Investigation of Performance Issues Affecting Optical Circuit and Packet Switched WDM Networks

A THESIS SUBMITTED FOR THE DEGREE OF DOCTOR OF PHILOSOPHY

To

Dublin City University

By

Frank Smyth, B.Eng, M.Eng

School of Electronic Engineering

Faculty of Engineering and Computing

Dublin City University

August 2008

Supervised by:

Professor Liam Barry

Approval

Candidate:	Frank Smyth	
Degree:	Doctor of Philosophy	
Thesis Title:	Investigation of Performance Issues affecting Optical Circuit and Packet Switched WDM Networks	
Examining Committee:	**Chairperson:**	_____
	External Examiner:	_____
		Prof. Antonio Teixeira
	Internal Examiner:	_____
		Dr. Martin Collier
	Supervisor:	_____
		Prof. Liam Barry

Declaration

I hereby certify that this material, which I now submit for assessment on the programme of study leading to the award of Doctor of Philosophy is entirely my own work, that I have exercised reasonable care to ensure that the work is original, and does not to the best of my knowledge breach any law of copyright, and has not been taken from the work of others save and to the extent that such work has been cited and acknowledged within the text of my work.

Signed: _____

ID No.: _____

Date: _____

Dedicated to Nic

Acknowledgements

I would like to thank my supervisor, Professor Liam Barry, for his initial faith in my ability, and for the support and guidance that he has given me throughout this PhD.

I am indebted to my colleagues past and present, for the role they have played, both academically and socially, in my time with the Radio and Optical Communications Group.

The researchers that I have collaborated with while working towards this PhD also deserve my gratitude, especially my mentor in Bell Labs, Dr. Dan Kilper.

Finally, I would like to thank my parents for their support, and my fiancée Nicola, for her initial encouragement of, and subsequent patience with my 'eternal' studentship.

Abstract

Optical switching represents the next step in the evolution of optical networks. This thesis describes work that was carried out to examine performance issues which can occur in two distinct varieties of optical switching networks.

Slow optical switching in which lightpaths are requested, provisioned and torn down when no longer required is known as optical circuit switching (OCS). Services enabled by OCS include wavelength routing, dynamic bandwidth allocation and protection switching. With network elements such as reconfigurable optical add/drop multiplexers (ROADMs) and optical cross connects (OXCs) now being deployed along with the generalized multi-protocol label switching (GMPLS) control plane this represents the current state of the art in commercial networks. These networks often employ erbium doped fiber amplifiers (EDFAs) to boost the optical signal to noise ratio of the WDM channels and as channel configurations change, wavelength dependent gain variations in the EDFAs can lead to channel power divergence that can result in significant performance degradation. This issue is examined in detail using a reconfigurable wavelength division multiplexed (WDM) network testbed and results show the severe impact that channel reconfiguration can have on transmission performance.

Following the slow switching work the focus shifts to one of the key enabling technologies for fast optical switching, namely the tunable laser. Tunable lasers which can switch on the nanosecond timescale will be required in the transmitters and wavelength converters of optical packet switching networks. The switching times and frequency drifts, both of commercially available lasers, and of novel devices are investigated and performance issues which can arise due to this frequency drift are examined. An optical packet switching transmitter based on a novel label switching technique and employing one of the fast tunable lasers is designed and employed in a dual channel WDM packet switching system. In depth performance evaluations of this labelling scheme and packet switching system show the detrimental impact that wavelength drift can have on such systems.

Table of Contents

Table of Figures

List of Acronyms

ACA	Amplifier Coupler Absorber
ACG	Applied Constant Gain
ADM	Add Drop Multiplexer
AM	Amplitude Modulation
AM-PSK	Amplitude Modulation-Phase Shift Keyed
AMZD	Asymmetric Mach-Zehnder Disinterleaver
AO	Acousto-Optic
APD	Avalanche Photodiode
AR	Anti Reflection
ASE	Applications Spontaneous Emission
ASON	Automatically Switched Optical Network
ATM	Asynchronous Transfer Mode
AWG	Arrayed Waveguide Gratings
AWGR	Arrayed Waveguide Grating Router
BER	Bit Error Rate
BERT	Bit Error Rate Tester
CG	Constant Gain
CW	Continuous Wave
CWDM	Coarse WDM
DB	Data Burst
DBR	Distributed Bragg Reflector
DC	Direct Current
DCF	Dispersion Compensation Fiber
DCM	Dispersion Compensation Module
DCS	Digital Cross Connect Switch
DFA	Doped Fiber Amplifiers
DFB	Distributed Feedback
DGD	Differential Group Delay
DPSK	Differential Phase Shift Keyed
DSB	Double Side Band
DSF	Dispersion Shifted Fiber
DWDM	Dense WDM
EAM	Electro Absorption Modulator
ECL	External Cavity Lasers
ED	Error Detector
EDF	Erbium Doped Fiber
EDFA	Erbium Doped Fiber Amplifiers
EML	Electro-Absorption Modulator Laser
EO	Electro Optic
EPS	Electronic Packet Switching
ETDM	Electrical Time Division Multiplexed
FBG	Fiber Bragg Grating
FDL	Fiber Delay Lines
FDM	Frequency Division Multiplexing

FEC	Forward Error Correction
FLM	Fiber Loop Mirror
FO	Fully Optimized
FP	Fabry-Pérot
FPGA	Field Programmable Gate Array
FSC	Fiber Switch Capable
FSR	Free Spectral Range
FTL	Fast Tunable Lasers
FWM	Four Wave Mixing
FXC	Fiber Cross Connect
GCSR	Grating Coupled Sampled Reflector
GEF	Gain Equalization Filter
GHz	Gigahertz
GMPLS	Generalized Multi Protocol Label Switching
IETF	Internet Engineering Task Force
IMD	Intermodulation Distortion
IP	Internet Protocol
ISDN	Integrated Services Digital Network
ISI	Inter Symbol Interference
ITU	International Telecommunication Union
ITU-T	ITU Telecommunications Sector
JET	Just Enough Time
JIT	Just in Time
L2SC	Layer 2 Switch Capable
LASER	Light Amplification by Stimulated Emission of Radiation
LD	Laser Diode
LO	Local Oscillator
LSC	Lambda Switch Capable
MEM	Micro Electro Mechanical
MEMS	Micro Electro Mechanical Systems
MGY	Modulated Grating Y
MHz	Megahertz
MPLS	Multi Protocol Label Switching
MZ	Mach-Zehnder
MZI	Mach-Zehnder Interferometer
MZM	Mach Zehnder Modulator
NF	Noise Figure
NNI	Network to Network Interface
NRZ	Non Return to Zero
NRZ-OOK	Non Return to Zero On/OFF Keyed
NZDSF	Non Zero Dispersion Shifted Fiber
OA	Optical Amplifier
OADM	Optical Add Drop Multiplexers
OBS	Optical Burst Switching
OCDM	Optical Code Division Multiplexed
OCS	Optical Circuit Switching

OCSS	Optical Carrier Suppression and Separation
OE	Opto-electronic
OEO	Optical to Electrical to Optical
OFS	Optical Flow Switching
OH	Hydroxil
OIF	Optical Internetworking Forum
OIS	Optical IP Switching
OLS	Optical Label Switching
OLT	Optical Line Terminals
OM	Opto-Mechanical
OPS	Optical Packet Switching
OSA	Optical Spectrum Analyser
OSNR	Optical Signal to Noise Ratio
OTDM	Optical Time Division Multiplexing
OTN	Optical Transport Networks
OXC	Optical Cross Connect
P-I	Power vs. Current
PD	Photodiode
PDG	Polarization Dependent Gain
PDL	Polarization Dependent Loss
PIN	Positive Intrinsic Negative
PM	Power Meter
PMD	Polarization Mode Dispersion
POL SCR	Polarization Scrambler
PPG	Pulse Pattern Generator
PRBS	Pseudo Random Bit Sequence
PSC	Packet Switch Capable
PSK	Phase Shift Keyed
PSTN	Public Switched Telephone Network
PT	Power and Tilt
PXC	Photonic Cross Connect
RAM	Random Access Memory
RF	Radio Frequency
ROADM	Reconfigurable Optical Add Drop Multiplexers
RZ	Return to Zero
SBS	Stimulated Brillouin Scattering
SCM	Subcarrier Multiplexed
SDH	Synchronous Digital Hierarchy
SDM	Space Division Multiplexing
SFP	Slotted Fabry-Pérot
SG	Sampled Grating
SG-DBR	Sampled Grating Distributed Bragg Reflector
SHB	Spectral Hole Burning
SLA	Service Level Agreements
SMA	Sub miniature Version A
SMSR	Single Mode Spectra

SOA	Semiconductor Optical Amplifier
SONET	Synchronous Optical Network
SPM	Self Phase Modulation
SRS	Stimulated Raman Scattering
SSB	Single Sideband
SSG	Super Structure Grating
SSMF	Standard Single Mode Fiber
STS-1	Synchronous Transport Signal
TAG	Tell and Go
TAW	Tell and Wait
TDM	Time Division Multiplex
TF	Tunable Filter
THz	Terahertz
TL	Tunable Laser
TLS	Tunable Laser Source
TO	Thermo-Optic
TOF	Tunable Optical Filter
TTL	Time to Live
TWC	Tunable Wavelength Converters
UDWDM	Ultra Dense WDM
UNI	User Network Interface
UNI/NNI	User Network Interface/Network Network Interface
USA	United States of America
V-I	Voltage - Current
VCF	Vertical Coupler Filter
VCSEL	Vertical Cavity Surface Emitting Lasers
VMZ	Vertical Mach Zehnder
VOA	Variable Optical Attenuator
WBXC	Waveband Cross Connect
WDM	Wavelength Division Multiplexed
WIXC	Wavelength Interchanging Cross Connect
WSS	Wavelength Selective Switch
WSXC	Wavelength Selective Cross Connect
XC	Cross Connect
XGM	Cross Gain Modulation
XPM	Cross Phase Modulation

Chapter 1 – Introduction

The widespread deployment of WDM technology has been driven by the massive growth in the volume of data traffic since the dawn of the internet. Optical fiber, originally used to carry a single wavelength channel now often carries 128 wavelengths or more. While the technology for optical transport flourished, the technology for optical switching lagged behind and this has led to a rigid, opaque network, in which OEO conversion is still performed at the nodes and reconfiguration of the network can take weeks. The ongoing deployment of optical switching components such as optical cross connects (OXCs) and reconfigurable optical add/drop multiplexers (ROADMs) brings greater transparency and reconfigurability to WDM networks and improves their efficiency, scalability and flexibility. The immediate advantage brought by the deployment of these components is centralized network management. Rather than having to deploy personnel to each node location, the network can be reconfigured from a central office.

The next step for optical networks will see a move away from human management of the network, to a network which will automatically self-reconfigure in response to changing traffic demands, network faults or user requests. The control and monitoring systems required for automatic operation represent a significant challenge and one aspect of this is examined closely in this thesis. As the channel configuration changes, gain dynamics of the amplifiers and the previous system arrangement can lead to channel power divergence that can result in OSNR and nonlinearity related transmission penalties. The re-optimization of the network for the new configuration can take seconds or longer and during this time transmission may not be possible leading to a significant reduction in network throughput.

While OCS represents a leap forward for optical networking, there are also potential drawbacks associated with its use for the backbone of the future Internet. Early arguments against OCS related to the poor bandwidth efficiency and reduced robustness in comparison to packet switching, however these arguments have largely been nullified [1]. More recent arguments include issues with signalling complexity, the inherent blocking probability of circuits and the fact that the current internet is designed for packets rather than circuits. As such great interest has been seen in the development of optical packet switched systems and

yet the challenges for the development of OPS may be even greater than those facing OCS. The lack of practical optical buffers and optical logic represent two of the major obstacles.

Wavelength tunable lasers (TLs) are becoming a mainstream component in today's optical networks due to the cost saving they offer, in terms of back-up transmitters and inventory reduction. However in these roles the dexterity of TLs is not fully exploited; they really come into their own as a key component in the transmitters and wavelength converters of OPS networks that require switching between hundreds of wavelengths on nanosecond timescales. As such, the accuracy of wavelength switching must be very precise. In this work the switching times, wavelength accuracy and drift are all examined and the impact of these properties on an OPS system is evaluated.

The work described in this thesis was supported by Science Foundation Ireland and was carried out in the Radio and Optical Communications Laboratory, Dublin City University, in the Photonic Systems Laboratory at the Tyndall National Institute, Cork and in Bell Laboratories, Crawford Hill, New Jersey USA. It contributes to the body of knowledge in three distinct areas:

Reconfiguration related performance penalties in OCS networks - This section of the work deals with slow reconfigurable networks and the performance issues which can be encountered after reconfiguration of the channels. To date, the effects of reconfiguration on transmission performance has not been widely studied and the aim of this work was to stimulate further experimentation in this area. Loading dependent gain variation in the EDFAs and the historical system arrangement can lead to severe channel power divergence and hence, transmission penalties due to OSNR degradation or non-linear effects. A technique was developed that allows the detailed study of the post reconfiguration and post re-optimization system performance in circulating loops. The experimental work was carried out on a WDM circulating loop testbed in Bell Laboratories and is described in Chapter 3.

Switching and modulation of a slotted Fabry-Pérot laser - The second set of experiments is based on the switching and modulation of a novel tunable laser developed by the III-V Devices and Materials Group at the Tyndall National Institute. Tunable lasers are a key component for future fast wavelength switching networks, however due to the complex fabrication processes; tunable lasers that can tune very quickly over a wide wavelength range are very costly. The fabrication process for the devices studied, which are known as tunable Slotted

Fabry-Pérot (SFP) lasers, is much simpler and it is expected that these devices could potentially be used as in cost effective transmitters for access networks, for example. It was shown for the first time in this work that these devices exhibit extremely fast wavelength switching and can operate error free up to 10Gb/s. The tunable SFP devices were characterised both in Dublin City University and in Bell Laboratories and the work carried out is detailed in Chapter 4.

Wavelength drift in SCM optical label switched networks - The final set of experiments is based on a commercially available Sampled Grating Distributed Bragg Reflector (SG-DBR) tunable laser module by Intune Networks. These devices exhibit all of the properties required of a tunable laser for use in an OPS network. To date, much of the literature in the area of OPS has focussed on the transmission, address recognition and routing of various OPS schemes, and the fact that these OPS schemes will be used in a multi-channel system with switching tunable lasers has been somewhat neglected. In this work, a novel subcarrier multiplexed (SCM) optical labelling scheme is developed and tested in a dual channel system employing switching tunable lasers. Characterization of the wavelength drift of the laser was performed and the impact of this drift in the optical packet switching system was examined. This work was carried out in Dublin City University and in the Tyndall National Institute and it is reported in Chapters 4 and 5.

The remainder of this thesis is structured into six chapters as follows:

Chapter One briefly discusses the history of optical communication and optical networking. Wavelength division multiplexing is introduced along with the basic components of a WDM optical network. Important issues relating to a number of the components are also considered in this chapter for example the section on optical fiber discusses dispersion, non-linearities, and attenuation. Where required these issues will be dealt with in greater detail in later chapters.

Chapter Two is concerned with reconfigurable WDM optical networks. It begins by presenting two of the trends observed in future optical networks, namely greater reconfigurability, and greater transparency. The various optical switching technologies are then discussed followed by a section describing the network elements that are currently being deployed. The remainder of the chapter then reviews the current state of the art in commercial networks, discussing optical circuit switching and the GMPLS control plane that

enables it, before turning to future optical switching techniques such as optical burst and packet switching.

In Chapter Three the first set of experimental work is described. Prior to this however, important background information that assists in the understanding of the experiment is given. The design and operation of EDFAs and their gain dynamics are explained along with performance degradation that can result from gain error induced power divergence. Also discussed are circulating loops, employed in this work to achieve long haul distances with limited resources. The remainder of the chapter goes on to describe the experimental process and set-up, the results and the conclusions arrived at.

Chapter Four moves away from slow optical switching and deals with the tunable laser (TL), a key enabler for fast optical switching. It begins by discussing the applications of TLs in WDM networks and the properties they must exhibit to be suitable for these applications. Some detail is given on the workings and mechanisms of TLs and some common designs are described. Then two types of widely tunable laser, namely the sampled grating distributed Bragg reflector (SG-DBR) and the tunable slotted Fabry-Pérot (SFP) are detailed along with experimental work which was carried out to characterise them.

Chapter Five then takes some of the characterisation work performed in the previous chapter and looks at how the issues raised affect an optical packet switching system. A review of the literature in the area of optical label switching is provided before a description of a novel optical labelling scheme developed within the confines of the project is given. This labelling scheme is then characterised in both single and dual-channel systems and the effects of wavelength drift of the TL is examined.

In Chapter Six the preceding work is summarized and the thesis conclusions are drawn.

References

[1] P. Molinero-Fernandez., N. McKeown "TCP Switching: Exposing Circuits to IP", Standford Knowledgebase.

Chapter 2 – Optical Networks and Wavelength Division Multiplexing

2.1 Optical Networks – A Brief History

In early telephone networks every user was connected to every other user via copper wire links as shown in Fig. 2.1(a). The fully interconnected network topology does not scale well, and as the network began to grow switching centres were introduced, changing the topology to a star (Fig. 2.1(b)), and the function of the switching office at the centre of the star was to connect any two users on request. As more and more networks emerged it was necessary for users on one network to talk to users on another, therefore the switching centres were interconnected, either directly or via higher level switching centres. This hierarchical model became known as the Public Switched Telephone Network (PSTN) and is depicted in Fig. 2.1(c) [1].

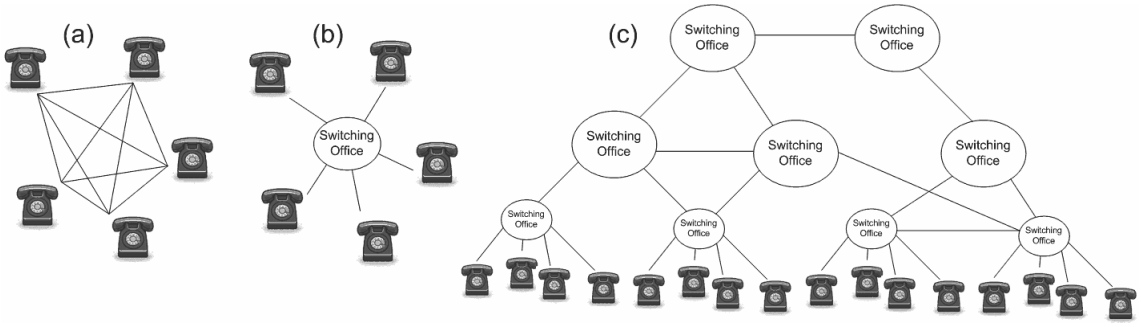

Fig. 2.1: Evolution of early telephone networks; a) fully interconnected users; b) users connected via switching centre; c) the PSTN

In 1977, live telephone traffic was carried on a fiber optic link for the first time in Long Beach, California, USA [2]. Early optical networks such as this were simple point to point links, installed in place of copper trunk transmission links to increase the bandwidth between different switching offices in the PSTN. The technology proved very popular, as carriers saw that the same amount of data which was then carried on tens or hundreds of copper wires could be carried on a single optical fiber. The subsequent rush to get products to market led to many incompatible proprietary technologies being developed as optical interfaces were added to electrical switching systems. Efforts to standardise led to the Synchronous Optical Network (SONET) and the Synchronous Digital Hierarchy (SDH), two similar and

compatible standards which define the standard optical signals, a synchronous frame structure and operating procedures [3,4]. SONET/SDH remains the dominant optical telecommunication standards in use today.

The fundamental component of a SONET/SDH network is the Add/Drop Multiplexer (ADM) that allows traffic to be taken off the network, and additional traffic to be coupled onto the network at intermediate nodes. SONET/SDH networks are generally based on a ring topology consisting of two optical fibers, one for each direction, or four fibers, one for each direction and two for protection. While the bandwidth of SONET/SDH links is scalable its upper bound was until quite recently limited to 10Gb/s by the electronics. As the demand began to outgrow this available bandwidth, optical multiplexing techniques were used to increase the capacity.

2.2 Optical Multiplexing

Optical multiplexing techniques allow multiple data streams to be transmitted simultaneously, thereby increasing total system capacity. The simplest method is Space Division Multiplexing (SDM) in which the capacity of a system is increased by transmitting additional data down a completely separate fiber. Unless the fiber plant is already place, this multiplexing technique is expensive and avoided where possible. For this reason, multiplexing techniques in which additional channels can be transmitted on a single fiber by changing the terminating equipment have been developed. Such techniques include Optical Time Division Multiplexing (OTDM) [5] in which short optical pulses are placed in a particular time slot depending on which optical channel they belong to, Polarization Division Multiplexing (PolDM) [6] in which channels are modulated onto orthogonal polarizations of the same light such that they don't interfere with each other, and Wavelength Division Multiplexing (WDM) [7] in which data is modulated onto optical carriers at different frequencies, which are then combined and transmitted down a single fiber. Each of the techniques has advantages and disadvantages and indeed, they have been used simultaneously in WDM/OTDM [8] for example.

At the time when bandwidth demand began to outgrow that available using time division multiplexing in the electrical domain, WDM was the most mature of the optical multiplexing techniques and it was adopted into many telecommunications carrier's networks.

2.3 Wavelength Division Multiplexing

WDM is analogous to Frequency Division Multiplexing (FDM) in Radio Frequency (RF) and satellite communications but at much higher frequencies. The concept is illustrated in Fig. 2.2. Typically, electrical data channels with either Non-Return to Zero (NRZ) or Return to Zero (RZ) line coding are modulated externally onto light at different wavelengths which are generated by a number of Distributed Feedback (DFB) lasers. The different 'colours' of light are combined using a multiplexer and transmitted over fiber to their destination. At their destination a demultiplexer splits the combined light signal back into individual channels which are then reverted to their original electrical form using photoreceivers.

In early WDM systems, regeneration of channels could only be carried out in the electrical domain. Hence, at each regeneration point, the channels were demultiplexed and detected, regenerated in the electrical domain and then re-modulated, re-multiplexed and re-transmitted. This process formed an electronic bottleneck; it was slow and expensive both in terms of the physical equipment required and in terms of power consumption.

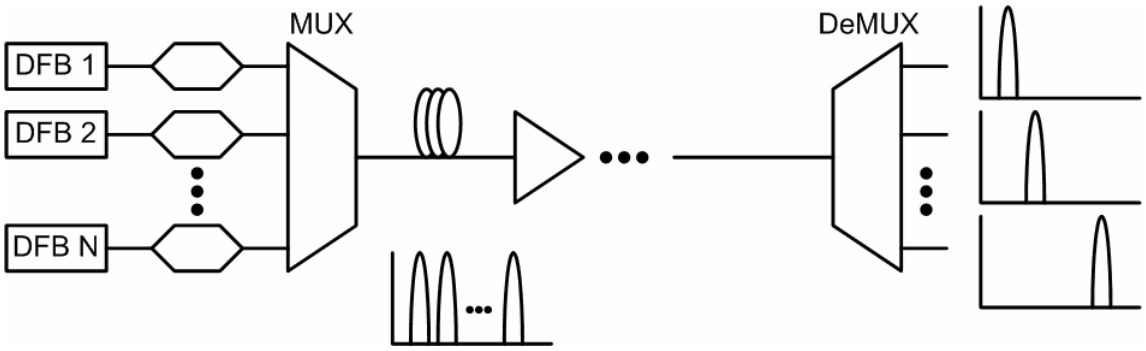

Fig. 2.2: Point to point Wavelength Division Multiplexing; light from a number of sources are modulated with different and multiplexed onto a single fiber for transmission. At the receiver the multi-wavelength signal is demultiplexed into the individual channels which are each detected separately.

The development of the Erbium Doped Fiber Amplifier (EDFA) in 1987 and the subsequent explosion in bandwidth demand due to the dawn of the Internet were the catalysts which led to widespread WDM deployment. It was discovered that light with a wavelength around 1550nm experienced strong gain when it was passed through silica fiber doped with erbium atoms and pumped at 980nm or 1430nm [9, 10]. This allowed WDM channels in this region to be amplified simultaneously without the need for demultiplexing

or Optical to Electrical to Optical (OEO) conversions. This important discovery prompted the industry to change the wavelength band of choice for telecommunications from the dispersion minimum at 1310nm to the EDFA gain peaks around 1550nm.

2.4 Classification of WDM Systems

The two main categories of WDM in use today are Coarse WDM (CWDM) or Dense WDM[1] (DWDM). The classification depends on the frequency spacing between individual channels. CWDM has channel spacing of 20nm spread evenly from 1270nm to 1610nm yielding 18 usable channels [11]. Wide channel spacing such as this allows for the use of inexpensive components and is suitable for systems with low bit rates, channel counts or distances, such as access networks. DWDM uses much narrower channel spacing, ranging from 3.2nm (400GHz) down to 0.4nm (50GHz) [12]. The DWDM channels are in the C and L band of the electromagnetic spectrum corresponding to the EDFA amplification band. As they require components of much higher specifications, they are generally only used in large metro and long haul networks.

2.5 Major Optical Components of a DWDM network

This section describes the major optical components used in current DWDM systems. Today, switching is still performed electrically in most instances and therefore it will not be discussed here. However, optical switching components will be covered in chapter 2.

2.5.1 Light Sources

The light sources used in DWDM systems must exhibit high output power, high Side Mode Suppression Ratio (SMSR), excellent wavelength stability, narrow line width and long lifetime. Fabry-Pérot laser diodes are the simplest form of diode laser. In these devices a semiconductor gain medium is sandwiched between two reflective surfaces to form a laser cavity. They emit light in multiple modes making them unsuitable for WDM but the basic structure can be adapted to form suitable WDM sources. Fabricated using Indium Gallium Arsenide Phosphide (InGaAsP) waveguides, Distributed Feedback (DFB) lasers are similar in structure to Fabry-Pérot laser but they include a frequency selective diffraction grating [13] which sets the emission wavelength to the ITU grid recommendation G.694.1 [12]. DFB lasers exhibit all of the desirable properties mentioned and are widely used in DWDM

[1] The terms Wideband WDM (referring to multiplexing a channel at 1310nm and a channel at 1550nm) and Ultra Dense WDM (referring to channel spacing's smaller than 50GHz for example 25GHz and 12.5GHz) are also sometimes used

networks. They generally incorporate temperature control to allow accurate fine tuning of the emission wavelength and subsequent wavelength stability. The operation and structure of laser diodes will be discussed in more detail in Chapter 5.

2.5.2 Modulators

Data can be modulated onto four properties of light: the intensity, the frequency, the phase and the polarisation. Intensity modulation is used almost exclusively in deployed networks, although advanced modulation formats are receiving considerable interest lately. Intensity modulation can be achieved via direct modulation of the drive current to the laser or through the use of an external modulator. Direct modulation is not suitable for DWDM because it causes an undesirable variation in the frequency of the emitted light known as chirp, and in addition, data rates are limited by the bandwidth of the laser.

Two main types of external modulator are employed in today's networks: The Mach-Zehnder modulator (MZM) is based on the Electro-Optic (EO) (or Pockels) effect by which the refractive index of a material changes with the application of an electric field, and the Electro-Absorption Modulator (EAM), which is based on the Electro-Absorption (EA) (or Franz-Keldysh) effect by which the absorption properties of a semiconductor are varied by applying an electric field. MZMs exhibit much higher extinction ratio than EAMs (~25dB vs. ~10dB) but in general they also need higher drive voltages [14]. In addition, while MZMs are fabricated on Lithium Nibate, EAMs are fabricated using the same materials as lasers and the two can be integrated on one chip to form an Electro-absorption Modulator Laser (EML) [15]. These devices are attractive due to their small size and low drive voltage, however while their chirp is small in comparison to direct modulation, it is non-zero and this limits the achievable transmission distance.

2.5.3 Multiplexers/Demultiplexers

Multiplexers are used to combine the various channels in the DWDM system into a single fiber for transmission. Demultiplexers conversely, are used to separate the channels either for switching at intermediate nodes or for detection at their destination. Multiplexers can be built from simple passive power combiners that couple light from two separate fibers into a single fiber although in practice, more sophisticated devices such as Arrayed Waveguide Gratings (AWGs) are generally used. The task of demultiplexing is more complicated because it requires specific wavelength selection, with good rejection of all other channels

and good stability over time. Most demultiplexers can also be used in reverse as multiplexers. Devices for multiplexing can be either passive or active, and are based on either diffraction or interference of the light signals.

Diffraction based demultiplexers make use of the Bragg effect. A Bragg grating or diffraction grating in the optical path disperses the light spatially into wavelength components which can then be focused into individual fibers using an array of grin lenses for example [16]. The interference based demultiplexers include the AWG, the Mach-Zehnder (MZ) demultiplexer and étalon filter based demultiplexers. The basic operation of an AWG is shown in Fig. 2.3. Light enters a free space star coupler which is followed by a number of waveguides of slightly different lengths which introduce a different phase shift for each path. The output light from each waveguide interferes constructively with the interference maximum at a spatial position dependent on the phase shift. Thus each individual wavelength can be focused onto an output fiber [17].

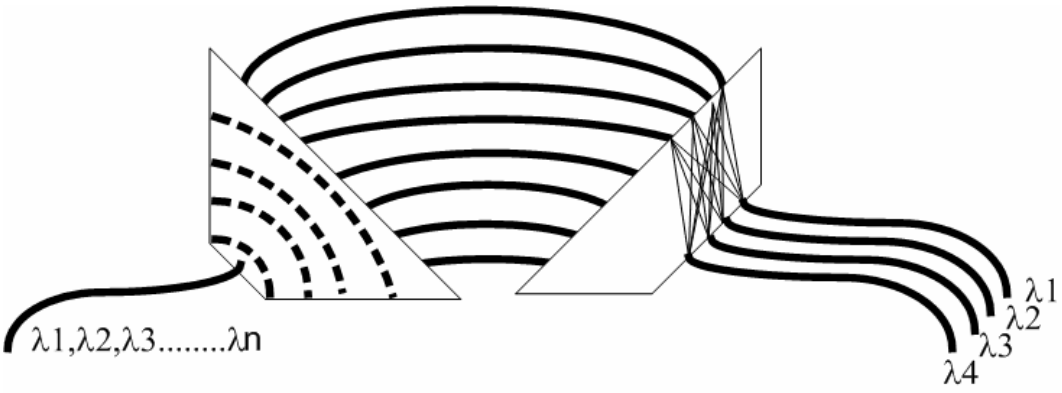

Fig. 2.3: An arrayed waveguide grating demultiplexer

MZ filters are created by splitting a light signal into two paths of different lengths and then recombining them in an interference recombiner. The two signals will interfere with each other constructively at periodic peak points and destructively elsewhere resulting in a periodic passband. The MZ demultiplexer is based on a cascade of MZ filters which each separate the spectrum into consecutively narrower portions. Because the insertion loss of each stage is additive, these devices are unsuitable for large channel counts.

Fabry-Pérot Etalon Filters [18] are resonant cavities consisting of two reflective surfaces designed such that while light at any wavelength can enter the cavity, only light which meets

the resonant conditions will be transmitted. Like the MZ filters, these are periodic filters which must be cascaded to form a demultiplexer.

2.5.4 Fiber

Most current DWDM systems use Standard Single Mode Fiber (SSMF) as their transmission medium. Fiber requirements in terms of attenuation, dispersion, nonlinear performance are stringent for long haul, high data rate networks.

Attenuation

Attenuation in optical fiber is primarily caused by absorption of the light by impurities in the glass (primarily hydroxide (OH) ions), and by Rayleigh scattering of the light caused by interactions between the photons and silica molecules. It is spectrally dependent and is at its lowest around 1550nm as shown in Fig. 2.4. Optical fibers with increased purity have been developed, [19] resulting in a significant reduction or elimination of the attenuation window at 1400nm and leaving massive bandwidth available for exploitation.

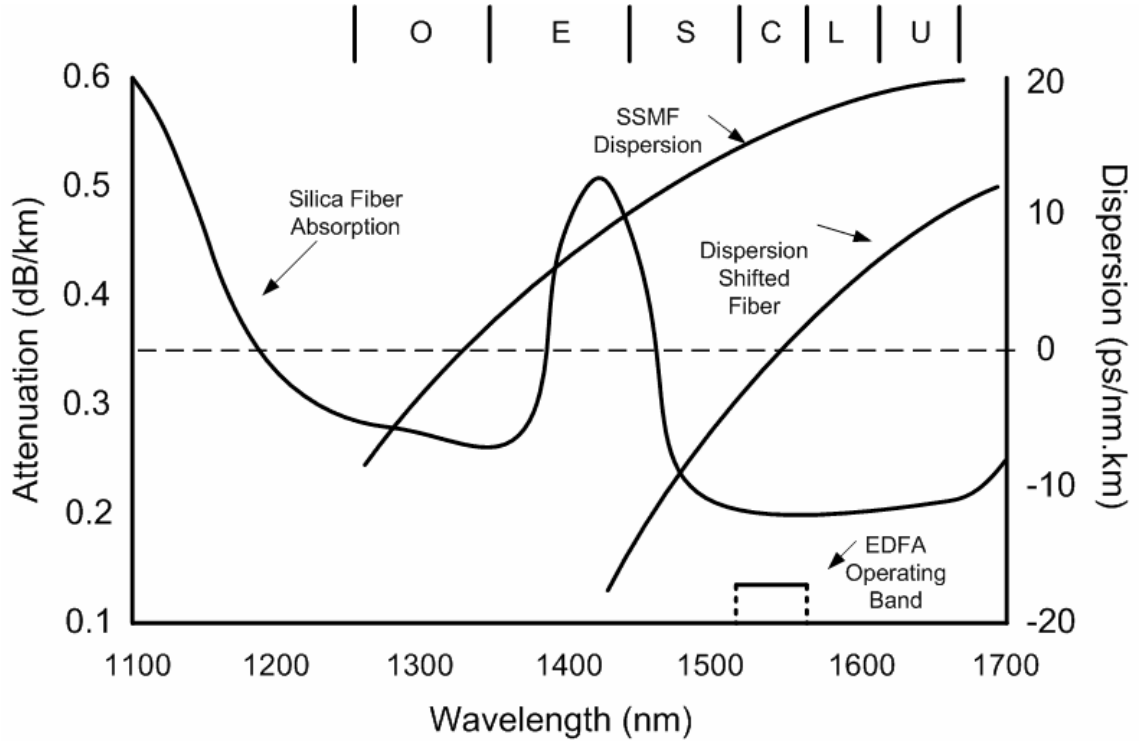

Fig. 2.4: Attenuation and Dispersion in optical fiber as a function of wavelength

Dispersion

Dispersion in SSMF causes light pulses to narrow or broaden as they travel through fiber. An optical channel actually consists of a narrow band of wavelengths as opposed to a single wavelength and because the refractive index of fiber is a function of wavelength, different wavelengths traverse a fiber at different speeds. The natural dispersion minimum of SSMF is at 1310nm but optical fibers have been designed with the dispersion zero shifted to other wavelengths [20] as shown in Fig. 2.4. In addition, dispersion compensation fiber (DCF) which has strong negative dispersion can be used to undo the negative effects of dispersion. A certain amount of dispersion is acceptable or even desirable in a DWDM system as it helps to reduce non-linear effects. However too much dispersion leads to data bits spreading as they propagate through the fiber leading to Inter-Symbol Interference (ISI) which causes bit errors at the receiver. The topic of dispersion will be re-visited in Chapter 4.

Non-linearities

Optical fiber nonlinearities cause optical pulses to alter each other or themselves, and have the effect of reducing the Optical Signal to Noise Ratio (OSNR) at the receiver. Two main categories exist: those which result from refractive index variations in fiber when it is exposed to different intensities of light such as Self Phase Modulation (SPM), Cross Phase Modulation (XPM) and Four Wave Mixing (FWM), and those which result from stimulated scattering such as Stimulated Raman Scattering (SRS) and Stimulated Brillouin Scattering (SBS) [21]. These nonlinear effects will be discussed in greater detail in Chapter 4.

2.5.5 Amplifiers

In a long haul link amplification is required to overcome losses in the system. There are three types of optical amplifiers in use in DWDM systems. Doped Fiber Amplifiers (DFAs) and especially the EDFA [9] are the most popular optical amplifier technology. Their fibers are heavily doped with rare-earth elements such as erbium, and ytterbium which are excited to a higher energy level by a pump laser. The excited ions emit a photon when they return to their regular energy level by one of two processes. A signal photon with the correct wavelength can disturb the excited atoms and in this case the recombination process will cause the stimulated emission of a coherent photon, thereby causing amplification of the signal. Alternatively, if the ion has not been disturbed it will recombine spontaneously after it's radiative lifetime and emit a photon with random wavelength and direction. Some of

these spontaneous photons will in turn be amplified causing amplified spontaneous emission (ASE) which competes with the stimulated emission reducing the efficiency of amplification and worsening the OSNR. Each rare earth element has a different emission wavelength, and Erbium's emission range is between 1530nm and 1565nm, which lies inside the absorption minimum of fiber, making it very suitable for communications. EDFAs can be designed with gain of up to 30dB, output power up to 30dBm and amplification windows of up to 50nm.

A DFA's gain is not constant over its entire emission spectral range. For this reason, gain flattening filters with a transfer function that is the inverse of the DFA's gain function are often used to flatten the spectrum [22,23]. In addition, the total gain is shared between all of the amplified signals, and hence the addition, reduction or even reconfiguration of the amplified channels leads to dynamic gain fluctuations. For long haul systems that may have many amplified spans these gain fluctuations can contribute to serious performance degradation. This issue will be closely examined in chapter 3.

Raman amplifiers [24] are the second common type of optical amplifiers used in telecommunication. A high energy pump signal, a few tens of nanometres shorter in wavelength that the signal to be amplified, is coupled into the transmission fibre. Due to Stimulated Raman Scattering (SRS), a signal photon stimulates the scattering of a pump photon in a process that creates a third photon identical to the incident signal photon. Essentially the original signal photons 'steals' some of the energy from the pump signal resulting in amplification of the original signal. Raman amplification generally occurs in the transmission fiber forming a distributed amplifier with improved noise performance over lumped amplifiers such as EDFAs. In addition, Raman amplifiers can provide gain at any wavelength simply by using a number of pumps at different frequencies.

The third type of amplifier uses the optical gain mechanism in semiconductor materials and is known as the Semiconductor Optical Amplifier (SOA) [25]. The structure of an SOA is similar to that of a simple Fabry-Pérot laser cavity but with anti-reflective facets. As such, the oscillation condition which causes lasing in a Fabry-Pérot laser does not exist. Electron-hole pairs are created by electrically biasing the device and incident signal photons stimulate recombination and the generation of a coherent photon, thereby causing gain.

SOAs can be integrated with lasers very easily and it is in this application, as transmitter boosters for single channels, rather than for inline amplification of many DWDM channels,

that SOAs are generally used in WDM networks today. In general they are not used for amplifying multiple channels because they suffer from Cross Gain Modulation (XGM), which can cause serious crosstalk between channels. This process however, does allow wavelength conversion using SOAs [26] and it seems likely that they will find a role in fast switched WDM networks of the future.

2.5.6 Photoreceivers

Two types of photodiode can be used to convert an optical signal back to the electrical domain. The first is the Positive Intrinsic Negative (PIN) photodiode which consists of an intrinsic layer sandwiched between a p-type layer and an n-type layer. When this structure is reverse biased, and light is incident upon it, it generates a current which is proportional to the intensity of the light. The ratio of the current generated to light absorbed is known as the responsivity. For PINs this current is usually very small, so they are often coupled directly to a transimpedence amplifier which converts the small current to a more useable voltage.

Receiver sensitivity can be greatly improved by using an avalanche photodiode (APD). The device structure is similar to that of a PIN but with the 'I' layer designed to encourage multiplication. A very large reverse bias is applied and this causes carriers to race across the depletion layer with so much energy that they can create further carriers which in turn can create further carriers and so on. The disadvantages of APDs are that they are noisier than PINs and also the multiplication process reduces the response time and hence the bandwidth of the device. Traditionally the bandwidth of APDs was limited to <5GHz but advances in the technology have yielded APDs with bandwidths of 10GHz and higher meaning that they could potentially be used in a DWDM system.

2.6 Conclusion and Perspective

This chapter gave an introduction into WDM optical networks and discussed the technology which enabled their widespread deployment. WDM eliminated the electrical bottleneck at the transmitter side by allowing the transmission of multiple Electrical Time Division Multiplexed (ETDM) signals on a fiber at the same time by placing them on WDM carriers, and the EDFA eliminated the electrical bottleneck in the transmission path by removing the need for OEO conversion of each channel at each regeneration point along the link. These advancements have greatly increased the number of wavelength channels and data rate per channel on the fiber links. At intermediate nodes however, switching is still performed in the

electrical domain requiring OEO conversions for every channel. This creates a bandwidth mismatch between link capacity and switching capacity. Terminating each wavelength at each node for routing is expensive, inflexible and scales poorly. Optical switching is seen as the solution to this problem. Its introduction into networks will mean that signals can remain in the optical domain throughout the network, and OE (or OEO) conversion will only be required at the edge of the network in order to enter a separate access or client network. Various forms of Optical Switching technologies and techniques will be discussed in detail in Chapter 2.

References

[1] T. S. El-Bawab, "Preliminaries and terminologies," in *Optical Switching* T. S. El-Bawab, 2006

[2] J. Hecht, *City of Light: The Story of Fiber Optics.* Oxford University Press, 1999

[3] ANSI T1.105: Digital Hierarchy Optical Rates and Formats Specification (SONET)

[4] CCITT (ITU) Recommendation G.707, "Synchronous Digital Hierarchy Bit Rates."

[5] R. S. Tucker, "Optical time-division multiplexing and demultiplexing in a multigigabit/second fibre transmission system", Electronics Letters 23(5), pp. 208-209, 1987.

[6] P.M.Hill, R. Olshansky, W.K Burns, "Optical polarization division multiplexing at 4 Gb/s," *IEEE Photonics Technology Letters*, vol.4, no.5, pp.500-502, May 1992

[7] S. Sugimoto, K. Minemura, K. Kobayashi et al, "High-speed digital-signal transmission experiments by optical wavelength-division multiplexing," *Electronics Letters* , vol.13, no.22, pp.680-682, October 27 1977

[8] H. Tanaka, M. Hayashi, T. Otani, K. Ohara, M. Suz, "60 Gb/s WDM-OTDM transmultiplexing using an electro-absorption modulator," *Optical Fiber Communication Conference and Exhibit, 2001. OFC 2001* , vol.1, no., pp. ME4-1-ME4-3 vol.1, 17-22 March 2001

[9] R. Mears, L. Reekie, I. Jauncey, and D. Payne, "High-gain rare-earth-doped fiber amplifier at 1.54μm," in Optical Fiber Communication, 1987 OSA Technical Digest Series (Optical Society of America, 1987), paper WI2.

[10] E. Desurvire, J. R. Simpson, and P. C. Becker, "High-gain erbium-doped traveling-wave fiber amplifier," Opt. Lett. **12**, 888- (1987)

[11] ITU Recommendation G.694.2, "Spectral Grids for WDM Applications: CWDM Wavelength Grid"

[12] ITU Recommendation G.694.2, "Spectral Grids for WDM Applications: DWDM Wavelength Grid"

[13] H. Kogelnik and C. V. Shank, "Stimulated Emission In A Periodic Structure" Appl. Phys. Lett. 18, 152 (1971)

[14] S. V.Kartalopoulos, *DWDM Networks Devices and Technology*, Wiley-Interscience, New Jersey, 2003

[15] H.Soda, M. Furutsu, K. Sato, N. Okazaki, S. Yamazaki, H. Nishimoto, H. Ishikawa, "High-power and high-speed semi-insulating BH structure monolithic electroabsorption modulator/DFB laser light source," *Electronics Letters* , vol.26, no.1, pp.9-10, 4 Jan 1990

[16] J. Lipson, W. Minford, E. Murphy, T. Rice, R. Linke, G. Harvey, "A six-channel wavelength multiplexer and demultiplexer for single mode systems," *Lightwave Technology, Journal of* , vol.3, no.5, pp. 1159-1163, Oct 1985

[17] C. Dragone, "An N*N optical multiplexer using a planar arrangement of two star couplers," *Photonics Technology Letters, IEEE* , vol.3, no.9, pp.812-815, Sept. 1991

[18] J.Stone, L.W. Stulz, "Pigtailed high-finesse tunable fibre Fabry-Pérot interferometers with large, medium and small free spectral ranges," *Electronics Letters* , vol.23, no.15, pp.781-783, July 16 1987

[19] A. K. Srivastava et al, "High-speed WDM Transmission in AllWaveTM Fiber in Both the 1.4-μm and 1.55-μm Bands," in *Optical Amplifiers and Their Applications*, D. Baney, K. Emura, and J. Wiesenfeld, eds., Vol. 25 of OSA Trends in Optics and Photonics Series (Optical Society of America, 1998), paper CA3

[20] L.G Cohen, C. Lin, W.G French, "Tailoring zero chromatic dispersion into the 1.5-1.6 μm low-loss spectral region of single-mode fibres," *Electronics Letters* , vol.15, no.12, pp.334-335, June 7 1979

[21] P. Bayvel, and R. Killey, , "Nonlinear Optical Effects in WDM transmission" in Optical Fibre Telecommunications IV-A: Components, Academic Press, California, USA 2002

[22] M. Yamada, T. Kanamori, Y. Terunuma, K. Oikawa, M. Shimizu, S. Sudo, and K. Sagawa, "Fluoride-based erbium-doped fiber amplifier with inherently flat gain response," *IEEE Photon. Technol. Lett.*, vol. 8, no. 6, pp. 882–884, Jun. 1996.

[23] P. F. Wysocki, J. B. Judkins, R. P. Espindola, M. Andrejco, and A. M. Vengsarkar, "Broad-band erbium-doped fiber amplifier flattened beyond 40 nm using long period grating filter," *IEEE Photon. Technol. Lett.*, vol. 9, no. 10, pp. 1343–1345, Oct. 1997.

[24] E. Desurvire, M. Papuchan, J. P. Pocholle, J. Raffy, , and D. B. Ostrowsky, 'High gain optical amplification of laser diode signal by Raman scattering in single mode fibres', *Electron. Lett.,* 1983,19, pp.751-753

[25] L. H. Spiekman, , "Semiconductor Optical Amplifiers" in Optical Fibre Telecommunications IV-A: Components, Academic Press, California, USA 2002

[26] B.C. Gopal, F.S. Choa, , "Comparative study of wavelength conversion schemes using semiconductor optical amplifiers," *Lasers and Electro-Optics Society Annual Meeting, 1995. 8th Annual Meeting Conference Proceedings, Volume 1., IEEE* , vol.2, no., pp.245-246 vol.2, 30 Oct-2 Nov 1995

Chapter 3 – Reconfiguration in WDM Networks and Optical Switching

3.1 Introduction

As discussed in the previous chapter, the tremendous growth of the internet throughout the 1990s and up to the present has led to extensive deployment of Wavelength Division Multiplexing (WDM). Initial WDM networks were point to point links between electronic end terminals. The development of the Erbium Doped Fibre Amplifier (EDFA), as well as improvements in each of the enabling technologies mentioned in Chapter 2 meant that large numbers of wavelengths could be transmitted over thousands of kilometres. However, because the technology for optical transport matured much earlier than the technology for optical switching, which is still maturing, a high capacity optical transport network was built on top of a legacy electronic switching system. This has led to a rigid network, in which Optical-Electrical-Optical (OEO) conversion is still performed at the intermediate nodes and changes to the network can take months, and to yet another electronic bottleneck – the switching bottleneck. Two major trends which have emerged in optical networking are the trend towards greater transparency and the trend towards higher levels of reconfigurability. Improvement in these properties of the network will enable a more flexible, more scalable, and more bandwidth efficient network suitable for the provision of next generation services.

This chapter will begin by discussing the trends of transparency and reconfigurability mentioned. It will then give some insight into optical switching technologies before discussing the main techniques of optical switching, namely Optical Circuit Switching (OCS), Optical Burst Switching (OBS) and Optical Packet Switching (OPS) as well as two other techniques, optical IP switching (OIS) and optical flow switching (OFS). OCS and OPS were actively studied as part of this PhD, and so will receive greater attention than the other methods.

3.2 Transparency

A transparent optical system is one in which the data remains in the optical domain throughout. Conversely, an opaque system requires the data to be converted back to

electronic form at some point. Transparency offers the advantages of format independence meaning that various bit rates, protocols and modulation formats can be carried simultaneously, and also reduced cost due to the removal of expensive OEO conversions. The main problem with transparency is that impairments in an all-optical system accumulate and while research in the area has been vibrant for some years [1], there are still no commercially available all-optical 3R regeneration (amplification, retiming and reshaping) solutions. Optical amplifiers facilitate transparent amplification but at present reshaping and retiming of the signal must be performed electronically. The lack of commercial wavelength converters and limited optical monitoring capability are also problematic for transparent optical transport networks (OTNs) [2,3].

It should be noted that in a *transparent* optical network, network and switch control are still carried out using electronics. A network, in which these functions are carried out optically, would be more accurately referred to as an *all*-optical network. Furthermore, there are varying degrees of transparency, ranging from opaque networks in which switching and regeneration remain entirely electronic, to fully transparent, in which no opto-electronic conversion is carried out. Between these two extremes exist partially transparent networks in which certain areas of the network permit all optical end to end transmission. Transponders bounding an 'island' of transparency (as shown in Fig. 3.1) limit the size of the transparent portion and through the use of OEO conversions for regeneration can keep impairment problems from occurring [4]. The main function of the transponder is to convert a signal, be it electrical or optical, into an optical signal at a specified DWDM wavelength. Currently, this is always done via OEO conversions. Many transponders also provide added functionality such as 3R regeneration and multiplexing.

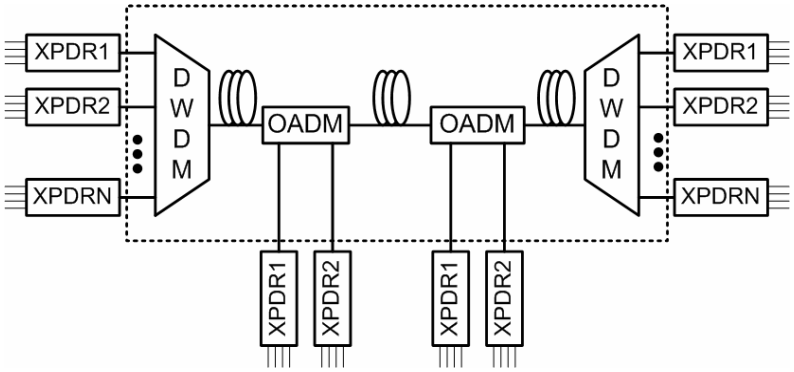

Fig. 3.1: An island of transparency bounded by transponders (adapted from [4])

3.3 Reconfigurability

The introduction of reconfigurable components into optical networks allows for automated provisioning of optical paths for dynamic bandwidth allocation, protection switching and wavelength grooming. Reconfigurability in a network enables the available capacity to be more fully exploited by reducing the inherent blocking conditions which exist in static networks [5]. Fig. 3.2 is an expansion of Fig. 3.1 which shows a larger island of transparency and illustrates the concept of blocking. If a certain wavelength is in use in path D-E, then without some form of reconfiguration that wavelength cannot be used anywhere in the path A-Z because it is blocked between X-Y.

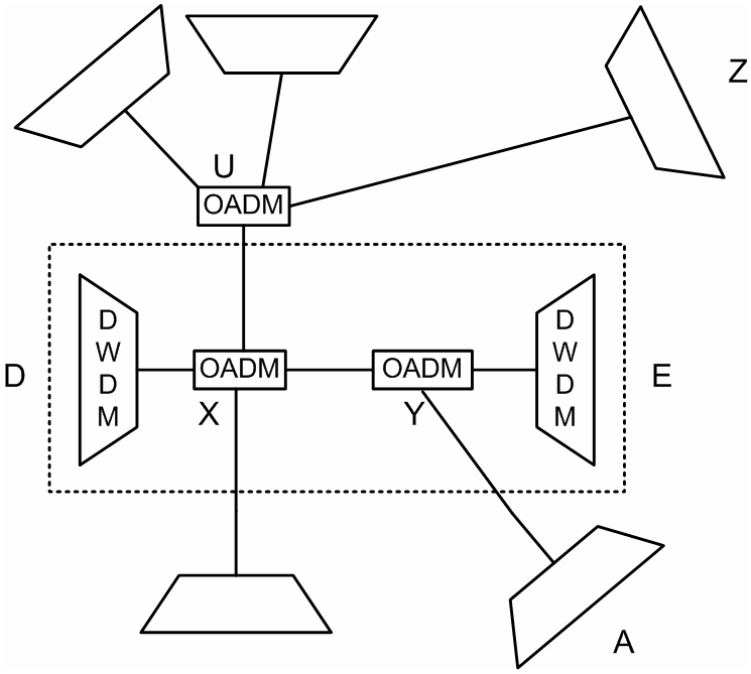

Fig. 3.2: The concept of blocking in a static WDM network (adapted from [4])

The reconfiguration speed of the networks determines the applications that can be run on it. As illustrated in Fig. 3.3, when reconfiguration of the network takes seconds or longer, the only applications enabled are sparing and wavelength provisioning. As the reconfiguration speed reaches milliseconds, protection switching, and automatic self-reconfiguration of the network become possibilities. Microsecond switching is required for OBS, while OPS needs switching times in the low nanoseconds.

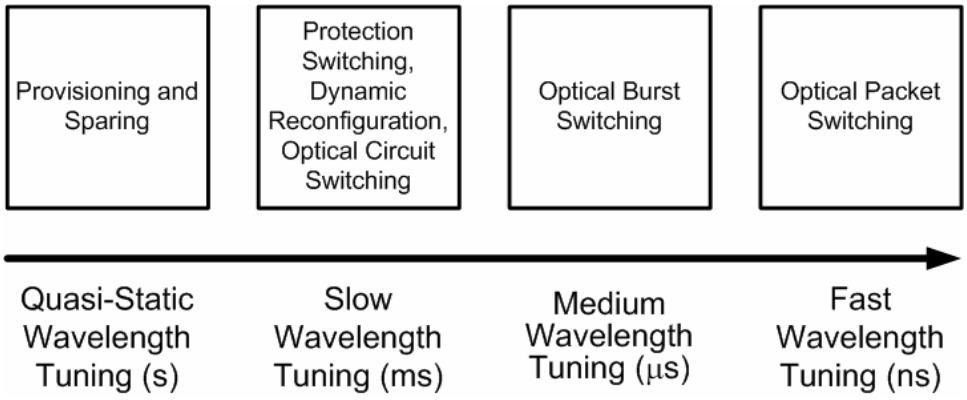

Fig. 3.3: Functions enabled by various reconfiguration speeds

Reconfiguration can be achieved using tunable transmitters and receivers, wavelength converters or optical switching elements. The vast majority of transmitters and receivers deployed today are of fixed wavelength; hence, reconfiguration of the network using the transmitters and receivers is not viable at present. Optical switching elements on the other hand, have been deployed in commercial networks [6,7], and their deployment represented the first steps towards the dynamically reconfigurable networks of the future. The majority of current optical switch fabrics perform their switching in the space domain, and have switching speeds in the order of milliseconds making them suitable for OCS.

A promising technology for faster reconfiguration which will be required for OBS and OPS performs its switching in the wavelength domain. An arrayed waveguide grating router (AWGR) takes an optical signal and routes it to a particular output port based on its wavelength. The switching speed of the fabric is therefore determined by the switching speed of the tunable laser used in the transmitter or wavelength converter. At present, tunable lasers have switching speeds in the low nanoseconds [8,9].

3.4 Evolution of Optical Network Topologies

One further trend which has been seen in transparent optical networks is a trend towards greater interconnection between nodes. Optical network topologies in the core network have evolved from simple point to point networks to tree and ring networks and from there to mesh networks where each of the nodes in the ring is connected not just to its nearest neighbours but also to other nodes [10]. This evolution is illustrated in Fig. 3.4.

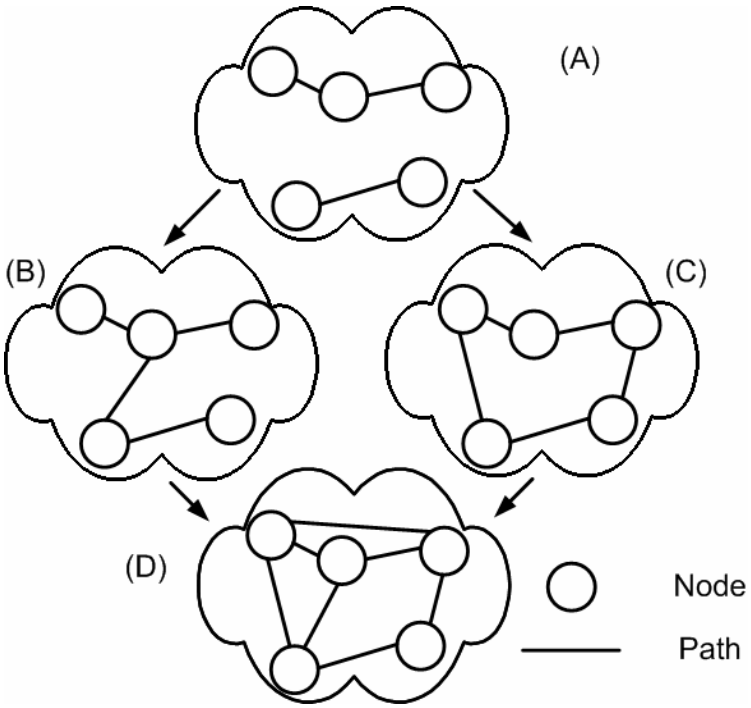

Fig. 3.4: Evolution of WDM network topologies; A) Point to Point; B) Tree; C) Ring; D) Mesh.

Mesh networks offer greater network efficiency and robustness over rings by providing multiple routing paths for restoration and protection without the need for dedicated protection fiber. However, network management for mesh networks is more complex than for rings due to the increased number of possible paths [11]. In addition, channels or bands of channels which have traversed very different paths may exist on a single fiber [12]. This means that techniques such as dispersion compensation, while improving performance of some channels may actually worsen others.

In the following section the technologies that can be used to enable reconfiguration in transparent mesh networks will be discussed. This will be followed by a section describing the building blocks of such networks that allow the interconnection of multiple optical paths typical of mesh networks, namely Reconfigurable Optical Add/Drop Multiplexers (ROADMs) and Optical Cross Connects (OXCs). These components are currently being deployed in commercial networks in order to allow greater levels of reconfiguration.

3.5 Optical Switching Technologies

This section will briefly discuss some of the optical switching technologies that have been demonstrated today. Optical switching technologies can be categorised into five main groups

depending on the method used to induce the switching. Numbers 1-3 and 5 below are generally based on guided wave switching (using optical fiber or waveguides) while switching in number 4 usually occurs in free-space (with the exception of the bubble switch). Note that here we only discuss the most common and promising technologies. More exhaustive lists and comparisons of techniques can be found in [13-15]

1. Electro-Optic switching

The most common Electro-Optic (EO) switches are based on the Pockels (or electro-optic) effect by which the refractive index of a material changes proportionally with an applied electric field. This refractive index change can be used to direct light through a waveguide. Lithium Nibate [16] ($LiNbO_3$) is the most common material used because it exhibits a large EO effect, and it is also readily fabricated into low loss planar waveguides [17]. EO switching has also been demonstrated in liquid crystals and in SOAs used as ON-OFF gates by varying the bias current [18]. Switching speeds ranging from microseconds to nanoseconds have been demonstrated using different EO switching technologies.

2. Acousto-Optic switching

Acousto-Optic (AO) switching has also been demonstrated with $LiNbO_3$ but Tellurium Dioxide (TeO_2) is more commonly used. In an AO switch, ultra-sonic waves are used to deflect light into different paths. On applying an RF electric field to the material, the piezoelectric effect generates an acoustic wave that modulates the refractive index of the material [19] enabling light to be directed through a waveguide. Typical switching speeds are in the order of hundreds of nanoseconds.

3. Thermo-Optic switching

Mainly fabricated using silica and polymers, Thermo-Optic (TO) switches use the TO effect by which the refractive index of the material is dependent on temperature. By supplying current to heating elements alongside the waveguide, the refractive index can be varied in order to direct the light in one direction or another. Switching speeds are generally in the millisecond range.

4. Opto-Mechanical switching

This category consists of a number of techniques in which the switching comes about through the movement of some component of the switch. Early OM switches involved the movement of optical fibers to switch the light [20]. More modern technology includes Micro-Electro-Mechanical Systems (MEMS) [14] that generally use matrices of tiny mirrors to block, pass or redirect light, and bubble switches [21], in which an air bubble at the crosspoint of a planar waveguide can be moved to redirect the light. The free space OM switches can switch on millisecond timescales.

5. All-Optical switching

Switching has also been demonstrated using an optical signal for control. In SOAs ultra-fast optical switching has been demonstrated using non-linear interferometry [22] whereby an optical control signal is used to interfere with the data signal either constructively or destructively in order to pass or block light. In addition, SOAs can be used as wavelength converters [23] that allow switching or routing in the wavelength domain using Arrayed Waveguide Grating Routers (AWGRs). Sub-nanosecond switching speeds can be achieved with SOAs.

The scalability of optical switches built using the aforementioned technologies is a very important issue. To be used in Cross-Connects (XCs) the switching technology must exhibit low loss in order to be highly scalable to hundreds or thousands of ports. Typically the low loss devices are the free space type based on beam steering and these exhibit slower switching speeds. On the other hand the waveguide based switches offer the potential for much faster switching with speeds matching or exceeding those required for OPS. The losses in these switches accumulate more quickly however, which makes it difficult to construct large port count XCs.

3.6 Elements of an Optical Switching Network

The main building blocks of the optical layer are illustrated in Fig. 3.5 and are described below. Note that in each case, transmission is only shown in a single direction. In reality, these components would support transmission in both directions.

3.6.1 Optical Line Terminals

Optical Line Terminals (OLTs), as shown in Fig. 3.5(a), are used to interface between fiber transmission links and the switching elements such as ROADMs and XCs. A generic OLT will contain a mux/demux to group a number of channels together and an amplifier to boost the signal prior to transmission or reception, and may also contain transponders to adapt the signal from client layers into a single WDM channel for transmission in the optical layer or to perform OEO conversions if an electrical switch fabric is used. OLTs can be included as part of a ROADM or XC, however due to poor standardization of WDM equipment; they are generally treated as separate components which prevents interoperability problems between equipment from different vendors.

3.6.2 ROADMs

Optical Add Drop Multiplexers (OADMs) were added to WDM networks to allow access to channels at intermediate points along a link that could be thousands of kilometres long. Essentially an OADM consists of a demultiplexer followed by a multiplexer with some filtration between the two. Channels or groups of channels can be dropped from and added to the main path using an OADM and the wavelengths that remain on their current path are known as the cut-through or express channels. One of the disadvantages of OADMs is that they are essentially fixed devices. The channels which are to be added and dropped must be chosen during the design phase and reconfiguring requires considerable Operational Expenditure (OpEx) because a technician must visit every node in order to configure the changes. The ROADM alleviates this problem by allowing remote reconfiguration of the channels which are added and dropped at the intermediate node. Rather than having static filtration elements between a mux/demux pair, ROADMs have a switching fabric as illustrated in Fig. 3.5(b). This gives them the ability to add or drop any wavelength and can enable, for example, dynamic provisioning of services in cases of unpredictable bandwidth demand. This flexibility is very desirable to carriers and they have begun to deploy ROADMs in their networks [7].

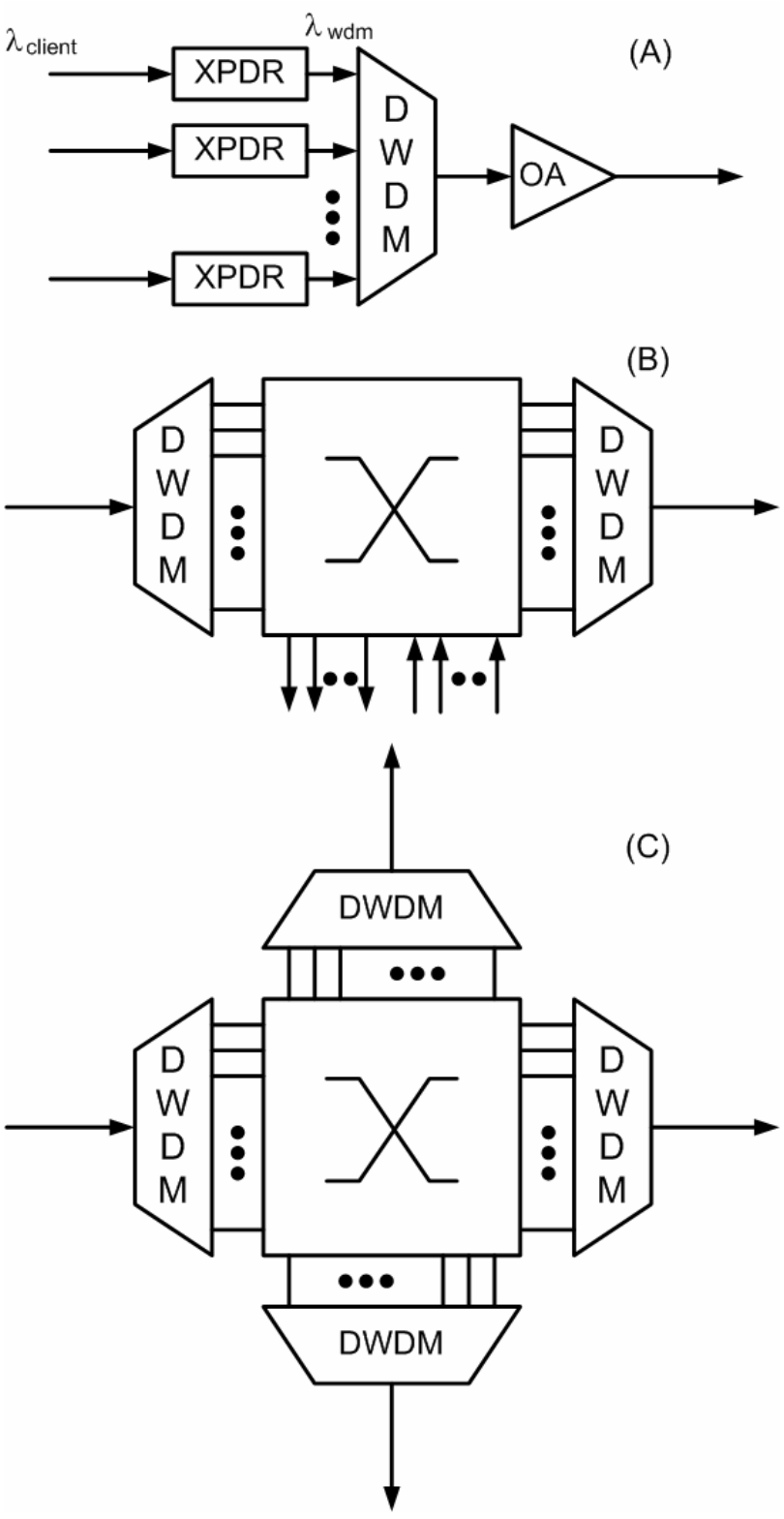

Fig. 3.5: Building blocks of reconfigurable transparent optical networks; A) A generic OLT; B) A generic 'degree 1' ROADM; C) A generic 'degree 4' PXC.

3.6.3 Cross Connects

While, in general a ROADM is used to add data to or drop data from a single WDM path, at a location where two or more WDM paths meet, there is a requirement for a XC. XCs switch data from an incoming WDM path onto any one of a number of outgoing WDM paths. In Fig. 3.5(c) the XC switches any channel from the West to either the North, South or East path. Note that in a practical XC, signals could arrive from any of the 4 directions. If this location also requires add/drop functionality (as is often the case) a multi-degree ROADM with XC functionality must be used. These devices have the ability to add or drop individual wavelengths from many paths or to switch them transparently onto any outgoing path if they are not required at the particular node.

Many varieties of XC exist [24, 25]:

1. Digital Cross-connect Switches (DCSs) accept a WDM signal but then demultiplex it in wavelength and time to a number of SONET STS-1 (50Mb/s) streams. All functions including switching, performance monitoring and regeneration are performed electrically. Such switches can be described as opto-electronic switches but because they do not employ optical switching they will not be discussed further here.

2. Optical Cross Connects (OXCs) are loosely and ambiguously defined and can be found in the literature with either electrical or optical switching cores and with varying levels of transparency. The advantages of these semi-transparent XCs over their fully transparent counterparts (described next) are that because OEO conversions are used, functions such as performance monitoring, wavelength conversion and 3R regeneration are readily available. The disadvantage is that these OEO conversions are expensive in terms of both equipment and power, and in general they are performed whether required or not, which is uneconomical.

3. Photonic Cross Connects (PXCs) are fully transparent XCs with an optical switching fabric however control and processing remains electronic. The advantages and disadvantages of total transparency are the converse of those listed above. Unless optical wavelength conversion is employed PXCs are blocking in the wavelength domain, which can complicate network management.

4. All-optical cross connects use photonics for signal processing and control of the switch as well as for the switching function itself. The technology to enable this is not yet mature although steps have been made towards it. These cross connects may find application in OPS switches due to the ultra fast switching speeds required.

Types 2, 3, and 4 described above can also be classified by their granularity. If the XC switches the entire contents of one fiber onto another it is deemed a fiber cross connect (FXC). If some filtration is employed to separate and then switch groups of adjacent channels it is known as a waveband cross-connect (WBXC). If the channels are fully demultiplexed and wavelengths are individually switched, the XC is termed a wavelength selective cross connect (WSXC). Each of these is blocking in the wavelength domain. A wavelength interchanging cross connect (WIXC) also switches with single wavelength granularity but uses either electronic or optical wavelength conversion to allow switching from any wavelength on any path to another wavelength on any other path thereby improving the blocking probability. Clearly, the finer granularity and lower blocking probability adds to the complexity and expense of a XC but these disadvantages are balanced by the increased flexibility.

3.7 Optical Circuit Switching

The switching of lightpaths (which may be wavelengths, wavebands, or entire fibers) is known as OCS because a lightpath is essentially analogous to an electrical circuit which must be requested, provisioned, and when it is no longer required, torn down. Currently, the provisioning or reconfiguring of wavelengths requires human intervention and is a process that can take anything from hours to weeks to complete with site visits generally being required. The deployment of centrally controlled hardware such as ROADMs and XCs represents significant cost savings for carriers. Networks that are still managed by humans are referred to as reconfigurable networks. In contrast, the next evolutionary step is the introduction of intelligent switching to the network, such that the network sets up lightpaths automatically as and when required. These automatically self-reconfiguring networks are referred to as OCS networks.

This section provides an insight to OCS. The main building blocks of a reconfigurable optical network have been discussed. Next, the network architecture, and the control plane

which will sit upon this network to manage the signalling and automation will be described, followed by the applications that this control plane enables.

3.7.1 Network Architecture

A generic illustration of an OCS network is shown in Fig. 3.6. It consists of optical switches such as ROADMs and XCs connected in a mesh topology in the core. Around the edges of this network lie the client networks which have traditionally been IP-over-ATM-over-SONET, although there is a trend towards thinning these layers out leaving an IP over DWDM stack (see Fig. 3.7).

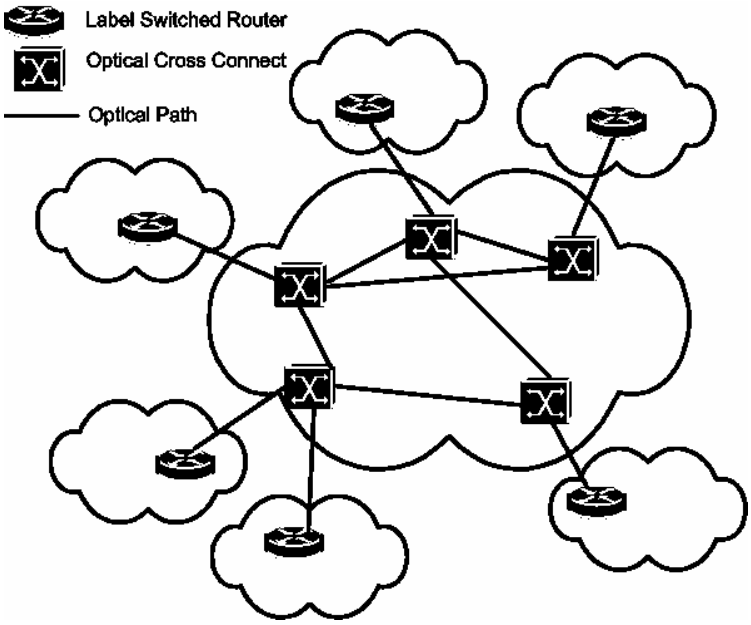

Fig. 3.6: A generic OCS Architecture

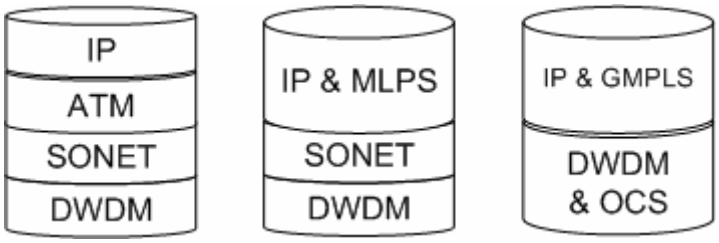

Fig. 3.7: Thinning out of the protocol stack

3.7.2 Control Plane

The control plane is the set of entities that controls and organizes the links between the network elements, determining the paths to other nodes in the network. The optical layer needs a large amount of human intervention for any type of modification. Currently, even the most basic functions, such as link and neighbour discovery, are either manually implemented or depend on non-standard protocol, which prevents interoperability between carriers. Provisioning a new circuit proves very inefficient in terms of cost and time.

Network service providers and vendors have attempted to overcome this deficiency by developing a standard for the optical control plane under the guidance of the International Telecommunications Union Telecommunications Standardization sector (ITU-T), the Internet Engineering Task Force (IETF) and the Optical Internetworking Forum (OIF). The general scope of the three standardization bodies is to develop an optical control plane capable of creating dynamic optical links triggered by user or management requests. In [26] the authors present a review of the standardization activity of the above cited bodies, emphasizing the interoperability aspects of their work.

ITU-T ASON

The Automatically Switched Optical Network (ASON) [27] is a control plane architecture being developed by the Study Group 15 of the ITU-T. It is not a protocol or a suite of protocols; rather it is an architecture which defines components in the control plane and the interactions between these components and those of the transport plane and management plane. ASON defines the requirements for an optical network capable of new functionalities like link and neighbour discovery, user interaction and fast dynamic provisioning of lightpaths, allowing the user to request bandwidth on-demand, and to reduce the bandwidth allocation time to the order of seconds.

The control plane supports connections requested either by users or by network management and is responsible for planning the route and signalling. It receives information from the transport plane regarding signal quality, faults etc and uses this data for provisioning and restoration.

Having a telecommunication-oriented background, the ITU-T group, has shaped its optical architecture more from concepts derived from standards such as SDH, ISDN and ATM than from the Internet protocols [28].

IETF GMPLS

The IETF has a more interactive approach to the development of Generalized Multi-Protocol Label Switching (GMPLS). In contrast to the ITU-T, where there is a designated group proposing and evaluating ideas for the protocol development, the IETF work group exchanges opinions with any Internet user who may want to actively participate to the discussions through an Internet mailing list.

GMPLS [29] is derived from Multi Protocol Label Switching (MPLS) [30], a technique that allows traffic engineering by creating switched virtual circuits through an IP network. Each time a packet enters a label-switched path it is marked with a label (similar to a packet header) which indicates the downstream neighbour to which the packet should be switched. After reading the label attached to the packet, this downstream neighbour replaces it with a new label that indicates to the subsequent downstream neighbour which route should be taken. This process continues until the packets reach the end of the circuit switched path. The practical advantages are that the short labels allow faster switching and cost reduction at the hardware level and that traffic engineering can be implemented without affecting the stability of the IP layer.

GMPLS extends this approach such that where MPLS could only accept packet switching capable interfaces, GMPLS can accept each of the following:

1. Packet Switch Capable (PSC) interfaces such as IP Routers which switch packets by reading information located in the packet header.
2. Layer-2 Switch Capable (L2SC) interfaces such as Ethernet and ATM switches which are able to switch frames or cells.
3. Time-Division Multiplex Capable (TDM) interfaces which switch data depending on it's time slot (for example SONET/SDH DCSs)
4. Lambda Switch Capable (LSC) interfaces such as WSXCs or WIXCs which switch optical signals with the granularity of a wavelength
5. Fiber-Switch Capable (FSC) interfaces such as FXC which switch the full contents of a fiber.

Aside from control plane architecture definitions, GMPLS also defines a suite of protocols which can be used on transport network architectures based either on the ASON overlay

network or its own GMPLS overlay or peer networks. Details of the GMPLS protocols are beyond the scope of this work but are described in detail in references [31-37]. While both networks can use very similar GMPLS protocols as an Internal Network to Network Interface (I-NNI) protocol, their User Network Interface (UNI) protocols are different from each other. Because different carriers use different GMPLS network architectures, a GMPLS based External Network to Network Interface (E-NNI) protocol has been introduced so that carriers/service providers can provide a seamless end-to-end call set up service between different architectures.

OIF UNI/NNI

ASON and GMPLS should be seen as complementary rather than competing technologies despite the fact that some of the literature suggests otherwise [28]. The OIF is a contribution-driven industry forum that encourages the cooperation between manufacturers, users and service providers. The OIF is generally recognized as a merging point between the ITU-T and IETF work in the optical control plane because it implements concepts and protocols defined by both the standardization bodies. For example the user network interface (UNI) concept is part of the ASON architecture and refers to ITU-T optical transport standards (as SONET/SDH); while it uses GMPLS signalling protocols and implements a GMPLS auto-discovery mechanism.

In 2004, the OIF organized an Interoperability demonstration [38], to show a practical implementation of the optical control plane, demonstrating the feasibility of their approach in a worldwide scale. The test brought together 15 vendors and 7 international carriers, connecting different laboratories located all over the world through trans-oceanic optical links and demonstrated the possibility of creating switched connections spanning multiple architectures. It represented the first real test of the automatic control plane standardization and its success helped to generate trust in an area that was viewed with scepticism by many service providers.

Since then many field trials and interoperability demonstrations have been conducted but carriers have only begun to deploy GMPLS recently. In late 2007 Verizon launched the United States' first bandwidth on demand service [39] which is run on a GMPLS network.

3.7.3 Applications

The applications which can be enabled and enhanced [40] through automatically and manually switched optical circuits in transparent optical networks are described below.

Network Management

'Point and click' centralized network management [41,42] significantly reduces a carrier's (OpEx) because it removes the need for an engineer to visit every site on the path in order to install the correct fixed wavelength components needed to re-arrange the network. If new wavelengths are required then only the end nodes need to be visited to install new transponders; if the wavelengths are already present, but need reconfiguring then no site visits are required at all.

Bandwidth Provisioning

Until recently, if a service provider for example, requested more bandwidth from a carrier, the delivery time ranged between a number of days and a number of weeks. With OCS enabled by GMPLS, this delivery time has been reduced to hours or even minutes. In addition, because traffic demand is generally quite predictable over weeks or months, bandwidth can be scheduled in advance in response to these predictable demands [39].

Traffic Management

A GMPLS control plane allows network managers to centrally re-route a portion of the traffic in the event of congestion for example [43]. Note that this is in response to real time events as opposed to network management mentioned above which would be in response to longer term trends.

Protection and Restoration

In today's world, reliable transfer of data is vital. Carriers often guarantee almost constant (99.999%) network up-time in their Service Level Agreements (SLAs) and failure to maintain such uptime can lead to financial penalties or loss of business. Nevertheless, failures do occur due to human error (e.g. fiber cuts) or equipment faults (e.g. amplifier fault). Heretofore, protection has often been provided by a dedicated protection fiber which would be automatically switched into place in the event of a failure [44]. This practice is highly inefficient because the maximum resource usage available with such a scheme is 50%. In other methods, the protection is shared by a number of resources [44,45]. For example, one

protection channel can be used for a number of service channels under the assumption that only one would fail at a time. Then the data of the failed channel is switched onto the protection channel until the fault is repaired.

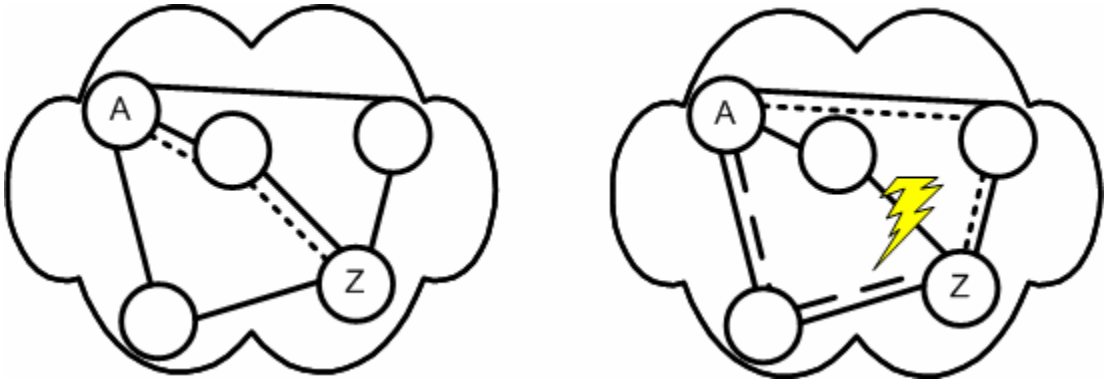

Fig. 3.8: Protection in Optical Mesh Networks; data is being transmitted from A-Z. Should its current path be disrupted, there are two additional paths that it can take therefore no dedicated protection fiber is required.

In transparent mesh networks, optical switching reduces the need for dedicated protection fiber even further. As shown in Fig. 3.8, with the higher degrees of interconnection, there is generally another route for the data to take in order to bypass a fault [44]. Although this requires greater complexity of signalling and route computation, these disadvantages are offset by the advantages of improved bandwidth efficiency and a more robust network.

3.7.4 OCS versus other Optical Switching Techniques

Some commentators maintain that the Internet is designed as a packet based network and that changing from Electrical Packet Switching (EPS) to optical circuit switching would represent a step backwards rather than a step forwards. Their solution is optical packet switching but the technology to enable OPS is not mature yet, so some intermediate solutions have been proposed, for example Optical IP Switching (OIS), Optical Flow Switching (OFS) and Optical Burst Switching (OBS).

3.8 Optical IP Switching

OIS [46] is a sub-genre of optical circuit switching, in which flows of optical packets which all have the same source destination can be switched onto a dedicated optical circuit. This can prove beneficial because it has been noted that of all internet traffic, a small number of flows carry a large proportion of the data [47]. While GMPLS circuits are usually provisioned in response to user requests or for long-term traffic management and once provisioned are

quasi-static, optical IP switching attempts to make greater use of the switching speeds available with OXCs by setting up circuits automatically in response to changing traffic conditions. This approach maintains the efficiency of IP routing for non-flow traffic but can save router resources such as memory and processing power. In addition, because it attempts to match traffic distribution with link utilization, it can improve the overall network throughput and diminish the probability of link congestion.

3.9 Optical Flow Switching

The goal of OFS [48] is to provide the end user with high bandwidth services sooner than other network architectures and switching methods might allow. It can be thought of as an intermediary between OCS and OBS. An end to end path or circuit through the network is requested by the user directly (see Fig. 3.9) and once an acknowledgement is received the entire flow is sent as a single entity. Note that this is in contrast to OBS and OPS in which data for transmission is broken down into packets at the user side and then reassembled at the destination. Not every lightpath request will be granted due to blocking probabilities so a trade-off between blocking, wavelength utilization and delay time must be made. This is seen as a method to offer various service levels to customers.

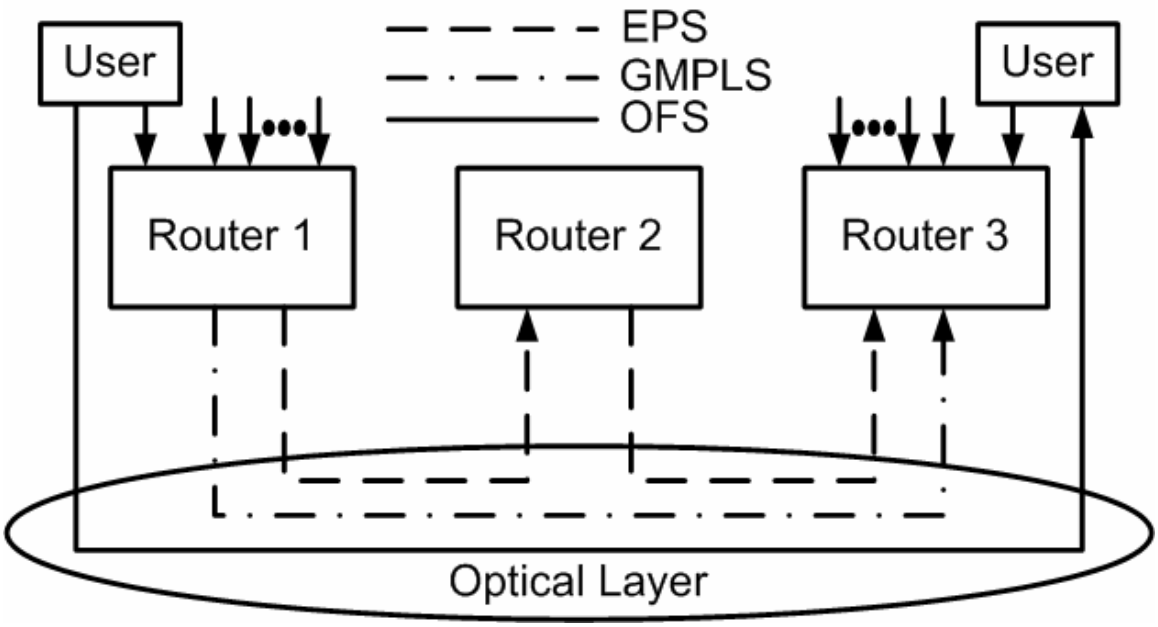

Fig. 3.9: Conceptual diagram of OFS vs. GMPLS and EPS

Circuits which are provisioned generally last >100ms before being torn down. Such timescales are short in comparison to typical GMPLS circuits but longer than typical data Bursts (DBs) in OBS (100μs – 100ms). The minimum granularity is a wavelength, so if a user does not have enough data to occupy a full wavelength, data from a number of users can be aggregated. Because scheduling is used and an end to end path is reserved, neither buffering nor contention resolution inside the network is required which can represent an advantage over certain forms of OBS.

3.10 Optical Burst Switching

OBS [49] is another method which has been proposed to bridge the gap between OCS and OPS in the core network. Data in today's networks is typically bursty in nature so in contrast with OFS, in OBS the user's data is 'packetised'. While still in the electronic domain these packets are then aggregated into bursts at the edge of the core network. Bursts are then converted to optical form, and routed through the entire core network in the optical domain. Only at the destination node it is converted to electrical domain. It is then disassembled, and all the IP packets are sent to their respective destinations.

In circuit-switched networks, the path is only considered to be complete after the initiating station has received positive acknowledgement, and no data can be sent before it happens. The delay between request and acknowledgement is of little consequence if the average length of connection is much greater than the required set-up time. Optical bursts, while larger than packets, are still relatively small, and waiting for a positive acknowledgement tends to be inefficient. Therefore, other switching protocols had to be developed.

There have been many different OBS schemes proposed in the literature but the two main categories are those implemented as fast reconfigurable 'packetised' OCS and those implemented with node-by-node routing where the route to the next node is decided at each individual node. The latter scheme is similar to optical packet switching but with large aggregated packets.

The fast OCS schemes can be further broken down into schemes with two way reservation protocols such as tell-and-wait (TAW) [50] which wait for an acknowledgement before sending the burst, and schemes with one-way reservation such as tell-and-go (TAG) which send the burst regardless of whether the network is ready for it or not, thereby reducing

latency but increasing blocking or contention probability. Common TAG signalling schemes include just-in-time (JIT) [51] or just-enough-time (JET) [52] Control signals are sent on a separate wavelength ahead of the burst in time, to reserve the path between two nodes for the duration of the burst. At each node they are converted to the electrical domain and analyzed in order to make the routing decision. A major advantage of this method of OBS is that optical buffers are not required inside the network.

In contrast, with the routed OBS [53], the latency is controlled and managed at each intermediate node by including optical buffers based on fiber delay lines (FDLs) in the node. This removes the need for pre-computation and estimation of the time it will take the burst to travel through the network and improves scalability. Routed OBS uses optical labels to control the switching and routing of bursts through the network and can work alongside OCS and OPS based on label switching also. This interoperability may prove very beneficial for supporting different services. Optical label switching will be discussed in greater detail in the next section.

3.11 Optical Packet Switching

Optical Packet Switching (OPS) is the forwarding of individual data packets one by one through a network directly in the optical layer [54]. In currently deployed transport networks the finest granularity which can be switched is a wavelength. Sub-wavelength traffic grooming must be performed in the electrical domain using expensive and slow OEO conversions. The main motivation for OPS is to allow more efficient use of the huge bandwidth available by switching at the packet level in the optical domain. It is also envisaged that optical packet switching may offer vastly reduced footprint and power consumption over electrical packet switching [55].

While research in the area has been going on for a number of years, and testbeds and demonstrators have emerged, the technology is far from being mature enough for commercial deployment. Many major technological obstacles must be overcome including the development of very high speed (nanosecond) switching fabrics, optical buffers, wavelength conversion and 3R regeneration, header recognition and optical clock recovery. Current systems generally combine optical and electrical technologies, with most of the switching and transport being performed optically and the control and processing being performed electrically.

3.11.1 Optical Label Switching

In order to enable OPS given the technology which is currently available, Optical Label Switching (OLS) has been proposed [56,57]. Fast, accurate header processing is a fundamental requirement of any packet switching network. While header processing in the optical domain is an active topic of research [58,59] it is still in its infancy. Indeed, as line rates continue to rise, traditional header processing[1] even in the electrical domain is becoming increasingly difficult. OLS separates the data from the routing information, thereby giving transparency to payload data rate, protocol and modulation format. Because the label, which contains the routing information, is much smaller than the payload it can be transmitted at a slower data rate and processed using simpler electronics whilst still arriving within the same time slot.

OLS Network Architecture

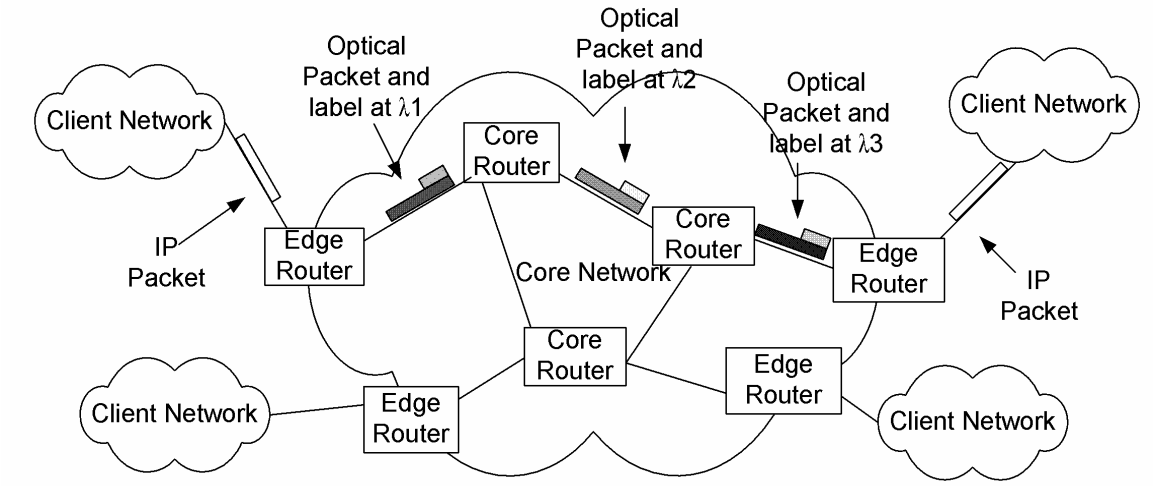

Fig. 3.10:The network architecture of an optical label switched network.

The basic network architecture of a label switched network is shown in Fig. 3.10. The routing information is extracted from the packet header at the ingress edge router and placed in a label that is separated from the payload. The payload remains in optical format throughout the network while the label is processed electronically at each node and used for routing. Labels can also be swapped at intermediate nodes, allowing their contents to be updated with locally significant information such as time to live (TTL) [60]. While label

[1] In which the header is transmitted at the same data rate as the payload and sits ahead of the payload in the time domain

swapping adds to the cost and complexity of each node, it allows for better network scalability [57].

OLS Node Architecture

A generic OLS node architecture is shown in Fig. 3.11. A number of input fibers each carrying optical packets on various wavelengths are demultiplexed into separate wavelengths and sent to the input interface, where the label information is extracted and sent to the switch controller. The switch controller analyses the label information, and adjusts the switch fabric as necessary to route the packet (which may involve buffering or wavelength conversion to avoid contention). If label swapping is used a new label is computed and passed to the output interface where it is attached to the payload. Packets on individual wavelengths are then re-multiplexed onto an output fiber and forwarded to the next node.

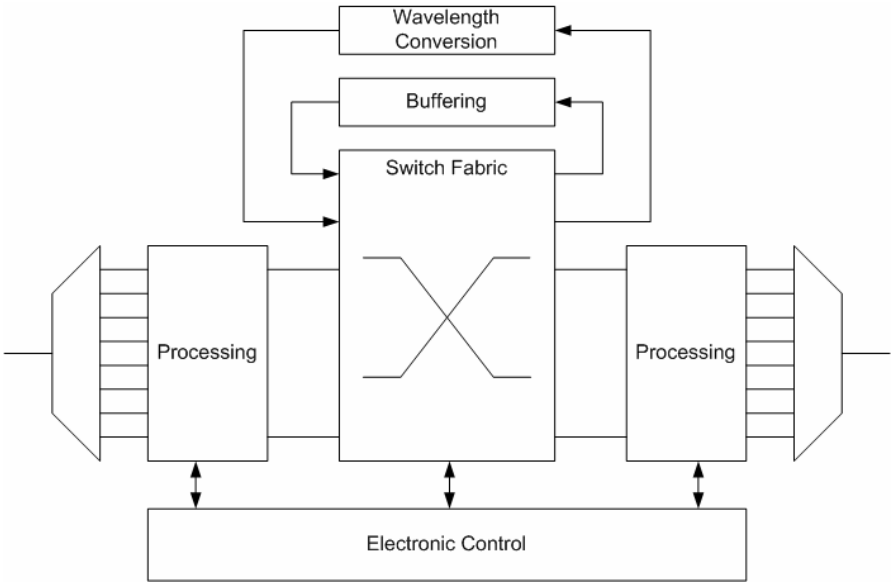

Fig. 3.11:A generic optical packet switching node architecture

Label Coding

The three most widely studied label coding techniques reported in the literature are bit-serial, subcarrier multiplexed and orthogonal [61]. Other techniques include WDM labelling and optical code division multiplexed (OCDM) labelling with the latter receiving a lot of interest in recent years. Fig. 3.12 shows a basic representation of the three main coding techniques and brief descriptions are given below. The labelling techniques will be discussed in greater detail in Chapter 6 and because sub-carrier labelling is the method employed in the OPS section of this work it will receive the greatest attention

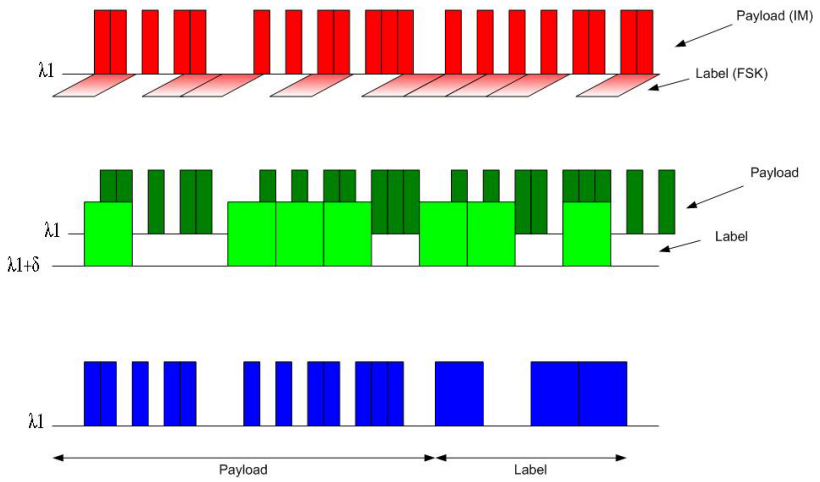

Fig. 3.12:Common Optical Label Coding Techniques

Bit serial labelling: In this technique the label is placed ahead of the payload in the time domain and on the same wavelength with guard bands in between [62, 63]. While this method is free from crosstalk between the payload and label which the other two methods suffer from, the main disadvantage associated with it is the strict timing required.

Subcarrier Multiplexed labelling: Here, the label data is modulated onto an RF sub-carrier, which is then combined with the optical carrier either optically [64], electro optically [65] or electrically [66, 67]. Simplicity and the lack of tight timing requirements are the main advantages of SCM labelling, while crosstalk, reduced spectral efficiency and dispersion induced fading are the major demerits.

Orthogonal labelling: The payload and label data are modulated onto different dimensions of the optical carrier in this method. For example the payload could be modulated onto the intensity of the light while the label is modulated onto the frequency or phase [68]. Like SCM labelling, crosstalk between label and payload is an issue and the receiver required is more complicated than that of SCM. However, the channel bandwidth remains the same even after the label is added giving better spectral efficiency.

3.11.2 Technology to Enable Optical Packet Switching

In this section some of the technologies which will be required to enable optical packet switching to be commercially realised are discussed.

Optical Buffering

Buffering is a vital function in a packet switching node. A fixed length buffer is required to store the data while the header information is read. Variable length buffers are required in switches to store data if resources are not available to serve them immediately. In electronic switches, the buffers may be in the form of Random Access Memory (RAM) which is useful because it can store information indefinitely and the information can be called on at any time. In the optical domain, however, this luxury is not available due to the fact that light cannot be stopped and stored. Instead it must be delayed by a certain amount of time. Fiber Delay Lines (FDLs) are the most widely used optical buffering technique at the moment. In general, groups of FDLs with different lengths are used to create variable delay lines [69] as shown in Fig. 3.13. Slow light waveguides are a possible alternative to FDLs. These devices can reduce the speed of light to a fraction of its usual speed [70]. Both methods are bulky and impractical as a direct replacement for current sized electronic buffers however recent work suggests that buffer sizes can be significantly reduced without impacting network throughput [71].

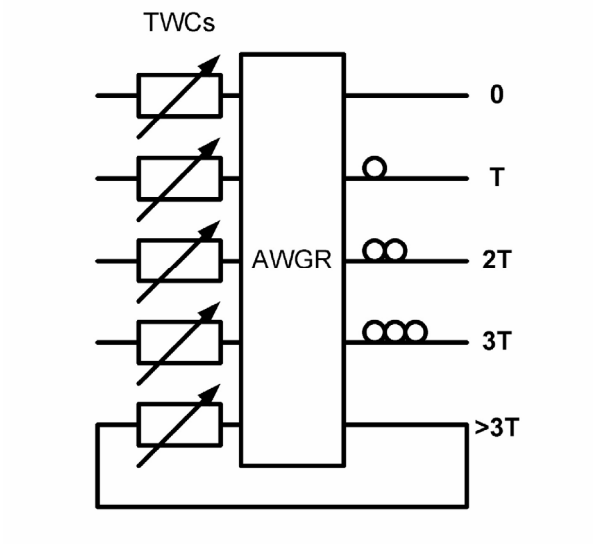

Fig. 3.13:Fiber delay lines used to create variable length optical buffer; the arrayed waveguide grating router (AWGR) routes the packet to the appropriate delay line depending on the wavelength of the packet which is set by the tunable wavelength converters (TWCs)

Fast Switching

As mentioned previously, switch fabrics for optical packet switching must have switching times of the order of a few nanoseconds. They also must be easily scalable and display

uniform operation over all channels. Most of the currently available switches are based on technologies such as MEMS, TO switching and AO switching. They have tuning speeds in the millisecond or microseconds range and are not suitable for packet switching [14]. Considerable research work is being done on SOA switching and electro-optic Lithium Nibate switching and these technologies may prove to be the basis of the first commercial optical packet switches. The interested reader is referred to [72] for more detail on these switching technologies. Another option to using a space switch is to use a passive routing device such as an AWGR [73] in conjunction with fast tunable wavelength converters based on fast tunable lasers to correctly route the packet. This method has been used in a number of projects including STOLAS [74], OPERA [65], WASPNET [75].

Header Recognition

As mentioned previously, line rates are continuing to rise and currently the routing information is transmitted separately in a slower data rate label which can be processed using electronics. However optical header recognition is still very desirable in the quest for an all optical packet switch. Most current research efforts are based on autocorrelation which is used to match streams of pulses which make up key words corresponding to output ports or destination nodes [76, 77]

Packet Delineation and Synchronization

Each packet will arrive at the OPS node at a slightly different time, due to path length differences throughout the network, dispersion, and jitter. The node must be able to determine the beginning and end of a packet so packet delineation is required. This involves locking the phase of the incoming signal at the bit level with the local clock [78,79], a process that must be completed within a few bit slots. In addition, in synchronous networks, where switching is only performed at the start of a slot, tunable delays similar to that shown in Fig. 3.13 are required to align packets with slots.

Wavelength Conversion

Wavelength conversion has an important role to play, not just in OPS but in WDM networks in general by offering improved transparency and reducing the number of optoelectronic conversions [80]. In OPS networks wavelength converters will be used in contention resolution schemes [81], in passive routing using AWGRs [82], and in signal regeneration [83]. Much research work is ongoing in this area and the three main

technologies being looked at are Cross Phase Modulation (XPM) and Cross Gain Modulation (XGM) in SOAs and Four Wave Mixing (FWM) [80,84]. Wavelength converters can be made tunable by using a tunable laser as the pump source.

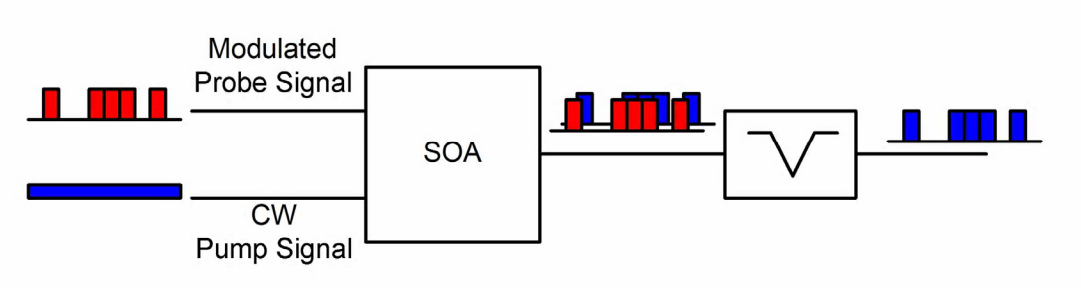

Fig. 3.14:Semiconductor Optical Amplifier based wavelength conversion

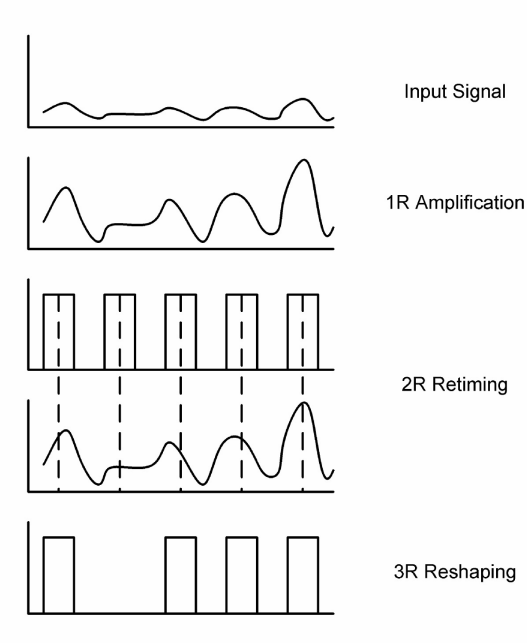

Fig. 3.15:3R Regeneration; amplifying, retiming and reshaping

3R Regeneration

As with wavelength conversion, optical 3R regeneration will prove beneficial in all transparent optical networks, not just packet switching systems. As optical signals travel in fiber they can be affected by a number of different factors such as dispersion, attenuation, interference from other channels, noise etc. These detrimental effects cause serious distortion of the signal which must be repaired at each node. 3R regeneration of a signal includes amplification, re-shaping and re-timing and is illustrated in Fig. 3.15. Currently 3R

regeneration is performed in the electrical domain with expensive OEO conversions required for each channel. SOA based MZIs have been used to demonstrate optical 3R regeneration but the technology is not yet mature [85].

3.12 Conclusion

This chapter reviewed a number of optical switching techniques and discussed the components and technologies required to enable them. In the remaining chapters, experimental work in the areas of OCS and OPS will be covered in detail. Chapter 4 will discuss work carried out at which focuses on issues relating to slow reconfiguration, typical of OCS. In Chapter 5, experimental work carried out on one of the primary enabling technologies for OPS, namely the Fast Tunable Laser (FTL) will be detailed, while Chapter 6 describes experiments which analyze a particular OPS transmitter built using FTLs, which was designed within the confines of this work.

References

[1] O. Leclerc, B. Lavigne, D. Chiaroni, E. Desuivre, "All Optical Regeneration: Principles and WDM Implementation" in *Optical Fibre Telecommunications IVA,* (I. Kaminov, T. Li., eds), San Diego, Academic Press, 2002, pp 732 – 783.

[2] Shoa-Kai Liu, "Challenges of all-optical network evolution," *Lasers and Electro-Optics Society Annual Meeting, 1998. LEOS '98. IEEE* , vol.1, no., pp.182-183 vol.1, 1-4 Dec 1998

[3] O. Leclerc, "Towards transparent optical networks: still some challenges ahead," *Lasers and Electro-Optics Society, 2005. LEOS 2005. The 18th Annual Meeting of the IEEE* , vol., no., pp. 418-419, 22-28 Oct. 2005

[4] J. Strand, "Optical Network Architecture Evolution" in *Optical Fibre Telecommunications IVB,* (I. Kaminov, T. Li., eds), San Diego, Academic Press, 2002, pp 57 – 153.

[5] O. Turkcu, S. Subramaniam, "Blocking in Reconfigurable Optical Networks," *INFOCOM 2007. 26th IEEE International Conference on Computer Communications. IEEE* , vol., no., pp.188-196, 6-12 May 2007

[6] M. O'Mahony, "Future Optical Networks" in *Optical Fibre Telecommunications VB,* (I. Kaminov, T. Li., A. Willner eds), San Diego, Academic Press, 2008, pp 611 – 640.

[7] M. Feuer, D. Kilper, S. Woodward, "ROADMs and their system applications" in *Optical Fibre Telecommunications VB,* (I. Kaminov, T. Li., A. Willner eds), San Diego, Academic Press, 2008, pp 293 – 343.

[8] F. Smyth, B. Roycroft, B. Corbett, P. Lambkin, and L. P. Barry, "Fast wavelength switching lasers using two-section slotted Fabry-Pérot structures," ***IEEE Photon. Technol. Lett.***, vol. 18, no. 20, pp. 2105–2107, Oct. 2006.

[9] J.E. Simsarian, et al, "Less than 5-ns Wavelength Switching with an SG-DBR Laser", IEEE Photonics Technology Letters, vol 18, pp 565-567, Feb 2006.

[10] D. Cavendish, "Evolution of optical transport technologies: from SONET/SDH to WDM," *Communications Magazine, IEEE* , vol.38, no.6, pp.164-172, Jun 2000

[11] J-F. Labourdette, E. Bouillet, C. Olszewski, "Operational Aspects of Mesh Networking in WDM Optical Netwoks" in *Emerging Optical Network Technologies: Architectures, Protocols and Performance,* (K.M Sivalingam, S. Subramaniam, eds), New York, Spring Science & Business Media, 2005, pp 219 – 241.

[12] S. Chandrasekhar, D. Kilper, "Using testbeds for optically-transparent mesh network experimentation" Lasers & Electro-Optics Society, IEEE Oct. 2006 Page(s):771 – 772

[13] T. S. El-Bawab, *Optical Switching,,* New York, Springer Science and Business Media, 2006, pp 333 – 379

[14] Ma Xiaohua, Kuo Geng-Sheng, "Optical switching technology comparison: optical MEMS vs. other technologies," *Communications Magazine, IEEE* , vol.41, no.11, pp. S16-S23, Nov. 2003

[15] R.A Jensen, "Comparison of optical switching technologies for intelligent optical networks," *Lasers and Electro-Optics Society, 2001. LEOS 2001. The 14th Annual Meeting of the IEEE* , vol.1, no., pp.230-231 vol.1, 2001

[16] R.S Weis, T.K Gaylord, "Lithium Niobate: Summary of Physical Properties and Crystal Structure," *Appl. Physics A.*, Vol. 37, No. 4, pp. 191-203, 1985.

[17] I. Bennion, L. Thylen, N. F. Whitehead, "Electro-optic switching systems," *Communications, 1990. ICC '90, Including Supercomm Technical Sessions. SUPERCOMM/ICC '90. Conference Record., IEEE International Conference on* , vol., no., pp.1130-1134 vol.3, 16-19 Apr 1990

[18] T. Kato, T. Shimizu, T. Tamanuki, "Hybrid-integrated SOAG array module for photonic packet switching application," *Lasers and Electro-Optics Society, 2001. LEOS 2001. The 14th Annual Meeting of the IEEE* , vol.2, no., pp.847-848 vol.2, 2001

[19] A. Yariv, P. Yeh, "Optical Waves in Crystals", John Wiley and Sons, 1984

[20] W.J. Tomlinson, R.E. Wagner, A.R Strnad, F. A. Dunn, F.A., "Multiposition optical-fibre switch," *Electronics Letters* , vol.15, no.6, pp.192-194, March 15 1979

[21] S. Hengstler, J.J. Uebbing, P. McGuire, "Laser-activated optical bubble switch element," *Optical MEMS, 2003 IEEE/LEOS International Conference on* , vol., no., pp. 117-118, 18-21 Aug. 2003

[22] A.V. Uskov, E.P. O'Reilly, R.J. Manning, R.P. Webb, D. Cotter; M. Laemmlin, N.N. Ledentsov, D. Bimberg, "On ultrafast optical switching based on quantum-dot semiconductor optical amplifiers in nonlinear interferometers," *Photonics Technology Letters, IEEE* , vol.16, no.5, pp.1265-1267, May 2004

[23] I. White, R. Penty, M. Webster, Yew Jun Chai, A. Wonfor, S. Shahkooh, "Wavelength switching components for future photonic networks," *Communications Magazine, IEEE* , vol.40, no.9, pp. 74-81, Sep 2002

[24] T. S. El-Bawab, "Optical Switching in Communications Networks" in *Optical Switching,* (T. S. El-Bawab, ed), New York, Springer Science and Business Media, 2006, pp 333 – 379

[25] M. Zirnigibl, "Applications for Optical Switch Fabrics" in *Optical Fibre Telecommunications IVA,* (I. Kaminov, T. Li., eds), San Diego, Academic Press, 2002, pp 374 – 404.

[26] D. Saha, B. Rajagopalan, G. Bernstein. "'The Optical Network Control Plane: State of the Standards and Deployment". *IEEE Communications Magazine*, Vol. 41, Issue: 8 , Aug. 2003

[27] "Architecture for the automatically switched optical network (ASON)". ITU-T Rec. G.8080.

[28] N. Larkin. "ASON AND GMPLS – The battle of the optical control plane". White paper, Data Connection, July 2004

[29] E. Mannie *et al.* "Generalized Multi-Protocol Label Switching (GMPLS) Architecture". IETF RFC 3945, Oct 2004

[30] E. Rosen *et al.* "Multiprotocol Label Switching Architecture". IETF RFC 3031, Jan 2001

[31] L. Berger *et al.* Generalized Multi-Protocol Label Switching (GMPLS) Signaling Resource ReserVation Protocol-Traffic Engineering (RSVP-TE) Extensions. *IETF RFC 3473*, Jan 2003.

[32] L. Berger *et al.* "Generalized Multi-Protocol Label Switching (GMPLS) Signaling Constraint-based Routed Label Distribution Protocol (CR-LDP) Extensions". IETF RFC 3472, Jan 2003.

[33] L. Andersson *et al.* "LDP Specification". IETF RFC 3036, Jan 2001

[34] R. Braden *et al.* "Resource ReSerVation Protocol (RSVP)--Version 1 Functional Specification". IETF RFC 2205, Sep 1997.

[35] K. Kompella *et al.* "OSPF Extensions in Support of Generalized Multi-Protocol Label Switching". IETF RFC 4203, Oct 2005.

[36] J. Lang, *et al.* "Link Management Protocol (LMP)". IETF RFC 4204, Oct 2005.

[37] A. Fredette *et al.* "Link Management Protocol (LMP) for Dense Wavelength Division Multiplexing (DWDM) Optical Line Systems". IETF RFC 4209, Oct.2005

[38] J.D. Jones, L. Ong,, M.A. Lazer. "Creating an Intelligent Optical Network Worldwide Interoperability Demonstration". *IEEE Communications Magazine*, Vol. 42, Issue 11, Nov. 2004.

[39] Liu, S. Lily Chen, "Deployment of Carrier-Grade Bandwidth-on-Demand Services over Optical Transport Networks: A Verizon Experience" *Optical Fiber Communication and the National Fiber Optic Engineers Conference, 2007. OFC/NFOEC 2007. Conference on* 25-29 March 2007 Page(s):1 – 8

[40] A. Banerjee, J. Drake, J. P. Lang, B. Turner, K. Kompella, Y. Rekhter, "Generalized multiprotocol label switching: an overview of routing and management enhancements," *Communications Magazine, IEEE* , vol.39, no.1, pp.144-150, Jan 2001

[41] www.polarisnetworks.com/images/PDF/GMPLSWhitePaperComplete.pdf

[42] "Optical Signalling Systems: Who's doing what?" *Light Reading*, Jan 08, 2002

[43] D. Shimazaki, E. Oki, K. Shiomoto, "Multi-layer Traffic Engineering Experimental System in IP Optical Network," *High Performance Switching and Routing, 2007. HPSR '07. Workshop on* , vol., no., pp.1-6, May 30 2007-June 1 2007

[44] S. Ramamurthy, L. Sahasrabuddhe, B. Mukherjee, "Survivable WDM mesh networks," *Lightwave Technology, Journal of* , vol.21, no.4, pp. 870-883, April 2003

[45] D. Elie-Dit-Cosaque, M. Ali, L. Tancevski, "Informed dynamic shared path protection," *Optical Fiber Communication Conference and Exhibit, 2002. OFC 2002* , vol., no., pp. 492-493, 17-22 Mar 2002

[46] G. Mulvihill; M. Ruffini; F. Smyth; L. Barry; L. Doyle; D. O'Mahony, "Optical IP Switching a Solution to Dynamic Lightpath Establishment in Disaggregated Network Architectures," *Transparent Optical Networks, 2006 International Conference on* , vol.3, no., pp.78-81, June 2006

[47] W. Fang, L. Peterson, "Inter-AS traffic patterns and their implications" *Global Telecommunications Conference, GLOBECOM '99* 3, Pages: 1859-1868

[48] V. W. S. Chan, G. Weichenberg, and M. Medard, "Optical Flow Switching," Proceedings of Workshop on Optical Burst Switching (WOBS 2006), San Jose, (Invited Paper) October 2006

[49] C. Qiao, M. Yoo, "Optical burst switching (OBS) – A new paradigm for an optical internet " *Journal of High Speed Networks*, Vol. 8, No. 1, pp 3-16,1999.

[50] M. Duser, P. Bayvel, "Performance of a dynamically wavelength routed optical burst switched network", *IEEE Photon. Technol. Lett.,* 14, 239-241, 2002.

[51] J.Y. Wei, R.I. McFarland, Jr., "Just-in-time signaling for WDM optical burst switching networks," *Lightwave Technology, Journal of* , vol.18, no.12, pp.2019-2037, Dec 2000

[52] Myungsik Yoo; Chunming Qiao, "Just-Enough-Time (JET): a high speed protocol for bursty traffic in optical networks," *Vertical-Cavity Lasers, Technologies for a Global Information Infrastructure, WDM Components Technology, Advanced Semiconductor Lasers and Applications, Gallium Nitride Materials, Processing, and Devi* , vol., no., pp.26-27, 11-15 Aug 1997

[53] S.J.B. Yoo, Hyuek Jae Lee, S. Vaidianathan, K. Okamoto, S. Kamei, "Optical-label switching and routing by rapidly tunable wavelength conversion and uniform loss cyclic frequency array-waveguide grating," *Optical Fiber Communication Conference and Exhibit, 2001. OFC 2001* , vol.3, no., pp. WDD49-1-WDD49-3 vol.3, 2001

[54] "Special Issue on Photonic Packet Switching Systems, Technology and Techniques", Journal of Lightwave Technology, December 1998

[55] S. J. B. Yoo, "Advanced optical components for next-generation photonic networks," Proc. SPIE 5246, 224-234 (2003)

[56] F. Xue, S. J. B. Yoo, "High Capacity Multiservice Optical Label Switching for The Next Generation Internet", IEEE Optical Communications, May 2004

[57] S. J. B Yoo, "Optical Label Switching, MPLS, MPLambdaS and GMPLS". Optical Networks Magazine, May/June 2003, p 17-31

[58] M. C. Cardakli, S. Lee, A. E. Willner, V. Grubsky, D. Starodubov, and J. Feinberg, "Reconfigurable optical packet header recognition and routing using time-to-wavelength mapping and tunable fiber Bragg gratings for correlation decoding," IEEE Photon. Technol. Lett., vol. 12, no. 5, pp. 552–554, May 2000.

[59] Hyun-Do Jung; Monroy, I.T.; Koonen, A.M.J.; Tangdiongga, E., "All-Optical Data Vortex Node Using an MZI-SOA Switch Array," *Photonics Technology Letters, IEEE* , vol.19, no.22, pp.1777-1779, Nov.15, 2007

[60] B. Meagher et al, "Design and implementation of ultra-low latency optical label switching for packet-switched WDM networks". Journal of Lightwave Technology, Vol 18, Iss 12, Dec 2000 pp 1978 – 1987

[61] D.J. Blumenthal, et al "All-optical label swapping networks and technologies", Journal of Lightwave Technology, Vol 18, Iss 12, Dec 2000, pp 2058 – 2075

[62] W. Wang, L. G. Rau, D. J. Blumenthal, "160Gb/s Variable Length Packet/ 10Gb/s Label All Optical Label Switching with Wavelength Conversion and Unicast/Multicast Operation",. Journal of Lightwave Technology, Vol 23, Iss 1, Jan 2005 pp 211 – 218

[63] J. J. V. Olmos, I. T. Monroy, A. M. J. Koonen, "All Optical Label and Payload Separator for a Time-Serial RZ-IM/IM Scheme", IEEE Photonics Technology Letters, vol 18, Iss 3, pp 496-498

[64] T. Dimmick, R. Doshi, R. Rajaduray, D. Blumenthal, "Optically Multiplexed Transmitter for hybrid baseband and subcarrier multiplexed signals". 26th European Conference on Optical Communication, 1996. ECOC '00. Vol 2, 3-7 Sept. 200 pp 155 - 156

[65] A. Carena, M. D. Vaughn, R. Gaudino, M Shell, D. J. Blumenthal, "OPERA: An Optical Packet Experimental Routing Architecture with Label Swapping Capability", Journal of Lightwave Technology, Vol. 16, Iss. 12, pp 2135-2145

[66] S.J.B. Yoo, H. J. Lee, Z. Pan, J. Cao, Y. Zhang, K. Okamoto, S. Kamei, "Rapidly Switching All Optical Packet Routing System with Optical Label Sapping incorporating tunable wavelength conversion and a Uniform Loss cyclic frequency AWGR", IEEE Photonics Technology Letters, vol 13, Iss 6, pp 635-637

[67] Z. Zhu et al, "RF Photonics Signal Processing in Subcarrier Multiplexed Optical-Label Switching Communication Systems", IEEE Journal of Lightwave Technology, vol 21, Iss. 12, pp 3155-3166

[68] T. Koonen, G. Morthier, J. Jennen, H. de Waardt, P. Demeester, "Optical packet routing in IP-over-WDM networks deploying two-level optical labeling" 27th European Conference on Optical Communication, 2001. ECOC '01. Vol 4, 30 Sept - 4 Oct. 2001 pp 608 - 609

[69] H. Yang, S.J.B. Yoo, "All-optical variable buffering strategies and switch fabric architectures for future all-optical data routers" Journal of Lightwave Technology, Vol 23, Iss 10, Oct. 2005 pp 3321 – 3330

[70] R.S. Tucker, P.-C.Ku, C.J. Chang-Hasnain, "Slow-Light Optical Buffers: Capabilities and Fundamental Limitations", Journal of Lightwave Technology, Vol 23, Iss 12, Dec. 2005 pp 4046 - 4066

[71] N. Beheshti, Y. Ganjali, R. Rajaduray, D. Blumenthal, N. McKeown, "Buffer sizing in all-optical packet switches" Optical Fiber Communication Conference 2006, OFC 2006 and the 2006 National Fiber Optic Engineers Conference 5-10 March 2006

[72] G.I. Papadimitriou, C. Papazoglou, A.S. Pomportsis, "Optical switching: switch fabrics, techniques, and architectures" Journal of Lightwave Technology, Vol 21, Iss 2, Feb. 2003 pp 384 – 405

[73] M.C. Chia, et al "Packet loss and delay performance of feedback and feed-forward arrayed-waveguide gratings-based optical packet switches with WDM inputs-outputs" Journal of Lightwave Technology, Vol 19, Iss 9, Sept. 2001 pp 1241 – 1254

[74] K.G. Vlachos, I.T. Monroy, A.M.J Koonen, C. Peucheret, P. Jeppesen, "STOLAS: switching technologies for optically labeled signals" IEEE Communications Magazine, Vol 41, Iss 11, Nov. 2003 pp S9 – 15

[75] D.K. Hunter, *et al* "WASPNET: a wavelength switched packet network," *Communications Magazine, IEEE* , vol.37, no.3, pp.120-129, Mar 1999

[76] H.J.S. Dorren, et al "Optical packet switching and buffering by using all-optical signal processing methods", Journal of Lightwave Technology, Vol 21, Iss 1, Jan 2003 pp. 2-12

[77] J. M. Martinez, J. Herrera, F. Ramos, J. Marti, "All-Optical Address Recognition Scheme for Label Swapping Networks". IEEE Photonics Technology Letters, vol 18, Iss 1, pp 151-153

[78] L. Zucchelli, M. Burzio, P. Gambini, "For optical packet delineation and in optical packet switched networks" 22nd European Conference on Optical Communication, 1996. ECOC '96. Vol 3, 15-19 Sept. 1996 pp 301 - 304

[79] C. Guillemot, et al "Optical packet switch demonstrator assessment: packet delineation and fast wavelength routing" 23rd European Conference on Optical Fibre Communications, Vol 3, 22-25 Sept. 1997 pp 343 - 346

[80] J.M.H. Elmirghani, H.T. Mouftah, "All-optical wavelength conversion: technologies and applications in DWDM networks", IEEE Communications Magazine, Vol 38, Iss 3, Mar 2000 pp 86 – 92

[81] S. Rangarajan, Zhaoyang Hu; L. Rau, D.J. Blumenthal, "All-optical contention resolution with wavelength conversion for asynchronous variable-length 40 Gb/s optical packets, IEEE Photonics Technology Letters, Vol 16, Iss 2, Feb. 2004 pp 689 – 691

[82] D. Klonidis, C.T. Politi, R. Nejabati, M.J.O'Mahony, D. Simeonidou, "OPSnet: design and demonstration of an asynchronous high-speed optical packet switch" Journal of Lightwave Technology, Vol 23, Iss 10, Oct. 2005 pp 2914 – 2925

[83] S. Hojfeldt, S. Bischoff, J. Mork, "All-optical wavelength conversion and signal regeneration using an electroabsorption modulator", Journal of Lightwave Technology, Vol 18, Iss 8, Aug. 2000 pp 1121 – 1127

[84] D. Nesset, T. Kelly, D. Marcenac, "All-optical wavelength conversion using SOA nonlinearities" IEEE Communications Magazine, Vol 36, Iss 12, Dec. 1998 pp 56 – 61

[85] M. Funabashi, Zuqing Zhu; Zhong Pan; S.J.B Yoo, L. Paraschis, "All-optical 3R regeneration in monolithic SOA-MZI to achieve 0.4 million km fiber transmission" 18th Annual Meeting of the IEEE Lasers and Electro-Optics Society, 2005. LEOS 2005. 23-27 Oct. 2005 pp 137 – 138

Chapter 4 – The Performance Impact of Reconfiguration in Optical Circuit Switched Networks

This chapter describes experimental work which was carried out to examine the performance impact of channel reconfiguration in a long-haul transparent optical network on slow timescales typical of Optical Circuit Switching (OCS). A circulating loop was employed to enable long haul transmission experiments and Section 4.1 describes the long haul system which was being represented with the experiment. The next 3 sections present important background information that assist in the understanding of the experiment. Optical amplification in long haul networks is often performed using Erbium Doped Fiber Amplifiers (EDFAs). These optical amplifiers have a wavelength dependent gain profile which varies with the loading conditions. The gain dynamics and their effect on performance is the focus of section 4.2. The transmission impairments encountered in long haul networks are the subject of section 4.3. Circulating loops are the subject of section 4.4 and then Section 4.5 and 4.6 describe the experiment which was performed and the results of the experiment, respectively. The final section is a discussion of what insights can be gained from the results obtained. The motivation behind the work described in this chapter was to stimulate further study of the effects of gain error in reconfigurable networks, an important issue for the realisation of automatically self-reconfiguring networks.

4.1 Reconfiguration in long-haul transparent networks

As discussed in the previous chapter, the reconfiguration of channels in transparent optical networks adds flexibility to the network by allowing wavelength re-routing for network applications such as dynamic bandwidth allocation and dynamic restoration. Key hardware required for automatic reconfiguration of channels, such as Reconfigurable Optical Add/Drop Multiplexers (ROADMs) and Optical Cross Connects (OXCs), has been deployed [1], however as yet, reconfiguration remains primarily a human-driven task albeit one that can now be carried out from a single central location. The new reconfigurable hardware allows the provisioning of wavelengths for example, to be carried out without

visiting each individual site on the path, significantly decreasing the associated time and cost. However, to fully exploit OCS networks, human-intervention must be minimized leaving a fully automated network that creates or reconfigures lightpaths when required, re-optimizes itself for each new configuration and tears down optical circuits that are no longer required. This full automation remains a significant challenge. An example of channel reconfiguration is illustrated in Fig. 4.1.

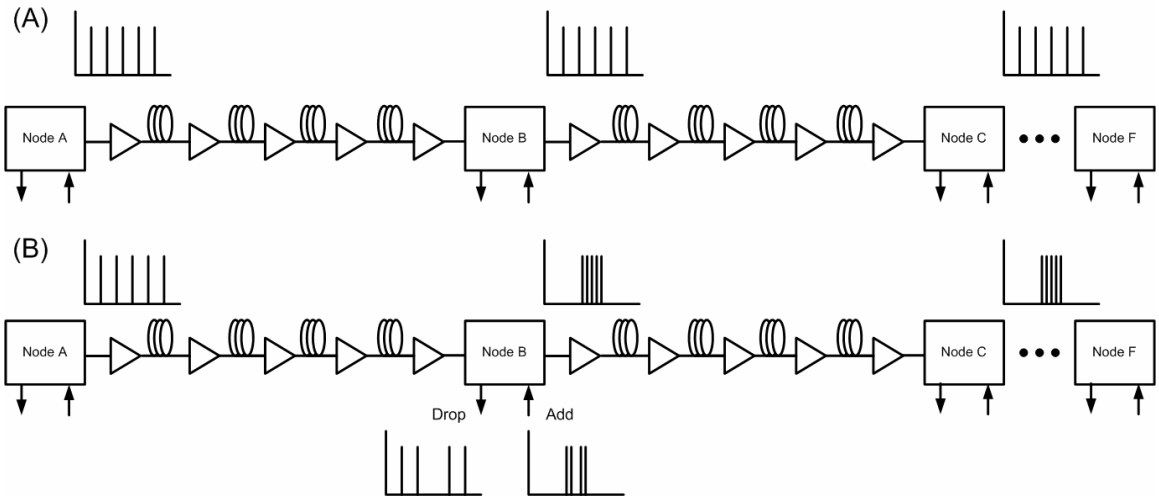

Fig. 4.1: Example of channel reconfiguration in a long-haul OCS network, showing the scenario before (A) and after (B) the reconfiguration event

Six nodes, labelled A to F constitute a point to point section of a network. Each node is separated by four 80 km spans with EDFAs to overcome the span losses. Prior to a reconfiguration request, five Wavelength Division Multiplexed (WDM) lightpaths are in place between Node A and Node F. At a certain point in time it is decided that it would be beneficial if four of these lightpaths were dropped at Node B and four new lightpaths added, and the ROADM switches are reconfigured to make it so, resulting in the spread configuration from node B to node F becoming a banded configuration. Indeed, the reconfiguration scenario illustrated is very similar to that being represented with the experiment detailed in a later section of this chapter. The system is reconfigured from a uniformly spread configuration to a number of waveband configurations and the transmission performance is measured as the system is re-optimized for this new configuration.

As will be discussed in the following section, the new loading conditions change the gain characteristics of the EDFAs. Hence, after reconfiguration takes place, the network must be re-optimized for its new channel configuration to prevent power divergence errors. In this work the re-optimization is considered to be a three-phase process as depicted in Fig. 4.2.

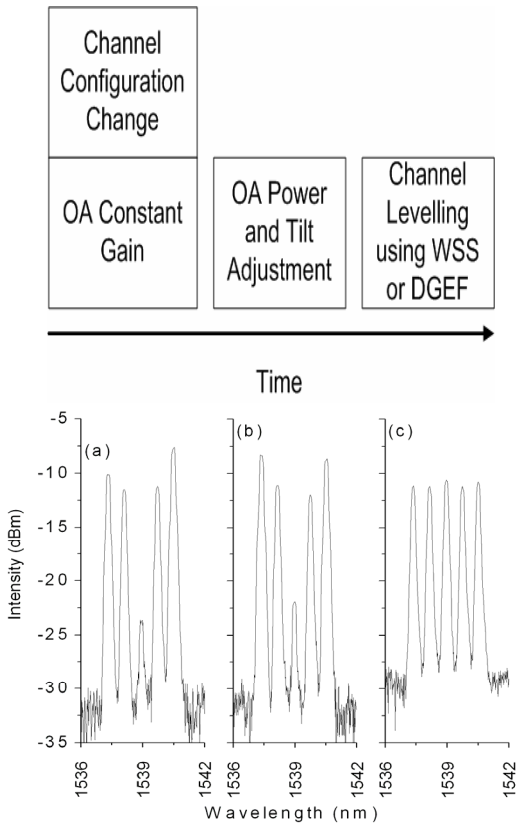

Fig. 4.2: (top) The three phases of optimization after channel reconfiguration; and (bottom) spectrum of one configuration corresponding to each optimization phase.

Phase 1. Immediately following a channel reconfiguration the fast control circuits of the EDFAs automatically adjust the pumps in order to maintain constant gain and reduce transient gain excursions. It should be noted that some transients may still occur prior to settling but because the effects are on very fast timescales (~microsecond) they are not considered here. This work focuses on the steady-state scenario.

Phase 2. While the constant gain operation serves to reduce gain transients, it can also cause EDFAs to deviate from their designed operating powers. The second phase occurs on a slower timescale than phase 1 and consists of adjustments to the EDFA

pumps and Variable Optical Attenuators (VOAs) in order to return to the designed operating output power and spectral tilt.

Phase 3. The third phase is a fine tuning phase in which residual gain ripple is levelled out using per channel VOAs or a dynamic Gain Equalization Filter (GEF).

The spectra in Fig. 4.2 show the effect of these optimization stages.

4.2 EDFAs in long haul networks

To assist with the description of EDFA gain dynamics and their effect on a long haul system, Fig. 4.3 depicts a schematic of a typical EDFA which may be used in a long haul network.

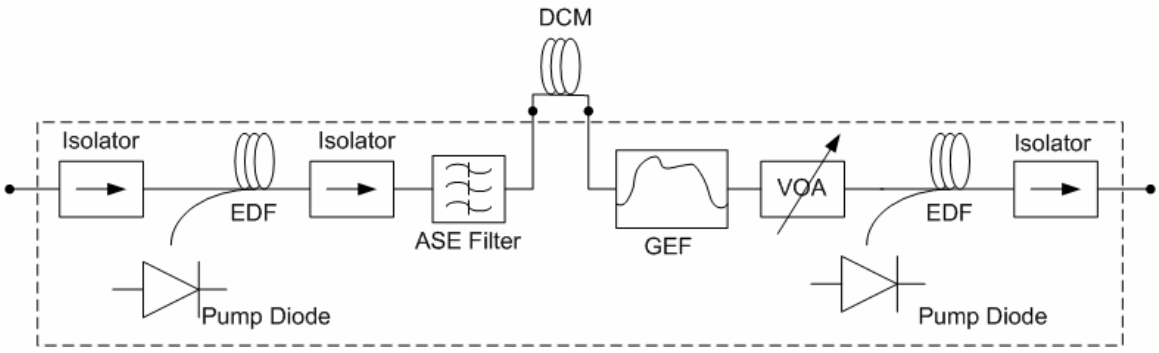

Fig. 4.3: Typical two-stage EDFA schematic incorporating two erbium doped fiber (EDF) gain stages, and an ASE Filter, external dispersion compensation module (DCM), gain equalization filter (GEF) and variable optical attenuator (VOA).

EDFAs have evolved from single gain blocks to multi-stage amplification sub-systems with many elements providing added functionality between the stages such as Dispersion Compensation Modules (DCMs), VOAs for gain tilt adjustment, filters to remove Amplified Spontaneous Emission (ASE) added in the first stage, and GEFs to flatten the gain profile of the EDFA. The mid-stage placement of these components reduces the Optical Signal to Noise Ratio (OSNR) impact that they would have if placed outside the amplifier. In addition, because they are passive components, they do not impact the noise figure. In general the input stage is operated with high gain and the output stage is operated in saturation with high output power. The overall noise figure is decided mainly by the input stage as can be seen from the following equation [2]:

$$NF = NF_1 + \frac{NF_2}{L_{MID} G_1} \tag{4.1}$$

where NF_1 and NF_2 are the noise figure of the first and second stage, respectively, L_{MID} is the mid-stage loss and G_1 is the gain of the first stage.

4.2.1 EDFA Noise and OSNR

The OSNR determines the reach of an optically amplified long haul system. A regularly used performance metric for long haul systems is the 'required OSNR'; a measurement of the minimum OSNR at which a certain Bit Error Rate (BER) can be achieved. In this work a BER of $1x10^{-3}$ was used for required OSNR measurements as this can be corrected to an error rate of $1x10^{-12}$ or better using Forward Error Correction (FEC). In WDM systems, the best case OSNR is set by the amount of ASE generated by the EDFAs in the path. OSNR penalties can then be introduced by many factors, including but not limited to, linear crosstalk, polarization effects, non-linear crosstalk, and dispersion. These impairments, which must be factored into the OSNR budget during system design, will be the topic of Section 4.3. In a reconfigurable mesh network this task becomes much more arduous given that signals can be routed to a particular destination via a number of paths.

ASE is the most severe limiter of reach in long haul systems. Its generation is an inevitable consequence of optical amplification that results in signal-spontaneous beat noise at the receiver and it represents the fundamental noise limit of the system. Each EDFA contributes ASE according to Equation 3.1, and the contributions along a chain of EDFAs add cumulatively.

$$P_{ASE} = 2h\nu \cdot \Delta\nu \cdot n_{sp}(G-1) \tag{4.2}$$

where P_{ASE} is the ASE power in an optical bandwidth $\Delta\nu$, h is Planck's constant, ν is the optical frequency, n_{sp} is the spontaneous emission factor and G is the gain of the EDFA.

The OSNR is defined as the ratio of optical signal channel power to the power of the ASE in a given bandwidth (usually 0.1nm). When designing the system, the target OSNR at the receiver must be sufficiently high, so as to give the required system performance, and must include sufficient margin to allow for any impairments which may be encountered.

For a chain of EDFAs the OSNR at the end of the chain is given by the following equation:

$$OSNR(dB) = 58 + P_{out} - L_{span} - NF - 10\log_{10}(N_{amp}) \tag{4.3}$$

where P_{out} is the channel output power of the EDFA, L_{span} is the loss through each span, NF is the noise figure of the EDFAs and N_{amp} is the number of amplifiers. While this equation is rarely accurate in practical networks because neither fiber spans nor EDFAs are likely to be uniform across the entire network, it gives a useful indication of some of the constraints due to amplifier noise. For circulating loops that by their very nature exhibit increased uniformity its accuracy improves and it is used later in this chapter to verify that the shape of the measured OSNR as a function of distance in the circulating loop agrees with expectations for a straight line system.

A 3dB increase in OSNR allows the reach to be doubled, and a 1dB increase allows a reach increase of approximately 25%. The equation shows us that a 1dB increase in final OSNR can be obtained by:

(a) increasing the output power by 1dB,

(b) reducing the span loss by 1dB, or by

(c) reducing the noise figure by 1dB.

Due to the logarithm in the final term of the equation, the number of amplifiers is a less important factor than these other terms. Increasing the output power is only viable to a certain extent due to the onset of nonlinearities at high optical powers. The noise figure in a high gain EDFA is limited to values above 3dB and typical values are 5dB with little scope for reduction. The other option is to reduce the span loss and while this is useful and common for underwater systems, limited availability of amplifier sites reduce it's viability for terrestrial applications. Distributed Raman amplification has improved noise characteristics over lumped amplification used in EDFAs and is seen as a promising technology to increase transmission reach.

4.2.2 EDFA gain flatness and the effect on OSNR

Amplifier gain flatness is a critical parameter for WDM networks. Through a chain of EDFAs, the non-uniformity of the gain spectrum accumulates and can lead to a large power divergence between channels in a network. Channels which experience low gain can suffer from OSNR related penalties whilst channels in a high gain region of the spectrum can reach powers above the non-linear threshold which also causes performance degradation. The GEFs used in EDFAs are optimized to flatten the spectrum of a fully loaded EDFA [2].

Under varied loading conditions that may be caused by reconfiguration or failure, the gain uniformity decreases, the GEF becomes less effective, and the gain ripple increases. The entire gain spectrum of an EDFA gets tilted when the average inversion level of the erbium is changed. Gain tilt is another effect with similar ramifications to gain ripple, including power divergence and OSNR penalties. As shown in Fig. 4.3 a VOA is often added to the midstage of the EDFA and this can be used to vary the gain tilt by controlling the average inversion level. Yet another effect, Spectral Hole Burning (SHB) is the result of a small amount of inhomogeneity in the gain spectrum and it causes loading dependent gain reduction around channels or groups of channels [3]. The depth of the gain reduction hole depends on how saturated the gain of the EDFA is, and is also strongly wavelength dependent, with the effect at 1532nm being four times stronger than at 1551nm [4, 5]. The performance penalties caused by each of these gain effects will remain in place until the system is optimized for the new loading configuration. As mentioned, re-optimization involves the adjustment of the amplifier powers and variation of the GEFs.

4.2.3 Transient gain dynamics

EDFAs in long haul networks are generally operated in saturation in order to reduce the amount of ASE generated, and the available gain is shared by all of the channels. If a channel or group of channels is added or dropped accidentally due to failure somewhere in the network, or intentionally due to channel reconfiguration, a transient gain excursion occurs due to the cross saturation effect [6]. The modelling [7], control [8] and effects [9, 10] of these gain transients have been studied by many groups. In early work, the time constant of gain recovery for a single stage EDFA was measured to be between 110 μs and 340μs [11]. Later reports stated that in a two stage EDFA the time constant is in the tens of microseconds range due to the higher saturation factors required in the today's high power EDFAs [12]. When a smaller percentage of channels are dropped, the time constant decreases further and in chains of EDFAs the effect is faster still [13]. If half of the channels are dropped, each EDFAs output power initially drops by 3dB at time t=0. In order to conserve the saturated output power, the gain in all of the amplifiers then begins to grow. This means that at the same time as the output power of the first EDFA is growing, the gain of the second EDFA is also growing and so on down the chain of EDFAs. This cascading effect means that the transient time gets faster and faster as the network size, or number of

amplifiers in a chain increases [14]. Transient effects can cause unacceptable errors in the system due to nonlinearities associated with high power spikes, and power dips at the receiver; they must therefore be minimized using dynamic gain control with a faster response time than the time constant of the transient. A number of channel protection schemes have been devised in order to reduce the effects of transients. Prior to these methods, EDFAs were operated in a constant output power mode such that a power change at the input to the EDFA did not result in a power change at the output. In contrast, these methods attempt to maintain constant gain, such that a proportional reduction in output power accompanies a reduction in input power. The techniques include:

(i) Pump control [15] operating on timescales of microseconds can be employed to limit the power transients on surviving channels. In [16] the authors reduce the power excursions from greater than 6dB to less than 0.5dB using this method. The control circuit acts within 8μs.

(ii) Optical control [17,18] achieves gain stabilization by feeding a portion of the output light back into the input of the EDFA.

(iii) Link control makes use of a control channel that is used for an entire link. It is coupled into the system at a node and decoupled out at the next node. An optical tap in the link monitors the power and this in conjunction with a feedback control circuit adjusts the power of the control channel in order to maintain constant input power for the first amplifier and hence constant power for the entire link.

4.2.4 Steady state gain dynamics

After the transient effects have settled down the EDFAs return to a steady state but there are also dynamic effects associated with the steady state gain due to variations in channel loading. Steady state gain dynamics of EDFAs in reconfigurable networks have received less attention than their transient counterparts, however recently a number of studies have illustrated the importance of gaining an in-depth understanding of the effects and the limitations that they can place on the system. Early work used constant-power controlled EDFAs and noted instabilities associated with particular network configurations and control strategies [19]. The use of Constant Gain Control (CGC) was found to reduce the impact.

More recent work [20] showed that residual steady state gain ripple and tilt can result in significant wavelength dependent gain error. The experimental section of the study focused on channel power and gain control of the steady state effects using per channel power levelling on a much slower time scale (the order of seconds) than the CGC use in the EDFAs to reduce transient effects.

Both transient and steady state responses to channel reconfiguration within cascades of EDFAs were examined in [21]. In contrast to this paper where measurements are taken as channel reconfiguration occurs, in this work, because the focus is on the steady-state effects of the EDFA gain dynamics the measurements are taken after the reconfiguration is complete and a steady state has been reached. A number of different channel configurations are put in place under identical gain conditions and measurements are then performed on each configuration under varying levels of post reconfiguration optimization.

4.3 Transmission Impairments in Long Haul Networks

The transmission impairments which can affect long haul reconfigurable mesh networks such as the one being represented by this experiment will be described in this section.

4.3.1 Dispersion

Dispersion in optical fibers was touched upon in Chapter 2 but this sub-section will discuss dispersion from the point of view of long haul networks. Dispersion causes different wavelengths to travel with different group velocities in fiber, and can result in broadening or narrowing of optical pulses depending on the operating wavelength, dispersion of the fiber and the initial chirp of the signal. In order to keep dispersion-related penalties low, it is necessary to keep dispersion below the dispersion limit, which is the distance after which a pulse has broadened by one bit interval. For an externally modulated Non-Return to Zero (NRZ) signal with a data rate of B, the dispersion limit, L_D is [22]:

$$L_D \approx \frac{10^5}{D \cdot B^2} \tag{4.4}$$

where D is the dispersion in ps/nm.km and B is in Gb/s. For a 10Gb/s signal in Standard Single Mode Fiber (SSMF) this corresponds to approximately 60km. Because noise limits allow much longer distances, it is necessary to compensate for dispersion in the path to maximize the reach.

If nonlinearities played no part then compensating for dispersion would simply require the use of Dispersion Shifted Fiber (DSF) for the entire path, with the required Dispersion Compensation Fiber (DCF) for each channel placed at the end to ensure that wavelengths that are not at the zero dispersion point do not exceed the dispersion limit. In long haul systems however, it is generally desirable to launch into each span of fiber with as much power as possible meaning that nonlinearities do come into effect. In order to maximize performance it is necessary to manage the dispersion, not only at the end of the system but throughout the entire path. The placement and amount of dispersion compensation forms the "dispersion map" and its design is critical to minimize penalties from nonlinearities and hence allow maximum launch power and OSNR [23]. Keeping the *accumulated* dispersion sufficiently low at all points in the system prevents nonlinear phase modulations from being converted into amplitude modulations. On the other hand, if *local* dispersion is too low, strong phase matching between signals and long distances over which wavelengths overlap, can cause certain non-linear effects such as Four Wave Mixing (FWM) to be severe.

Much of the fiber installed today is SSMF which has a dispersion of 0ps/nm.km at 1300nm and approximately 17ps/nm.km at 1550nm. This large dispersion at the EDFA operating wavelength led to the development of DSF which has its dispersion zero at 1550nm. As was mentioned previously however, a small amount of dispersion is beneficial because it spreads pulses out, thereby reducing the peak power and reducing the FWM intermodulations which are most deleterious at high power peaks. Non-Zero Dispersion Shifted Fiber (NZDSF), is the compromise between SSMF and DSF. With a dispersion of 3-8ps/nm.km at 1550nm, it is large enough to reduce FWM but small enough to keep total accumulated dispersion low. Many transmission fiber designs exhibit a large wavelength dependence (dispersion slope), while the slope of DCF is often much flatter. Hence the best dispersion map for the central channel in the band is non-ideal for wavelength channels above or below this wavelength and dispersion "walk-off" can occur. This walk-off is illustrated in Fig. 4.4 which shows the dispersion map for the central channel as a solid line and a higher wavelength channel as a dotted line. In this plot the dispersion for the central channel and higher wavelength channel are 17 and 20ps/nm.km respectively. Because the DCF (placed every 80km) compensates each channel for 17ps/nm.km the higher wavelength channels experiences the walk-off. More recent fiber designs have lowered the wavelength dependence (dispersion slope) making it easier to keep the entire band of channels within the dispersion limit. Walk-off can

also occur due to the fact that dispersion compensation modules (DCMs) are generally available in discrete values and are generally not matched exactly to the spans.

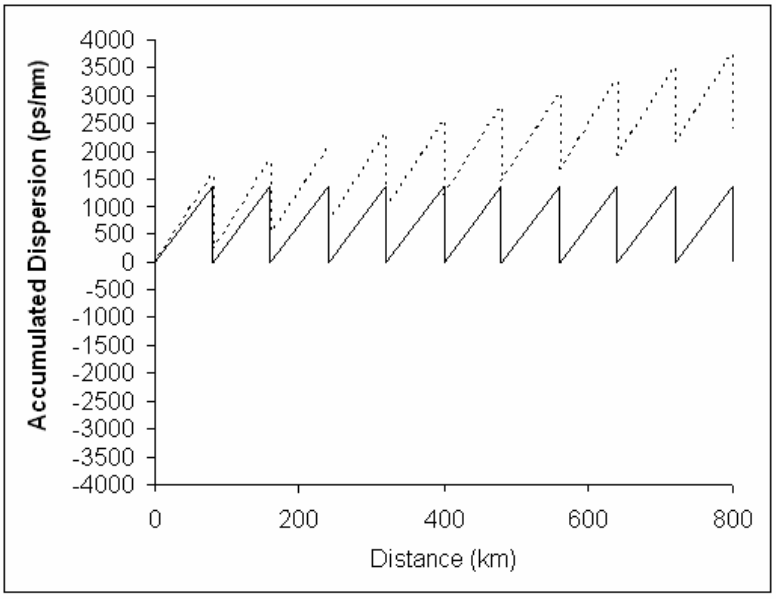

Fig. 4.4: Dispersion map for two channels. The solid line represents the zero-dispersion wavelength and the dotted line represents a higher wavelength. Mismatch between the dispersion slope of the span fiber and the compensating fiber leads to the walk off shown.

Optimized dispersion map design is critical for long haul networks. The use of dispersion pre-compensation and post compensation has been shown to reduce the effects of nonlinearities and improve performance [24]. In mesh networks channels that have travelled various distances and over different fiber plant can be present on the same fiber, making dispersion map design an even greater challenge. The work detailed in this chapter makes use of two dispersion maps which will be described in the experimental section.

4.3.2 Nonlinearities

Nonlinear effects occur in fiber when the response of the fiber is a nonlinear function of the amplitude of the electromagnetic field applied and they can be categorized into two distinct types:

1) Stimulated scattering effects (including Raman and Brillouin scattering) and,

2) Effects arising from the Kerr effect (including Cross-Phase Modulation (XPM), Self-Phase Modulation (SPM) and FWM).

The experimental results described in this chapter show the detrimental effects of nonlinearities on system performance and also demonstrate that careful management of the dispersion in the system can reduce their effects considerably, allowing much higher launch powers and greater transmission distances.

Stimulated Scattering Nonlinearities

Scattering occurs when light passing through a fiber is forced to deviate from its path by non-uniformities in the fiber. The processes of Raman and Brillouin scattering are examples of inelastic scattering in which the frequency of the scattered photon is different to that of the incident photon. In general, the scattered photon is reduced in frequency. The two processes are very similar with the difference being that in Raman scattering the energy difference between the initial photon and the scattered photon is released as an optical phonon while in Brillouin scattering the energy is released as an acoustic phonon.

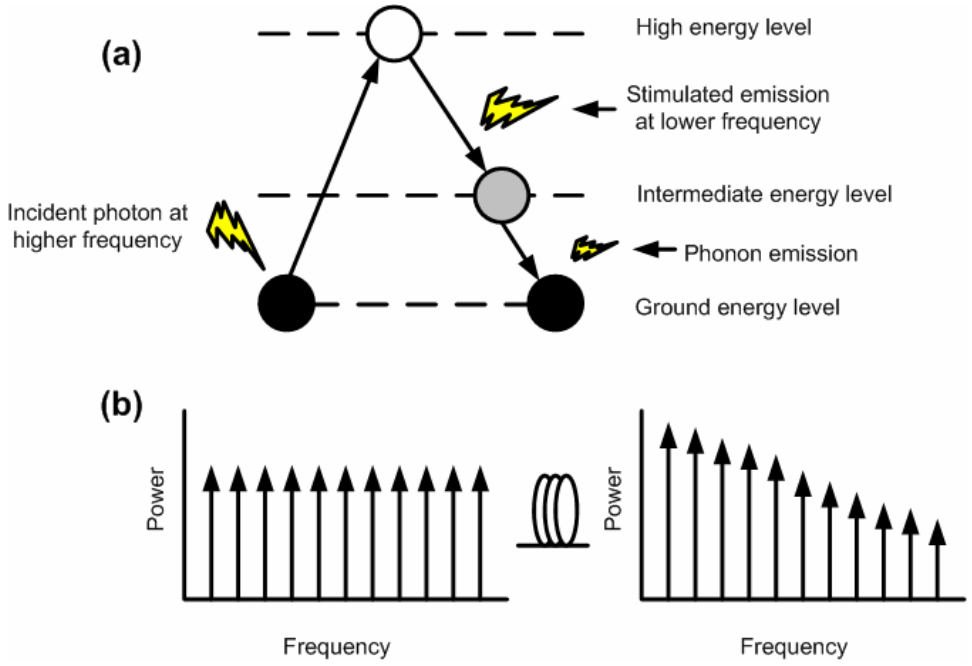

Fig. 4.5: Stimulated scattering (a) and Raman tilt (b)

Stimulated scattering (illustrated in Fig. 4.5(a)) occurs when a photon with high energy is incident on an optical or an acoustic phonon. The phonon is raised to a higher energy level and after a short time drops back down to an intermediate energy level with the release of a photon which is lower in frequency than the initial photon. Eventually the phonon will drop back to the ground state by releasing the remaining energy in the form of an acoustic

phonon for Stimulated Brillouin Scattering (SBS) or in the form of an optical phonon for Stimulated Raman Scattering (SRS).

The main differences in the two effects, caused by the difference in dispersion for optical and acoustic phonons are as follows:

(iv) SBS only occurs in the backward direction while SRS can occur in both directions

(v) The frequency shift is approximately 10GHz for SBS but 13THz for SRS.

(vi) The Brillouin gain spectrum has a very narrow bandwidth (<100MHz) whereas the Raman gain spectrum is of the order of 30THz.

The SBS process results in signal loss in the direction of propagation and distortion in the backwards direction caused by reflections. SBS has the lowest threshold of all the optical nonlinearities [25] and can impact a system at optical channel powers as low as 1mW. However, this is for very narrow light sources and the effects are reduced by using a light source of relatively broad spectral width or through the use of phase shift keying or other modulation schemes.

The use of Raman scattering for amplification was described in Chapter 2. However, Raman scattering can also occur between signal channels, when lower wavelength channels pump (transfer energy to) higher wavelength channels. This leads to wavelength dependent loss and spectral tilt in a WDM system as shown in Fig. 4.5(b). The effect grows in each fiber span so in long haul systems consisting of many spans it is often compensated for, either through the use of per-channel VOAs in the nodes, or by tilting the gain spectrum of the EDFAs using a VOA in the mid-stage section of a two-stage EDFA for example.

Kerr Effect Nonlinearities

The refractive index, n, of silica optical fibers varies with optical power, P, according to the following equation:

$$n = n_0 + n_2 \frac{P}{A_{eff}} \tag{4.5}$$

where n_0 is the refractive index at low powers, A_{eff} is the effective area of the optical mode in the fiber and n_2 is the nonlinear index co-efficient which is typically around 2.6 x 10^{-20} m^2/W in SSMF [26]. The intensity dependence of the refractive index causes an intensity dependent phase shift in the optical field, known as the Kerr effect. The manifestations of the Kerr effect will be described below.

Self phase modulation (SPM)

SPM occurs when the high peak power of an optical signal increases the refractive index of the fiber it is travelling through, thereby reducing its group velocity. The result is a change in the phase of the optical signal and a broadening of its frequency spectrum, which has been caused by the signal's own intensity. The envelope of the optical signal in the time domain does not change due to SPM. However, in any real system dispersion will act on the pulse at the same time as SPM. In the normal dispersion regime pulses will broaden in time while in the anomalous dispersion regime pulse compression is caused and the counteracting effects of SPM. Anomalous broadening can be used to extend the reach of long haul systems which would otherwise be limited by SPM [27]. The combined broadening by SPM and compression by anomalous dispersion can also be used to form optical solitons [28]. SPM is significant when the nonlinear length, L_{NL} (defined as the length of fiber over which nonlinear effects are significant [28]) is less than the dispersion length, L_D (defined as the length of fiber over which an isolated '1' broadens by $\sqrt{2}$). In WDM systems with wider channel spacing SPM is the dominant nonlinear effect however in fiber with high dispersion, pulses broaden rapidly and hence the high peak powers are quickly reduced, causing a reduction of the effects of SPM.

Four Wave Mixing (FWM)

FWM occurs when closely spaced channels at different frequencies beat together causing phase modulation of the signals and giving rise to modulation side bands at new frequencies according to the following equation:

$$f_{FWM} = f_1 + f_2 - f_3 \tag{4.6}$$

The order of the frequencies across the band will then be f_1, f_{FWM}, f_2, f_3. If f_{FWM} lies within the passband of another channel it will be detected as noise at the receiver. FWM is most efficient in systems with low channel spacing and low dispersion. It can be avoided by

designing the system with unequal channel spacing such that generated components lie in unoccupied portions of the spectrum [29]. A more effective technique however is to use transmission fiber with high local dispersion.

Cross Phase Modulation (XPM)

XPM is similar to SPM in that a high intensity optical pulse varies the refractive index of the fiber it is travelling through but for XPM this variation affects overlapping pulses on different channels. In itself the effect of XPM is stronger than that of SPM, however because pulses on different channels will have different group velocities, they will not overlap indefinitely. In addition, differences in polarization between channels will also reduce the effect. The manifestations of XPM are the same as those of SPM, whereby the phase modulations of the pulses result in spectral broadening. Dispersion simultaneously acts to broaden or compress the pulses in the time domain. The strength of the interactions depend largely on the channel spacing, and as with FWM, the effects are reduced by high local chromatic dispersion because walk-off occurs very quickly and high peak powers are also quickly reduced.

4.3.3 Linear crosstalk

Crosstalk occurs whenever optical power is transferred from one channel to another and this results in noise on a signal which can degrade system performance. Crosstalk can occur due to nonlinear effects in optical fibers, but also in perfectly linear channels due to non-ideal optical equipment in the nodes. Linear crosstalk can be broken down into in-band and out-of-band varieties. Out-of band cross talk occurs due to the finite extinction ratios in filters and demultiplexers, which allow a portion of the light from neighbouring channels to fall on the receiver. Generally, this is incoherent and is less of a problem than in-band crosstalk. In-band crosstalk comes about in optical switches, when a portion of the signal which was to be switched, remains in the path. When another optical signal of the same wavelength is then switched onto that path, interference occurs.

In-band and out-of-band crosstalk are illustrated in Fig. 4.6. It is clear that in an OXC for example, consisting of demultiplexers and switches (and possibly cascades of switches), that the crosstalk will build up, causing serious degradation to individual channels. Linear crosstalk was not a significant factor in these experiments because no switching took place. The measurements were carried out on static channel configurations.

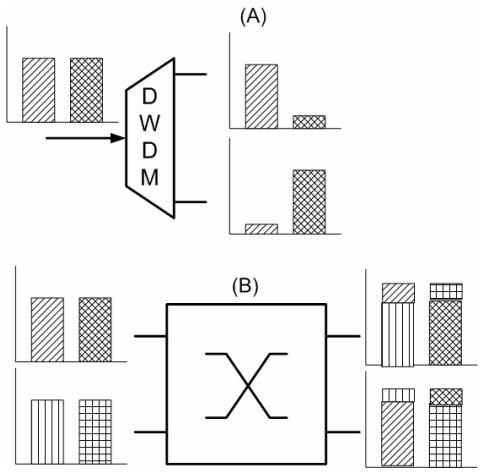

Fig. 4.6: a) Out-of-band crosstalk in a demultiplexer; and b) in-band crosstalk in a switch

4.3.4 Polarization Effects

There are three main polarization effects which come into play in long haul systems, Polarization Dependent Loss (PDL), Polarization Dependent Gain (PDG), and Polarization Mode Dispersion (PMD). PDG is a weak effect which only comes into play in very long chains of amplifiers, the likes of which may be used in trans-oceanic systems and will not be discussed further here. PDL arises from the fact that the components in the system exhibit different insertion loss depending on the polarization of the light incident on them. In a practical system PDL affects the OSNR and must be taken into account in the OSNR budget. It can be kept under control by simply ensuring that low-PDL components are used in the system. In a circulating loop apparatus PDL plays a larger role because light will pass through components with the same PDL many times [30]. A polarization scrambler can be used to reduce this effect and more closely match the PDL performance of a straight-line system.

PMD comes about because the two orthogonal modes in a fiber have different group delays due to manufacturing imperfections or stress. The result is that the different polarizations travel at different speeds through the fibre [31]. PMD is illustrated in Fig. 4.7 with the Differential Group Delay (DGD) being the group-delay difference between the fast and slow modes. When the delays approach a significant percentage of the bit period the data gets distorted and errors occur. Hence, PMD becomes more of a problem at higher bit-rates, especially above 10Gb/s.

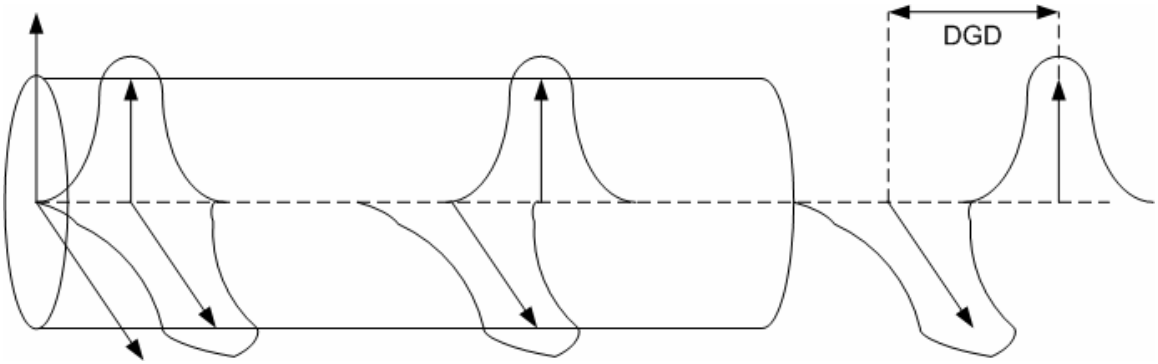

Fig. 4.7: PMD causing the orthogonal axes of a light pulse to experience different group delay.

4.4 Circulating Loops

In the lab, long haul transmission distances can be achieved using a circulating loop [32]. In such a configuration a number of amplified spans are used repeatedly to achieve the transmission characteristics of long haul systems, while using the hardware of only a few spans. A pair of optical switches is generally used to open and close the loop as shown in Fig. 4.8. When the switches are in the load position, data channels are loaded into the loop for a time which approximately equals the time that it takes light to propagate once around the loop. When the switches are in the loop position, they seal the loop allowing the light to circulate the loop components many times. Measurement equipment can be synchronised to the loop switching signal to take measurements corresponding to a certain distance traversed.

Circulating loop experiments to study a reconfigurable mesh network are more complicated than straight line systems as amplifier loads will vary due to groups of channels being added or dropped at intermediate nodes [33]. Traditional circulating loop experiments lacked the flexibility to examine irregular path lengths, fiber types and other transmission characteristics. However, recent works have used novel techniques to increase the flexibility of circulating loops. Multi-loop experiments have been used to vary the fiber type over different transmission segments [34]. In [35], fast optical switches synchronous with the loop are used to switch in different lengths of SSMF and DCF creating a dynamically reconfigurable circulating loop that enables long haul transmission experiments to examine the impact of dispersion map variation.

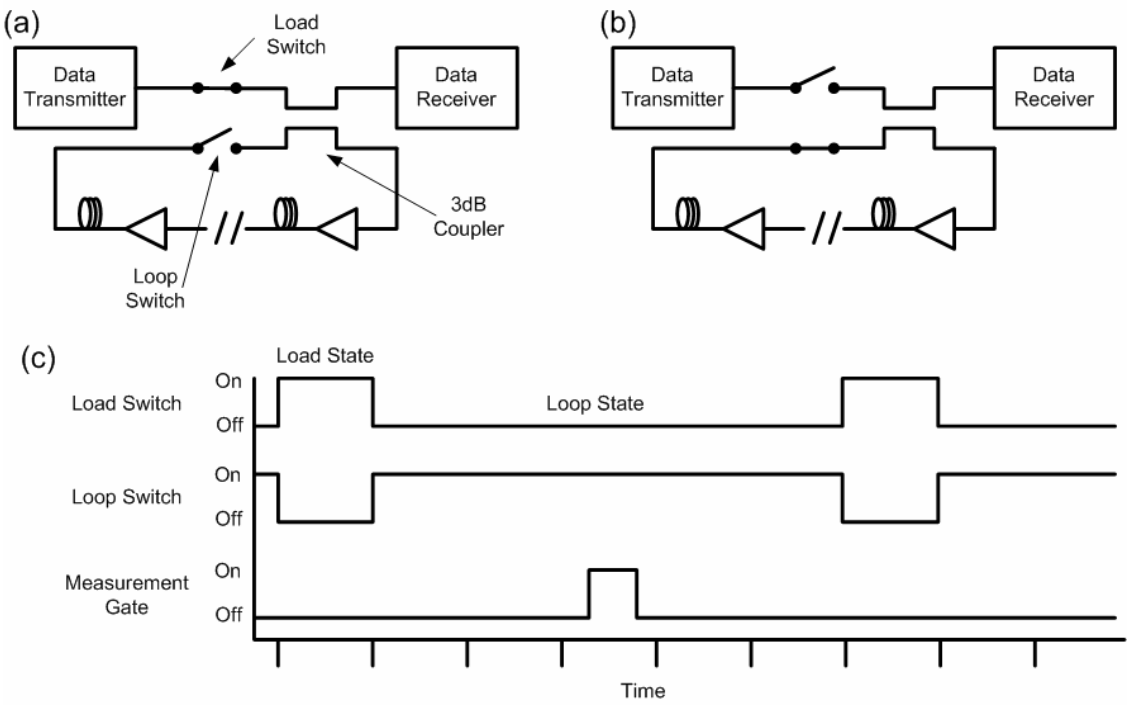

Fig. 4.8: Circulating loop in: a) the load position; b) the loop position. c) sample timing diagrams for a circulating loop

Normally, the amplifiers in a circulating loop configuration are operated in constant output power mode because, in constant gain mode, any power deviation at an amplifier output will propagate around the loop and due to the constant gain condition, grow or diminish until the amplifier power limits are reached. This poses a problem for circulating loop-based study of reconfigurable networks in which the amplifiers are generally operated in a constant gain regime to suppress the transient effects discussed in section 4.2. In [36] the authors use constant gain control in a four channel circulating loop using custom high speed control. This configuration is unsuitable for detailed testing as it requires careful matching of the gains and losses in the loop and is prone to instability. In addition it may be difficult to differentiate between effects caused by the constant gain in the loop and transmission effects related to constant gain. In work presented here, a technique known as Applied Constant Gain (ACG) was developed. Based on the technique used in [37], the constant gain control of the amplifiers is turned off so that they operate with the more stable constant power. Constant gain is then applied by measuring the input powers and setting the output powers accordingly. This technique allows performance to be measured as it would be after constant gain control had re-established the correct gain, but before any further network re-optimization had taken place.

4.5 Experiment

In order to study the effect of channel reconfiguration on performance the ACG method is applied to seven channel configurations that represent some of the extreme channel loading scenarios. Quantitative post-reconfiguration performance measurements are taken using the experimental setup described in the following sub-sections.

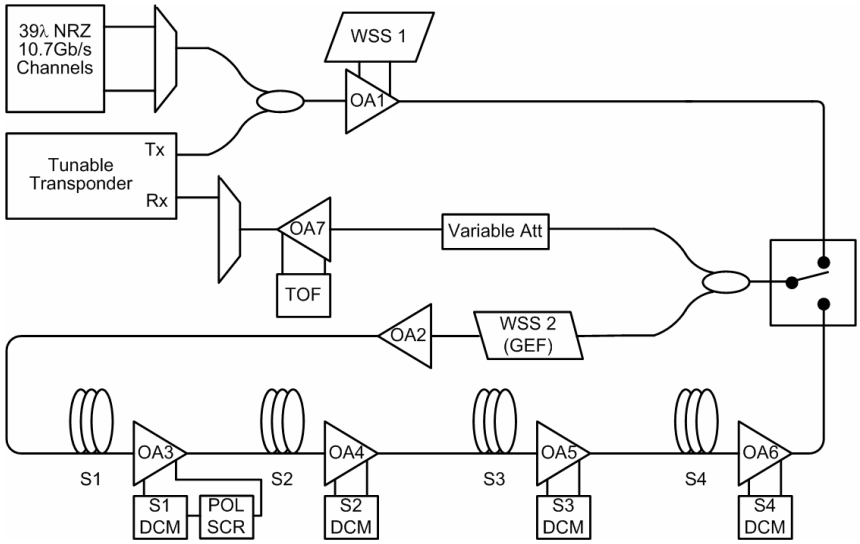

Fig. 4.9: Schematic of the Experimental Setup. (OA: Optical Amplifier, ROADM WSS: Reconfigurable Add/Drop Multiplexer Wavelength Selective Switch, TOF: Tunable Optical Filter, DCM: Dispersion Compensation Module, POL SCR: Polarization Scrambler)

4.5.1 Setup

The recirculating loop setup shown in Fig. 4.9 was used throughout the experiment. Forty 100 GHz-spaced channels were generated using Distributed Feedback (DFB) lasers and multiplexed together. The DFB for the channel of interest was switched off and a tunable transponder was tuned to the corresponding wavelength and inserted in its place to yield a 40 channel comb. Each channel was modulated with a 2^{31}-1 Non-Return to Zero On-Off-Keyed (NRZ-OOK) Pseudo-Random Bit Sequence (PRBS) at 10.7Gb/s. The modulated channels were amplified using a two-stage EDFA, and as this EDFA was outside of the loop, it could be used in constant gain mode. A 1x4 Wavelength Selective Switch (WSS) at the mid-stage of the input EDFA had two functions; to set up the desired channel configuration by blocking the unwanted channels, and to level the power of the input channels using individual per channel VOAs such that their power levels were the same regardless of the configuration.

The loop consisted of four amplified spans of Standard Single Mode Fiber (SSMF). The nominal spans lengths were 80km, 80km, 70km and 90km respectively and the average span loss was 25.8dB. The amplifiers inside the loop were also two-stage EDFAs. DCMs were inserted mid-stage in each EDFA and OA3 also had a polarization scrambler in line with its DCM. An additional two-stage EDFA was placed before the first span to compensate for component losses between the transmitter and the first span. Each of these EDFAs was used in constant output power mode. A second WSS used inside the loop represents a node every five spans in a long haul link. In future work channels can be added or dropped at this node, but in this work it simply provides channel levelling/gain equalisation and ASE removal. It was located at the beginning of the loop to represent its position on the add side of an east/west separable ROADM and was adjusted in order to give a flat and level spectrum at its own input at all times. This ensured that the loading channels (which were flattened using WSS1) experienced the same filtration as the looping channels. Due to the low channel count for the majority of the channel configurations considered, the ASE grew very rapidly in the loop. In order to improve the OSNR, unused ports on WSS2 were closed to block any out-of-band ASE.

At the output of the loop the OSNR was varied by attenuating the signal power, while maintaining constant power on the receiver. A 5nm tunable optical filter in the mid-stage of the output EDFA was used to reduce the ASE and the signals were demultiplexed using a 100GHz Arrayed Waveguide Grating (AWG) based demultiplexer. The channel of interest was sent into the receiver of the transponder. The required OSNR for a BER of $1x10^{-3}$ was recorded, along with the delivered OSNR at the receiver for each round trip.

4.5.2 Channel Configurations

Configuration 1 consisted of forty 100GHz spaced C-band channels. Configuration 2 consisted of five of these channels spread across the C-band. The wavelengths of these channels were 1532.68nm, 1538.98nm, 1546.12nm, 1553.33nm and 1559.79nm. Configurations 3 – 7 consisted of a band of five channels with one of the channels from Configuration 2 as the centre channel together with its two nearest higher frequency neighbours and its two nearest lower frequency neighbours. Three of the configurations are shown in Fig. 4.10 after one round trip. These configurations represent extreme cases of

channel loading that may occur in a reconfigurable network and so provide some insight into some of the worst case scenarios.

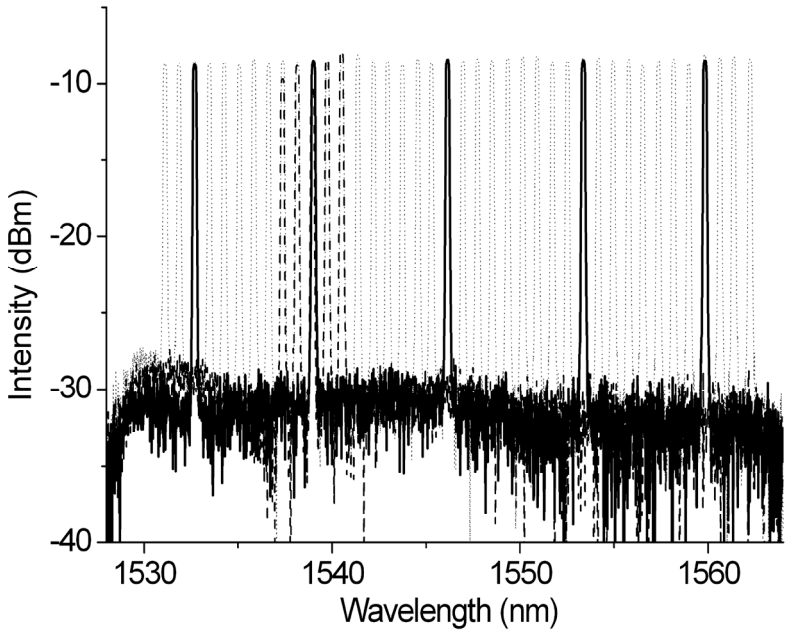

Fig. 4.10:Three of the configurations used. The dotted spectrum shows configuration 1, the solid black line shows configuration 2 and the dashed black line shows configuration 4.

4.5.3 Experimental Process

The experimental process is depicted in the flowchart in Fig. 4.11 and will be described in this section.

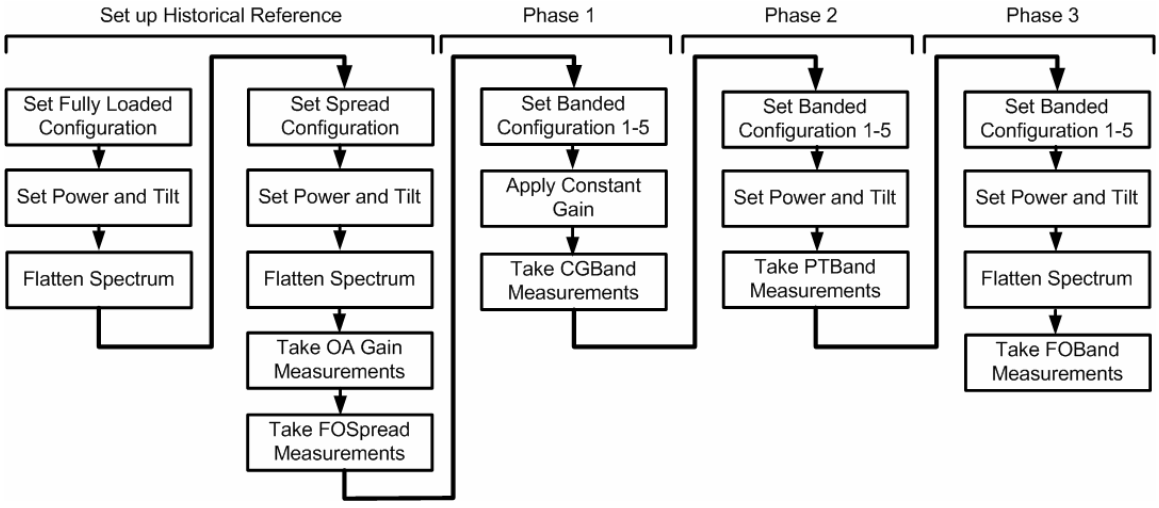

Fig. 4.11:Flow chart depicting the experimental process.

Historical System Arrangement

The system arrangement (including EDFA and channel levelling settings) that is in place when a channel reconfiguration takes place will have a major impact on the transmission performance until such time as re-optimization takes place. For this reason a consistent starting point was used for each measurement. The EDFAs are designed to operate fully loaded so this configuration was used as the historical reference point. Initially, each EDFA was set to give the desired output power and spectral tilt for this fully loaded configuration, and WSS2 was then set to flatten any residual gain ripple and Fig. 4.12(a) shows the per channel attenuation of WSS2 at this point.

From this reference point the channels were set to configuration 2 (5 channels spread uniformly across the band). This represents the starting point of the example presented in Fig. 4.1 on page 57. To maintain the gains in the loop, the amplifier output powers were reduced by 9dB to correspond to the input power drop caused by a reduction from 40 channels to 5 channels. The WSS was then adjusted to flatten the reconfigured spectrum. Note that only the open channels were adjusted as shown in Fig. 4.12(b) which shows the shape of WSS2 after optimizing configuration 2. Performance measurements were taken for each of the five channels of configuration 2 and these results are referred to as "fully optimized for the spread configuration" (FOSpread). In Fig. 4.11 this corresponds to the end of the "set up historical reference" phase.

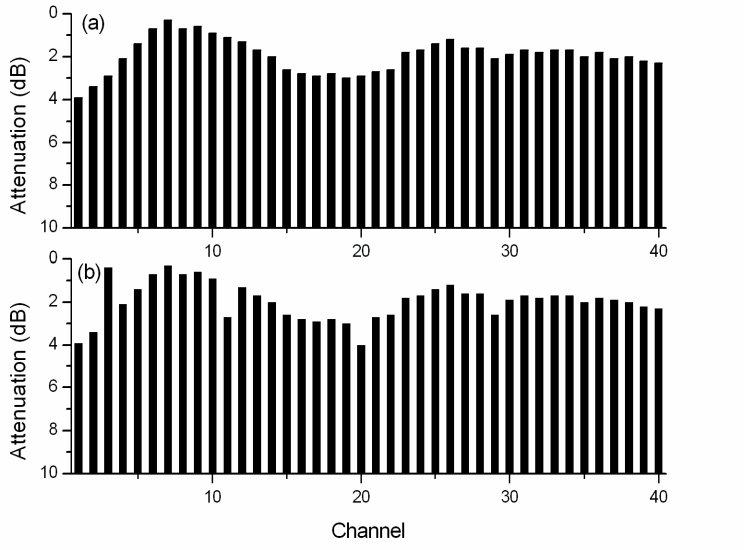

Fig. 4.12:WSS1 channel attenuations after: a) 40 channel optimization; and b) uniformly spread optimization

It is seen that in order to flatten the spectrum for configuration 2, the shortest wavelength had to be boosted while the three central channels are attenuated further indicating that the gain spectrum had varied despite the total gain remaining constant. This gain error is one of the effects that cause the post-reconfiguration performance issues being studied here. It is expected to be a complex function of the configuration dependent SRS and amplifier gain ripple and tilt and SHB. The effect of the WSS settings is illustrated in Fig. 4.13. In part (a) the spectrum of the fully optimized uniformly spread configuration after 7 round trips is shown. The WSS settings in Fig. 4.12 allow this spectrum to remain flat after long transmission distances. Fig. 4.14(b) however, shows that when the configuration changes, the suboptimal WSS settings for the new configuration cause significant channel power mismatches at long distances. It is not until phase 3 re-optimization takes place (Fig. 4.13(d)) that the channel powers are once again levelled.

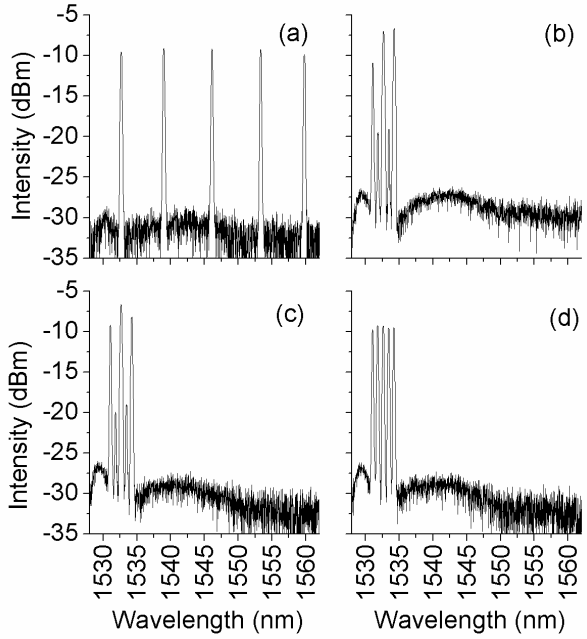

Fig. 4.13:Evolution of the optical spectra after 7 round trips for the 1532nm channel during the reconfiguration and re-optimization process, showing: a) the uniformly spread configuration; b) the reconfigured banded configuration after ACG; c) after power and tilt optimization; and d) after full optimization

Phase 1 measurements - Simulating Constant Gain in a circulating loop

The next step of the experimental process is the phase 1 adjustments and measurements as seen in Fig. 4.11. As was previously mentioned the EDFAs in a circulating loop configuration must operate with constant output power in contrast to the straight line

reconfigurable system being represented in which the amplifier's gains are kept constant. In order to make meaningful measurements on phase 1 of the optimization cycle it was necessary to use the ACG technique described previously on the EDFAs used in the loop. The gain of each loop amplifier was measured prior to reconfiguring away from Configuration 2. When changing configuration the powers of the loading channels were kept constant and this, combined with the use of constant gain on the loading amplifier ensured that the total input power to the loop was kept constant. Inside the loop however, the non-ideal WSS settings for the new configuration caused the power into the first EDFA to change. A change in input power to a constant-power-controlled EDFA causes its gain, and hence its ripple and tilt to change. This effect will propagate through the loop and cause similar gain changes for all of the other amplifiers in the loop. This situation is undesirable as it departs from what would occur in a network operating with constant gain. The EDFA output powers required to revert to the pre-reconfiguration gain can be calculated by measuring the new input powers to each EDFA. These output powers can then be set while maintaining the stable constant-power mode in the circulating loop. A change to any EDFA affects every other EDFA so changes are made iteratively until the gain of each EDFA is within tolerance. The algorithm achieved a tolerance between desired and achieved gain of ±0.4dB for the total EDFA gain and the EDFA monitor photodiodes were accurate to ±0.1dB. Performance measurements taken at this point are referred to as "constant gain for the banded configuration" (CGBand). This process is then repeated for configurations 4 – 7.

Phase 2 and Phase 3 Measurements

As mentioned in the previous section, channel configuration changes can cause variations in the wavelength dependent gain even if the EDFA control maintains constant total gain. Hence, after a reconfiguration it will often be necessary to adjust the amplifiers to re-obtain the desired channel powers and total spectral tilt. At this point configuration 3 was reconfigured and the EDFAs output power and tilt were adjusted until target levels were reached. Fig. 4.13(c) clearly shows the effect of the tilt adjustment however, the channel power mismatch is still evident despite the mean channel power being correct at this point. Performance measurements taken after phase 2 re-optimization are referred to as "power and tilt for the banded configuration" (PTBand). The same process was then repeated for configurations 4 – 7.

Note that up to this point the per-channel levelling shape has not been adjusted for the new channel configuration and remains as shown in Fig. 4.12(b), optimized for configuration 2. Clearly this arrangement is non-ideal for configuration 3 (a 5 channel waveband) so phase 3 of the re-optimization process consisted of iteratively adjusting the power and tilt of the EDFAs, and the shape of the WSS in order to get a flat spectrum with all channels at the desired mean channel power as shown in Fig. 4.14(d). Once this was achieved, measurements were taken and these are referred to as "fully optimized for the banded configuration" (FOBand). Again, similar measurements were taken for configurations 4 – 7 and this completed the experimental process.

To summarise, the configuration is changed from five uniformly spread channels to five banded channels as shown in Fig. 4.14 (a & b) for the 1532nm channel. Performance measurements are taken at both of these points as well as at two further optimization stages Fig. 4.13 (c & d). The same measurements are taken for each of the five initial channels, yielding a total of 20 sets of measurements. The naming conventions used in figures and text to describe these are as follows:

(i) Fully Optimized (phase 3 measurements) with five channel spread across the band are referred to as FOxxxxSpread.

(ii) Applied Constant Gain (phase 1 measurements) with 5 channels banded together are referred to as CGxxxxBand.

(iii) Power and Tilt (phase 2 measurements) with 5 channels banded together are referred to as PTxxxxBand.

(iv) Fully Optimized (phase 3 measurements) with five channels banded together are referred to as FOxxxxBand.

For example CG1538Band refers to Constant Gain (phase 1 measurements) of the 1538 channel in the banded configuration and FO1559Spread refers to the Fully Optimized (phase 3 measurements) of the 1559 channel when it is part of the configuration with 5 channels spread across the band.

4.5.4 Channel Launch Powers and Dispersion Maps

The process outlined above was performed using four different channel launch powers (0dBm, 2dBm, 4dBm and 6dBm). 'Return-to-zero' dispersion maps (where the DCMs and

span lengths are nominally matched to each other) were used for the 0dBm and 2dBm cases. For the 4dBm and 6dBm launch powers, pre-compensation of 500ps/nm was used in addition to a singly periodic dispersion map with a residual dispersion per span of 34ps/nm. This dispersion map helped to reduce the non-linear penalties associated with the high channel powers as described in section 4.3

4.6 Experimental Results

4.6.1 Power Evolution

It was important to ensure that the power evolution in the loop system closely matched that of the straight line system being represented. Two methods of power control were examined initially and these are illustrated in Fig. 4.14. The solid white boxes represent the power in the channels, the solid grey areas represent ASE growth and the hatched grey areas represent ASE removal by the WSS. In addition the measurement points are indicated by black dots and the dashed line represents the observed power evolution at these measurement points. Note that to simplify the illustration the WSS removes all built up ASE including in-band and out-of-band. In reality, the out of band ASE removal is less complete and in band ASE would not be removed at all.

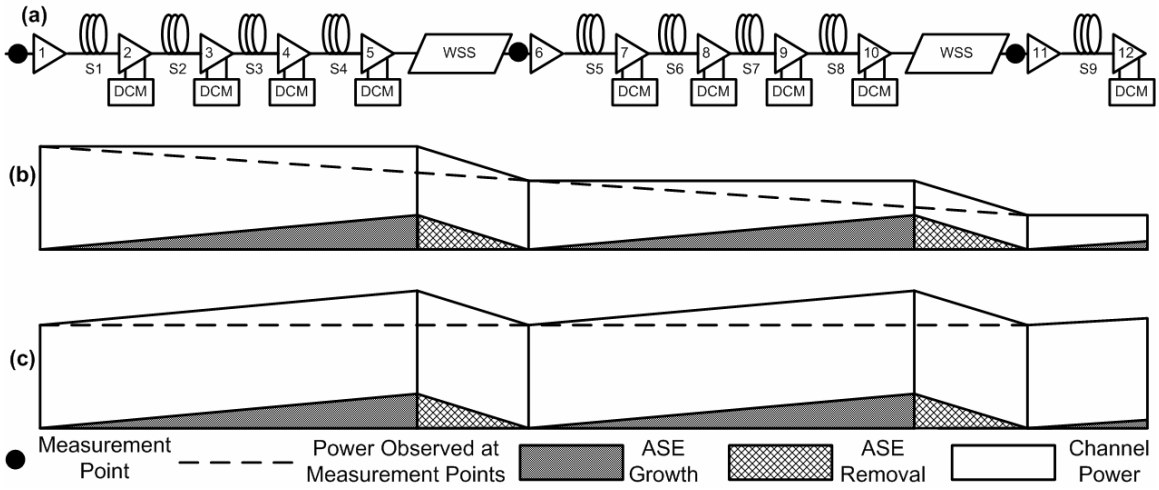

Fig. 4.14:Power evolution in a straight line system. a) block diagram of the straight line system; b) the mean channel power method of amplifier adjustment; and c) the total output power method of amplifier adjustment.

Both methods involved the setting of the total EDFA output power. With the first method (Fig. 4.14(b)), the EDFA output power is simply set to match a target, while with the second method (Fig. 4.14(c)) it is set such that the power in the channels alone (out-of-band ASE

power was ignored) matched a target. The first method is faster because a photodiode power reading will suffice, whereas the second method requires a spectrum analyser sweep to calculate the power in the channels. However, with the first method the ASE growth is not taken into account and as the ASE grows, the power in the channels is reduced proportionally. Hence, the removal of the ASE leaves the total power and therefore the mean channel power well below target as shown in Fig. 4.14(b). With the second method, when the WSS removes the ASE the mean channel powers remain close to their target because extra power has been added to keep the mean channel power constant. This method exhibited far superior resilience to OSNR degradation and was used throughout the experiment.

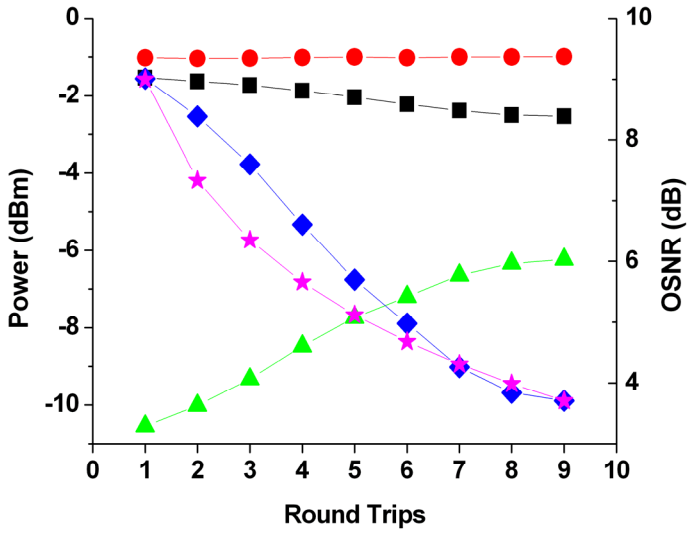

Fig. 4.15:Power evolution for Spread configuration. Total power including channel power and noise (●) and total power in channels only (■) were measured and noise power (▲) and OSNR (◆) calculated from these. The theoretical OSNR evolution of a system without the ASE removal is also shown (★)

Measurements were taken to ensure that the power evolution matched well to that of the system being represented. The total power plot shown in Fig. 4.15 (●) shows the total power measured at the input to the WSS filter for each round trip with the uniformly spread configuration. The fact that this power remains almost constant indicates that the loop power evolution quite closely matched that of a straight line system adjusted for a target mean channel power. From the total power and channel power measurements, the noise power and hence OSNR can be calculated. In a cascade of EDFAs the OSNR is expected to

decay exponentially as shown in Fig. 4.15(★). In this experiment the OSNR deviates from the perfect exponential because the WSS filters much of the ASE, causing a boost in OSNR after every 5 amplifiers.

4.6.2 Performance

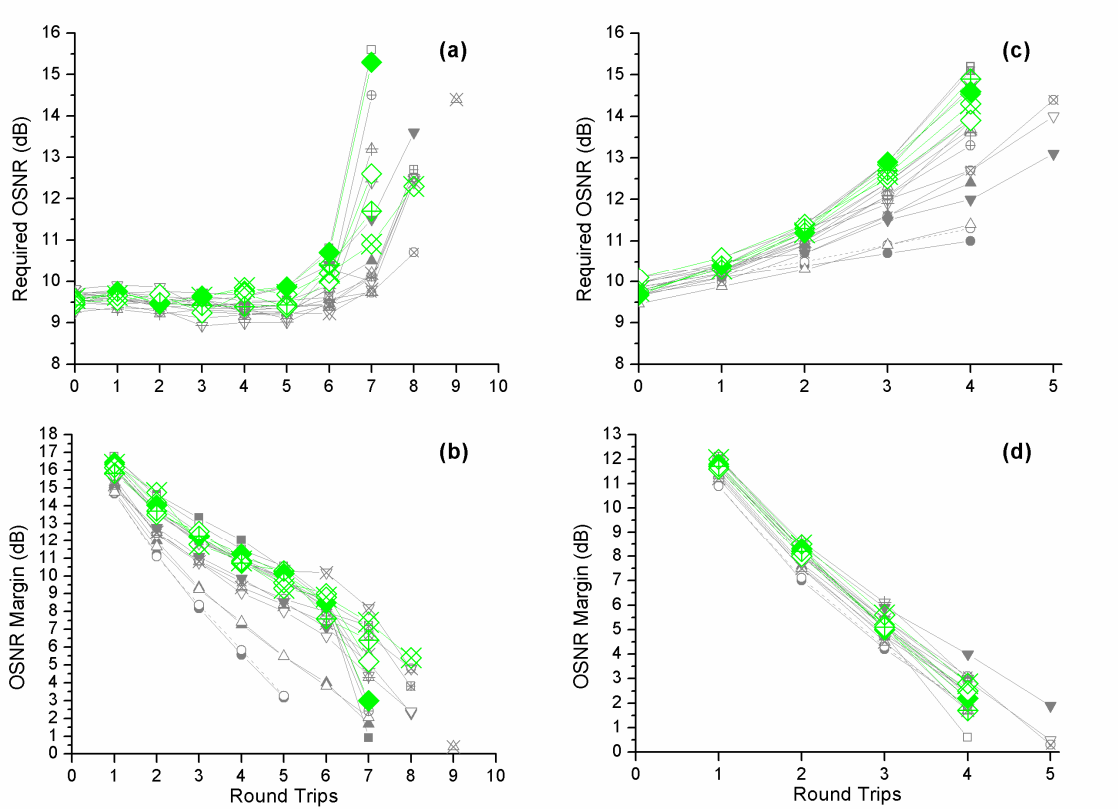

Fig. 4.16:Required OSNR and OSNR Margins as a function of distance for 6dBm launch power (a & b respectively) and required OSNR and OSNR margins for 2dBm launch power as a function of distance (c & d respectively). 1532nm (■), 1538nm (●), 1546nm (▲), 1553nm (▼), and 1559nm (◆) channels. Solid = CGBand, Hollow = PTBand, + = FOBand, X = FOSpread

Fig. 4.16 shows the required OSNR and OSNR margin measurements as a function of distance for the 6dBm launch power and the 2dBm launch power. The highlighted plots correspond to the four reconfiguration scenarios for the 1559nm channel. The first point of note is that the 6dBm per launch power allows for a greatly extended reach. In some cases the reach is twice that of the 2dBm launch power. The reason for this is the optimized dispersion map, which allows high launch powers while keeping nonlinear distortion low. The effect of the dispersion map can be seen by the difference in the shape of the 6dBm curves when compared to the 2dBm curves. In Fig. 4.16(a) it is seen that the required OSNR for all channels stays quite constant for the first five round trips. In contrast, Fig. 4.16(b)

shows that despite the lower launch power, the required OSNR increases from the offset and many of the channels cannot reach five round trips with an acceptable BER even when fully optimized. Focusing on the highlighted 1559 channel, the OSNR margin plot of Fig. 4.16(b) shows that although the required OSNR remains almost constant for the first five round trips, the OSNR margin falls quite linearly on account of the degrading delivered OSNR with each round trip. After this distance the nonlinear effects take hold and a change in slope is observed. It is seen that the OSNR margin drops by approximately 5dB over the first 4 round trips. For the 2dBm launch power, the reduction in OSNR margin over the same distance is approximately 10dB indicating that a reduction in delivered OSNR caused by the EDFAs and an increase in required OSNR caused by nonlinearities are both affecting the margin. The change in the slope of the required OSNR curve seen for the 1559nm channel is not present for the 1538nm channel for example. The reason for this is that the large WSS attenuation for this channel causes the power for the 1538nm to be too low for nonlinearities to affect it. The evolution of the channel power for both of these examples will be seen in Fig. 4.18.

Another interesting point to note from Fig. 4.16(a) is the role played by the reconfiguration and subsequent re-optimization. Looking at the highlighted 1559nm channel after 7 round trips it can be seen that the required OSNR varied substantially for each of the scenarios. At this distance the initial configuration of FO1159Spread exhibits a required OSNR of 10.9dB. When the configuration changes from spread to banded and constant gain is applied the required OSNR increases dramatically to 15.3dB due to increased nonlinear effects caused by XGM between the closely spaced channels, and also the suboptimal WSS setting. Phase 2 optimization involves re-optimizing the power and tilt of the EDFA and results in a 2.7dB improvement in required OSNR to 12.6dB. When the WSS is adjusted for the new configuration in phase 3, a further 0.9dB improvement is achieved bringing the required OSNR to 11.7dB. The 0.8dB difference between the FO1559Spread and FO1559Band is due to the increased nonlinear penalty associated with the narrower channel spacing.

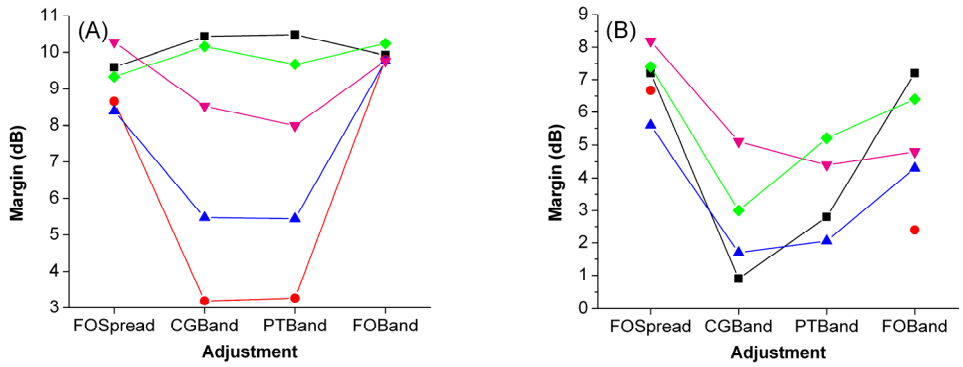

Fig. 4.17:Margin after (a) 1600km, (b) 2240km for each adjustment step. (■ - 1532) (● - 1538) (▲ - 1546) (▼ - 1553) (◆ - 1559)

Fig. 4.17 presents similar reconfiguration and re-optimization data for each of the five channels after five round trips or 1600km (Fig. 4.17(A)) and after seven round trips or 2240km (Fig. 4.17(B)). At 1600km the 1532nm and 1559nm channels experience a slight positive penalty when reconfigured, whereas the margin is reduced by up to 5.5 dB for the other channels. Despite this penalty, each channel maintains a margin of at least 3dB to this distance. Little improvement is registered after tuning the power and tilt of the amplifiers, but when the channel powers are fine tuned using the WSS, FOBand margins recover to within 1dB of the FOSpread in the worst case. At 2240km, all of the channels suffer a margin penalty when reconfigured; indeed at this distance the 1538nm required a higher OSNR at this distance than is delivered indicating that error free transmission is not possible. With the exception of the 1532nm channel, the FOBand cases show lower OSNR margins than their FOSpread counterparts. This penalty may be caused by nonlinear interaction between neighbours in the band or by variation in the gain spectrum due to SHB.

A number of factors that can affect the post reconfiguration performance are evident from Fig. 4.18, which shows the optical spectra after reconfiguration for 3 configurations at four different distances. The first point to note is that in (a), (e) and (i) the channel powers are relatively uniform. The signals have only passed through a single gain equalization element at this point and the maximum power divergence is approximately 2.5dB. Clearly as they travel longer distances this divergence grows considerably with a worst case of 15dB power divergence after passing through seven gain equalization elements. The shape of the WSS shown in the lower plot of Fig. 4.12 correlates to these spectra. It is seen that for the 1532nm channel (Fig. 4.18(a - d)) the level of attenuation has been lowered in order to level

the uniformly spread configuration and this results in a high powered central channel. In contrast, for the 1538nm channel (Fig. 4.18(e - h)) the attenuation has been increased and so the power in the central channel degrades rapidly with distance.

The next point of interest is the channel broadening with distance, which is especially prominent in the shorter wavelengths. This broadening of channels may be attributed to ASE growth in the channel and to spectral broadening associated with the nonlinear effects of SPM and XPM. While the central channel of (d) appears to be broadened further than that of (l), the two perform similarly. In contrast the power of the central channel of (h) is too low to display much broadening. The performance of this OSNR limited channel is worst of all.

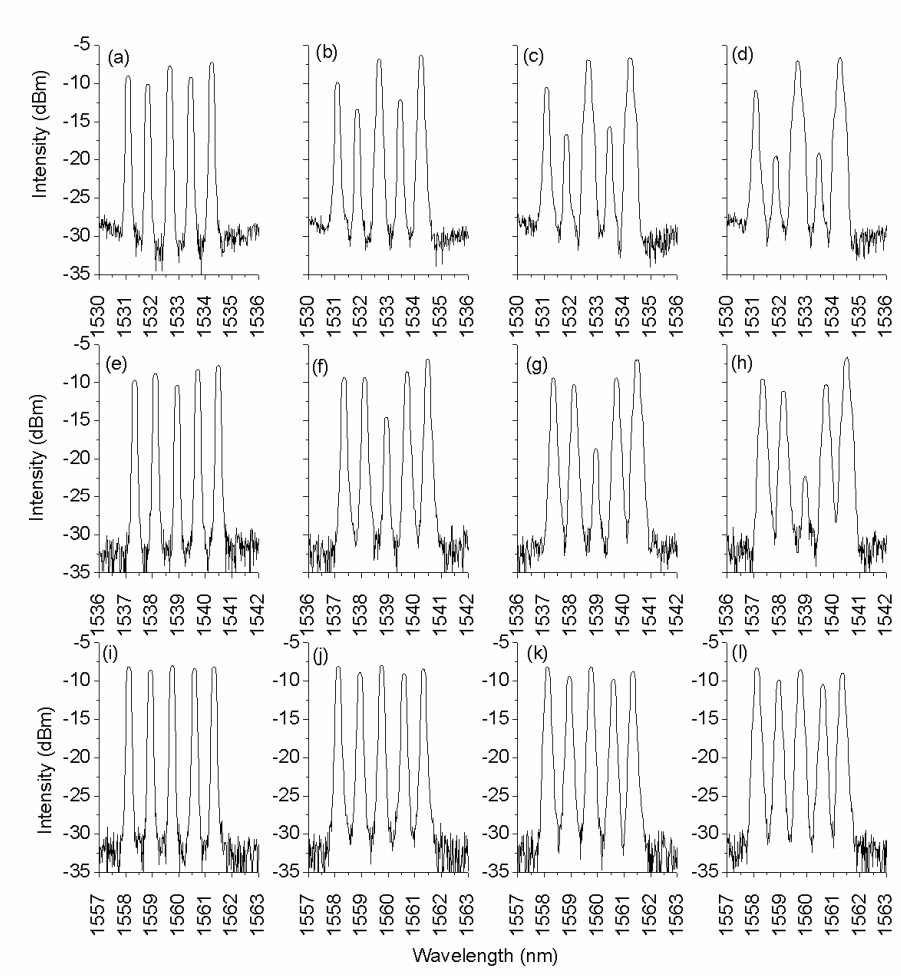

Fig. 4.18:Evolution of the optical spectra of CG1532Band after 1 (a), 3 (b), 5 (c), and 7 (d) round trips, CG1538Band after 1 (e), 3 (f), 5 (g) and 7 (h) round trips and CG1559Band after 1 (i), 3 (j), 5 (k) and 7 (l) round trips with 6dBm launch powers.

Evidence of SHB can be seen in the spectra of Fig. 4.18. If the effects of the WSS on the central channels are ignored, a smooth hole in the gain profile around the central channel can be imagined. As expected, the effect is more prominent for the short wavelength bands such as those at 1532nm and 1538nm than for the 1559nm band. Despite only the central channels of the waveband having been adjusted with the WSS, a large power divergence is also seen on the adjacent channels, and while performance measurements were not taken for these adjacent channels the detrimental effect of the gain hole is clear.

After full optimization the behaviour of the network will be more predictable because the channels will all be levelled to a known power. However, Fig. 4.19 shows that full optimization does not always improve performance. The margins after each round trip for the 1538nm and 1553nm channels are presented. Full optimization for the 1538nm channel results in a transmission distance improvement of 2 round trips (>600km). However, for 1553nm, when the system is "fully optimized" this process actually degrades the transmission distance by one round trip. In this case the performance with CG and PT optimization was better due to a slight reduction in power by the WSS. When the WSS is readjusted to hit the target power it pushes the channel power higher causing non-linear effects to reduce performance.

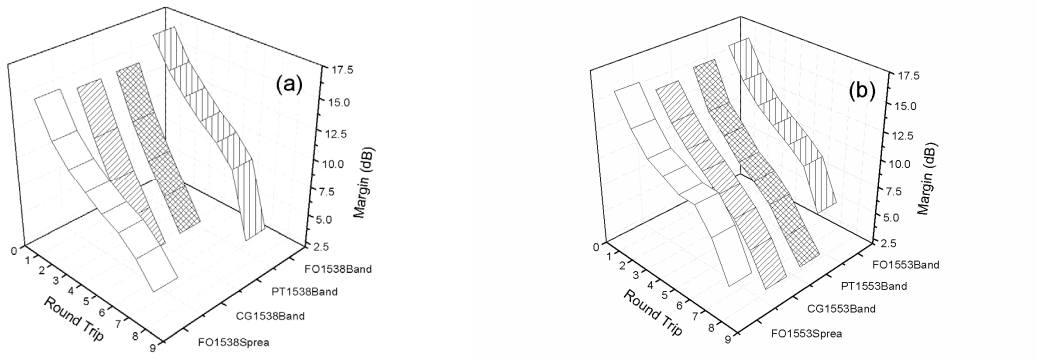

Fig. 4.19:Margin after each round trip for the four set of performance measurements on: a) the 1538nm; and b) the 1553nm channels.

4.6.3 Comparison of different launch powers and dispersion maps

Fig. 4.20 compares the overall performance of each of the measured channels under the various phases of optimization and for four different launch powers. The optimized dispersion map is used for the 4dBm and 6dBm cases and without it the high channel launch powers would cause severe non-linear distortion and limit the transmission distance

achievable as it does with the 0dBm and 2dBm cases. By comparing the transmission distances of the 0dBm/channel launch power without optimized dispersion mapping, and the 4dBm/channel launch power with optimized dispersion mapping for the 1532nm channel, it can be seen that the reach has been extended from 4 round trips to 9 round trips corresponding to 1600km, a 125% increase. This shows the tremendous value that can be gained through the use of dispersion mapping.

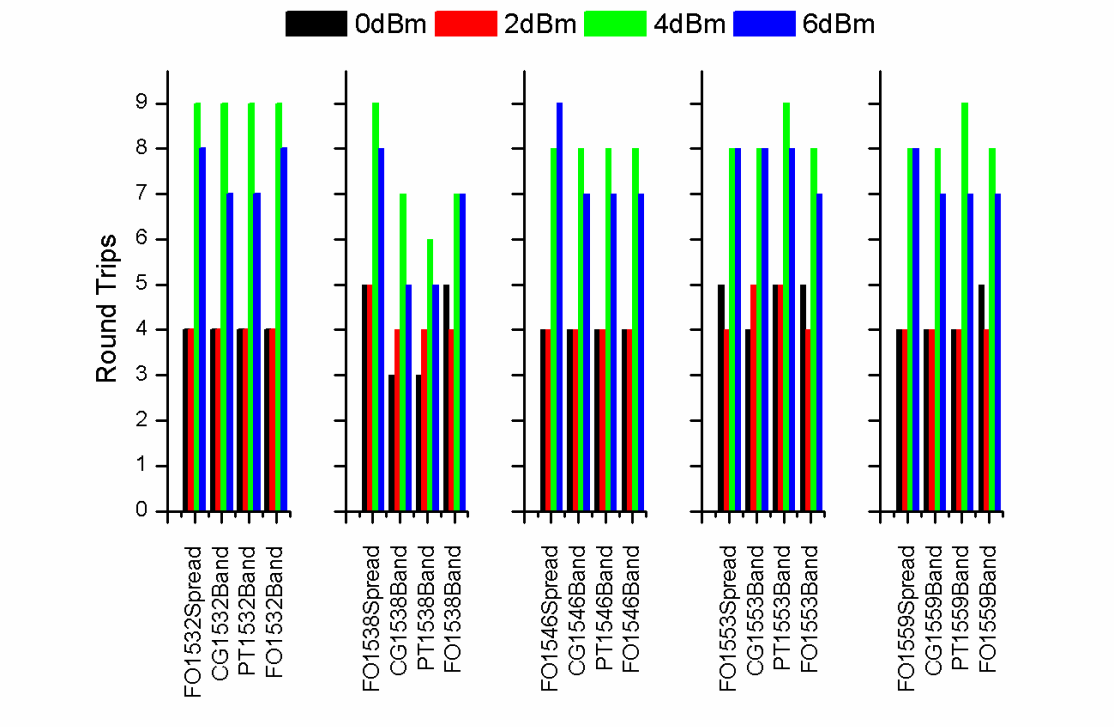

Fig. 4.20:Number of round trips completed for each configuration using 4 different launch power levels.

Another point to note from Fig. 4.20 is that in only one case out of 20 does the FOBand outperform the FOSpread case while the FOSpread outperforms the FOBand in 6 cases. This is to be expected due to the increased non-linear interactions associated with the narrow channel spacing.

In the majority of cases, reconfiguration, and subsequent re-optimization tends to impact the reach by a maximum of one round trip. The major exception to this rule is the 1538nm channel where reach can be changed by up to three round trips (almost 1000km). The reason for this is its severe delivered OSNR reduction caused by the large increase in WSS attenuation required to level the spectrum for the uniformly spread case. Consider again the reconfiguration example described in Fig. 4.1 on page 57 where 4 of the 5 channels in

Configuration 2 required re-routing, but the 1538nm channel was to stay on its current path. A configuration change from Configuration 2 to Configuration 4 (FO1538Spread to CG1538Band) for this purpose causes an initial reduction in possible transmission distance of up to 960km for the 1538nm data channel. Only when this new configuration is fully optimized will the 1538nm channel reach its intended destination once more. This post reconfiguration reach reduction has serious implications for reconfigurable networks.

4.7 Conclusion

In current WDM networks, when wavelengths are provisioned or reconfigured, the process is slow and methodical and the system is monitored throughout to ensure that no adverse effects occur. With greater levels of automation, and shorter connection times, this manual monitoring process becomes unfeasible. The automatic switching of channels at network nodes can result in significant performance degradation due to channel power divergence caused by EDFA gain dynamics and the historical system arrangement. EDFAs in reconfigurable networks operate with constant gain to prevent instabilities associated with strong channel power coupling. EDFA control circuits can effectively maintain the total gain in the presence of channel reconfiguration; however the wavelength dependent gain still varies. The result of this gain error is that the system arrangement (including EDFA settings and gain equalization settings) optimized for the initial configuration is non-ideal for the new configuration. The motivation of the work detailed in this chapter was to demonstrate the possible transmission problems which can be caused by channel reconfiguration and to stimulate further study and development of techniques which can predict the post-reconfiguration behaviour of the network based on amplifier gain models and known historical network states.

In order to study these issues, a method was developed which allowed the study of constant gain based networks using a constant power based circulating loop apparatus. A number of extreme channel loading configurations were inspected during three phases of post reconfiguration optimization and showed that immediately after reconfiguration transmission performance could be severely affected by the wavelength dependent gain error and the historical network state. Subsequent optimization of the network for the new configuration normalized performance but the length of time that re-optimization takes could result in a significant reduction in throughput. Results showed that in the worst case

studied, reconfiguration from a spread configuration to a waveband configuration caused a reduction in transmission distance of 37.5% (3 round trips of the circulating loop) for a channel at 1538nm. Subsequent re-optimization for the new configuration improved the reach by 2 round trips. Of the five channels whose performance was measured it was shown that the 1538nm channel suffered the largest penalties due to reconfiguration.

The remaining chapters of this thesis move away from slow reconfiguration, typical of OCS where connections may last anywhere from minutes to months or even years, and towards Optical Packet Switching (OPS), a much faster form of optical switching, where reconfiguration takes place on timescales of the order of nanoseconds. Chapter 5 will describe work which was carried out on fast tunable lasers, which represent one of the key components required to enable OPS. In Chapter 6, a novel optical labelling scheme, employing these tunable lasers will be detailed.

References

[1] P. Morkel, ”Edge-to-Core Optical Switching in Metro Apps”, Lightwave Europe, January 2008.

[2] A. Srivastava, Y. Sun, “Advances in Erbium Doped Fiber Amplifiers” *Optical Fiber Telecommunications, Vol IVA*, I. P Kaminow and T. Li, Eds. San Diego, CA: Academic 2002.

[3] H. Chou and J. Stimple, "Inhomogeneous Gain Saturation of Erbium-Doped Fiber Amplifiers," in Optical Amplifiers and Their Applications, Vol. 18 of 1995 OSA Technical Digest Series (Optical Society of America, 1995), paper ThE1.

[4] J. W. Sulhoff, A. K. Srivastava, C. Wolf, Y. Sun, J. L. Zyskind, “Spectral-Hole Burning in Erbium Doped Silica and Fluoride Fibers,” *IEEE Photon. Tech. Lett.* Vol 9, No 12, Dec 1997, pp 1578-1579.

[5] G. Luo, J.L. Zyskind, J.A. Nagel, M.A. Ali, "Experimental and theoretical analysis of relaxation-oscillations and spectral hole burning effects in all-optical gain-clamped EDFA's for WDM networks," J. Lightwave Technol. , vol.16, no.4, pp.527-533, Apr 1998

[6] J.L Zyskind et al, “Fast Power Transients in Optically Amplified Multi-Wavelength Networks”, Proc. Tech. Dig. Optic. Fiber Commun. OFC'96, San Jose, CA, paper 1996.

[7] C.R. Giles, E.Desurvire, "Modeling erbium-doped fiber amplifiers," J. Lightwave Technol., vol.9, no.2, pp.271-283, 1991

[8] F. Shehadeh, R. S. Vodhanel, C. Gibbons, and M. Ali, “Comparison of gain control techniques to stabilize EDFA's for WDM networks,” Proc. Tech. Dig. Optic. Fiber Commun. OFC'96, San Jose, CA, paper WM8, 1996.

[9] M.I. Hayee, A.E. Willner, "Transmission penalties due to EDFA gain transients in add-drop multiplexed WDM networks," IEEE Photon. Technol. Lett. , vol.11, no.7, pp.889-891, Jul 1999

[10] D. Kilper, C. Chandrasekhar, and C. A. White, " Transient Gain Dynamics of Cascaded Erbium Doped Fiber Amplifiers with Re-Configured Channel Loading," in Optical Fiber Communication Conference and Exposition and The National Fiber Optic

Engineers Conference, Technical Digest (CD) (Optical Society of America, 2006), paper OTuK6.

[11] C. R. Giles, E. Desurvire, and J. R. Simpson, "Transient gain and cross talk in erbium-doped fiber amplifiers," Opt. Lett. 14, 880- (1989)

[12] A.K. Srivastava; Y. Sun; J.L. Zyskind; J.W. Sulhoff, "EDFA transient response to channel loss in WDM transmission system," *Photonics Technology Letters, IEEE* , vol.9, no.3, pp.386-388, March 1997

[13] J. L. Zyskind, Y. Sun, A. K. Srivastava, J. W. Sulhoff, A. J. Lucero, C. Wolf, and R. W. Thach, "Fast Power Transients in Optically Amplified Multiwavelength Optical Networks," in *Optical Fiber Communication Conference*, Vol. 2 of 1996 OSA Technical Digest Series (Optical Society of America, 1996), paper PD31.

[14] Y. Sun, A.K Srivastava, J.L. Zyskind, J.W. Sulhoff, C. Wolf, R.W. Tkach, "Fast power transients in WDM optical networks with cascaded EDFAs ," *Electronics Letters* , vol.33, no.4, pp.313-314, 13 Feb 1997

[15] A.D. Ellis, R.M. Percival, A. Lord, W.A. Stallard, "Automatic gain control in cascaded erbium doped fibre amplifier systems," *Electronics Letters* , vol.27, no.3, pp.193-195, 31 Jan 1991

[16] A. K. Srivastava, et al "Fast Gain Control in an Erbium-Doped Fiber Amplifier," in *Optical Amplifiers and Their Applications*, R. Jopson, K. Stubkjaer, and M. Suyama, eds., Vol. 5 of OSA Trends in Optics and Photonics Series (Optical Society of America, 1996), paper PP4.

[17] J.L. Jackel, D. Richards, "All-optical stabilization of cascaded multichannel erbium-doped fiber amplifiers with changing numbers of channels," *Optical Fiber Communication. OFC 97., Conference on* , vol., no., pp.84-85, 16-21 Feb 1997

[18] M. Zirngibl, "Gain control in erbium-doped fibre amplifiers by an all-optical feedback loop," *Electronics Letters* , vol.27, no.7, pp.560-561, 28 Mar 1991

[19] S. J. B. Yoo, W. Xin, L. D. Garrett, J. C. Young, G. Ellinas, J. C. Chiao, M. Rauch, J. E. Baran, B. Meagher, H. Leblanc, and G.-K. Chang, "Observation of prolonged power

transients in a reconfigurable multiwavelength network and their suppression by gain-clamping of optical amplifiers," IEEE Photon. Technol. Lett., vol. 10, pp. 1659–1661, 1989.

[20] D.C Kilper, C.A. White, S. Chandrasekhar, "Control of Channel Power Instabilities in Constant-Gain Amplified Transparent Networks Using Scalable Mesh Scheduling," *Lightwave Technology, Journal of* , vol.26, no.1, pp.108-113, Jan.1, 2008

[21] D.C. Kilper, S. Chandrasekhar, C.A White, "Transient gain dynamics of cascaded erbium doped fiber amplifiers with re-configured channel loading," *Optical Fiber Communication Conference, 2006 and the 2006 National Fiber Optic Engineers Conference. OFC 2006* , vol., no., pp. 3 pp.-, 5-10 March 2006

[22] A. Gnauck, R. M. Jopson, "Dispersion Compensation for Optical Fibre Systems" *Optical Fiber Telecommunications, Vol IIIA*, I. P Kaminow and T. Koch, Eds. San Diego, CA: Academic 1997.

[23] F. Forgheiri, R. W. Tkach, A. R. Chraplyvy, "Fibre Nonlinearities and their impact on transmission systems" *Optical Fiber Telecommunications, Vol IIIA*, I. P Kaminow and T. Koch, Eds. San Diego, CA: Academic 1997.

[24] T. Naito, T. Terahara, T. Chikama, M. Suyama, "Four 5-Gb/s WDM transmission over 4760-km straight-line using pre- and post-dispersion compensation and FWM cross talk reduction," *Optical Fiber Communications, 1996. OFC '96* , vol., no., pp. 182-183, 25 Feb.-1 March 1996

[25] D. Marcuse, "Selected Topics in the Theory of Telecommunications Fibers" *Optical Fiber Telecommunications, Vol II*, S. E Miller and I. P Kaminow, Eds. San Diego, CA: Academic 1988.

[26] P. Bayvel, R. Killey, "Nonlinear Optical Effects in WDM transmission" *Optical Fiber Telecommunications, Vol IVB*, I. P Kaminow and T. Li, Eds. San Diego, CA: Academic 1997.

[27] G. Belloti, A. Bertaina, S. Bigo, "Impact of residual dispersion on SPM-related power margins in 10Gb/s-based systems using standard SMF" *Proc. ECOC '98*, vol. 1, pp 681-682.

[28] G.P. Agrawal, *Nonlinear Fiber Optics*, Academic Press, San Diego, CA, USA, 1997.

[29] F. Forghieri, R.W. Tkach, A.R. Chraplyvy, "WDM systems with unequally spaced channels," *Lightwave Technology, Journal of* , vol.13, no.5, pp.889-897, May 1995

[30] C. Vinegoni, M. Karlsson, M. Petersson, H. Sunnerud, "The statistics of polarization-dependent loss in a recirculating loop," *Lightwave Technology, Journal of* , vol.22, no.4, pp. 968-976, April 2004

[31] S. Kartalopoulos, *DWDM: Networks, Devices and Technology*, Wiley, NJ, USA, 2003.

[32] N. S. Bergano and C. R. Davidson, "Circulating loop transmission experiments for the study of long haul transmission systems using erbium-doped fiber amplifiers," J. Lightwave Technol., vol. 13, pp. 1553–1561, May 1995.

[33] S. Chandrasekhar, D. Kilper, "Using testbeds for optically-transparent mesh network experimentation" Lasers & Electro-Optics Society, IEEE Oct. 2006 Page(s):771 – 772

[34] P. Peloso, D. Penninckx, M. Prunaire, and L. Noirie: Optical transparency of a heterogeneous pan-European network, J. Lightwave Technol., vol. 22, pp. 242-248, 2004.

[35] D. Kilper, S. Chandrasekhar, E. Burrows, L. L. Buhl, and J. Centanni: Local dispersion map deviations in metro-regional transmission investigated using a dynamically re-configurable re-circulating loop, in Proc. OFC/NFOEC 2007, paper OThL5.

[36] T. Yoshikawa, K. Okamura, E. Otani, T. Okaniwa, T. Uchino, M. Fukushima, and N. Kagi, "WDM burst mode signal amplification by cascaded EDFAs with transient control," Opt. Express 14, 4650-4655 (2006)

[37] C. Fürst, R. Hartung, J.-P. Elbers, C. Glingener, "Impact of Spectral Hole Burning and Raman Effect in Transparent Optical Networks", *Proc of the European Conference on Optical Communications, (ECOC 2003),* Paper Tu:4.2.5, Rimini, Italy, Sept 21-25 2003.

Chapter 5 – Characterization of Tunable Lasers for use in Reconfigurable Optical Networks

While the previous chapter was concerned with slow reconfiguration in Optical Circuit Switched (OCS) mesh networks, the remainder of this thesis focuses on faster methods of optical switching. This chapter is concerned with Fast Tunable Lasers (FTLs), which are seen as a key component for future optical networks. More specifically, the chapter describes Tunable Lasers (TLs) and details some experimental work carried out to examine their suitability for deployment in Optical Packet Switching (OPS) and optical burst switching (OBS) Wavelength Division Multiplexing (WDM) networks. The chapter begins by discussing the roles of the tunable laser (TL) in WDM networks and the different properties they must exhibit to fulfil these roles. Sections 5.3 to 5.4 provide background information regarding TLs and the basics of their operation. In Sections 5.6, 5.7, and 5.8 the discussion becomes more focused. Electronically tuned laser diodes are discussed, including specific lasers which are essentially static but do exhibit some tunability, and also the structures used to fabricate widely tunable lasers. The final two sections then detail two individual types of widely tunable laser, namely the Sampled Grating Distributed Bragg reflector (SG-DBR) and the tunable Slotted Fabry-Pérot (SFP) along with experimental work which was carried out to characterise them.

5.1 Tunable Lasers - Applications

Tunable lasers find application in many diverse fields, from astronomy to medicine, but this chapter focuses on their applications in telecommunications. The two major applications are inventory reduction/sparing and reconfiguration.

5.1.1 Inventory Reduction

Prior to the commercial availability of widely tunable lasers, telecommunications carriers were obliged to carry large inventories of laser diodes at every WDM channel in their system in case of failure of a laser in the field. As WDM networks can often consist of 128 channels or more, inventory maintenance quickly becomes cumbersome. Lasers which can be tuned

to any wavelength channel on the ITU allow the inventory size to be reduced considerably which represents a logistical, as well as a financial benefit.

5.1.2 Reconfiguration

TLs will play a part in enabling a number of the features available in reconfigurable optical networks such as dynamic provisioning and bandwidth allocation, lightpath routing, protection and restoration, and burst and packet switching. They will be employed in tunable wavelength converters and transponders within network nodes and also in transmitter subsystems. For provisioning new wavelengths in a system, where more bandwidth is required, tunable lasers in the transmitter can be used to provide channels at any available wavelength. In this case, tuning speeds do not need to be very fast because the channel will be turned on slowly, while monitoring the network for problems. In addition, the channel will likely be in place for a long time, so switching times of seconds are adequate.

For dynamic reconfigurability and fault restoration, in transparent systems which are being deployed currently, reconfiguration is generally performed using space switching techniques, rather than wavelength switching due to the fact that the majority of lasers in the transmitters are static devices. Sub-second switching times are required in order to minimize data loss and maximize network throughput. In protection systems, carriers have long been offering their customers 50ms protection with SONET/SDH systems so switching times of the order of a few tens of milliseconds would be suitable. Wavelength switching could be enabled in these networks through the installation of tunable lasers and AWGs as the switching fabric, or by replacing the current static transmitters with tunable ones; however it seems more likely that wavelength switching will be commercially deployed in future systems such as OBS and OPS which require much faster switching times. In conjunction with a passive Arrayed Waveguide Grating (AWG), TLs can be used to build an optical router in which the light is directed to a certain output port by tuning the laser's wavelength. With switching speeds in the low nanoseconds available with the state of the art tunable lasers, such optical routers are suitable for OBS and OPS applications. In these systems the transmitters in the edge nodes of the core network use FTLs as their source. The FTL is tuned to a certain wavelength depending on the output port onto which the packet or burst should be placed. In the core nodes, data is not detected and retransmitted; rather it remains in optical format throughout the network. As such, tunable transmitters are not required,

rather tunable wavelength converters using an FTL for tunability, re-route the light by changing the wavelength of the FTL.

5.2 Tunable Lasers – Requirements

In this section the various requirements of tunable lasers for suitability in WDM networks are listed and described. In the experimental section of this chapter, the characterization and investigation of some of these properties are carried out. For a packaged, commercial laser, the focus is on wavelength drift, while for the novel device; single mode operation, switching speed, and tuning range etc were of greatest concern.

5.2.1 Single Mode Operation:

It is generally accepted that tunable lasers must offer equal performance to their static counterparts. As such, good single mode operation is required with a Side Mode Suppression Ratio (SMSR) of greater than 30dB generally required. In addition, output powers of 13dBm or higher are often desired by carriers and the power of every channel must be uniform to within approximately 0.5dB.

5.2.2 Tuning Range:

For use in a WDM network, a TL must have a wide tuning range which covers the entire C-band. In the future, as EDFAs become available with C+L-Band operation, it is likely that TLs will have to do likewise in order to pack more wavelengths into a WDM system, or spread wavelengths further apart to reduce interference as bit-rates climb.

5.2.3 Tuning Continuity

Related to the tuning range is the tuning continuity and there are three modes of continuity considered[1]: A discontinuously tuned TL allows only a finite number of defined wavelengths at discrete points within the tuning range to be accessed, while a continuously tunable device allows any wavelength within its range to be accessed. The output wavelength is a simple function of a single tuning parameter, such as current. Between these two extremes is the quasi-continuous laser in which all wavelengths within the range can be accessed, however not as a simple function of a single tuning parameter. In these lasers, a lookup table defines the parameters required to access the various wavelengths. These three tuning mechanisms are illustrated in Fig. 5.1

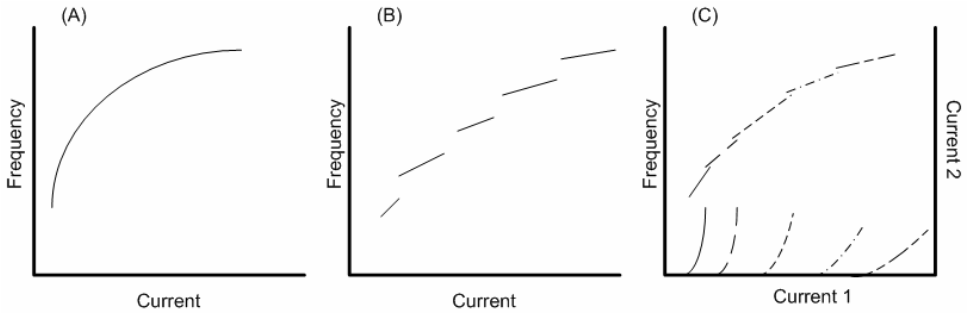

Fig. 5.1: Tuning continuity; A) continuous tuning; B) discontinuous tuning; C) quasi-continuous tuning

5.2.4 Tuning Speed

The tuning speed required is application dependent and some rough approximations for various applications were given in the previous section. An important issue relating to the switching or tuning speed is the latency. This is defined as the time between the switch being requested and the time when the device actually begins the switching process as seen in Fig. 5.2. Poor latency is generally a result of the processing time required to set up the switch and the electronics used in the module. The switching time is defined as the time from when the device begins to change wavelength until the time it reaches its desired wavelength and remains within tolerance.

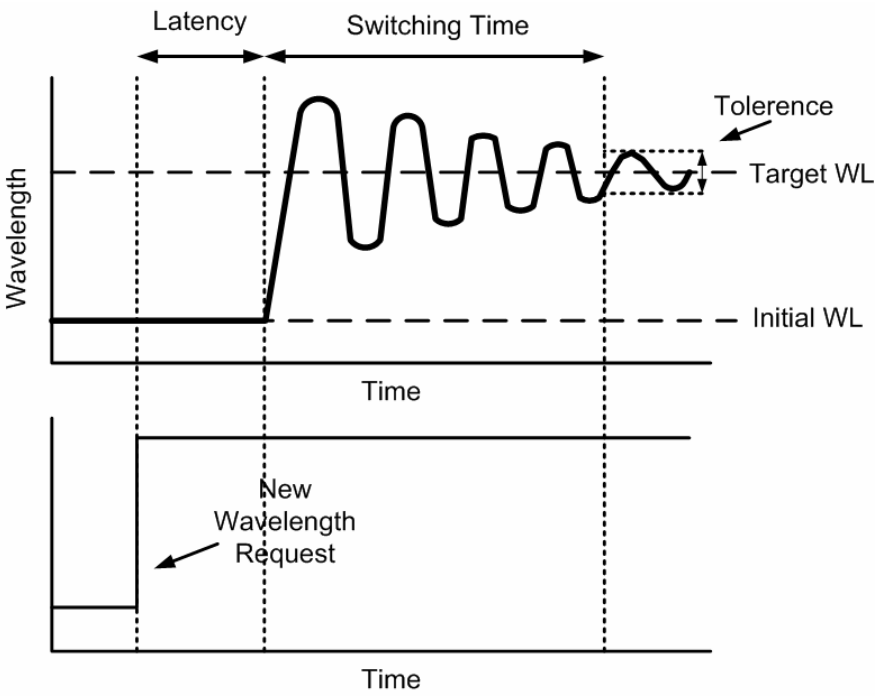

Fig. 5.2: Total tuning time consisting of latency and switching time.

5.2.5 Tuning Accuracy and Stability

The tuning accuracy and stability is a very important property of TLs. For use in WDM systems the laser must be able to tune to and remain within ± 5% of the channel spacing. Any drift outside this range can result in unacceptable crosstalk caused by power leakage into the passband of an adjacent channel. The age of the device and environmental factors can cause wavelength drift. Feedback loops known as wavelength lockers can be used to keep the TL within specification.

5.3 Semiconductor Laser Background

There are three processes of interest that may occur in a two-level atomic system such as that of a semiconductor laser diode. In stimulated absorption, an electron at the lower energy valence band may absorb an incoming photon, and in the process, rise to the higher energy conduction band. In spontaneous emission, an electron in the conduction band can spontaneously return to the valence band with the emission of a photon of random phase and energy. Finally, in stimulated emission, an incoming photon can "knock" an electron in the conduction band, back to the valence band and in doing so, cause the emission of a second photon, coherent to the incident photon. When more carriers are at the higher level energy than the lower energy level the system is said to be in a state of *population inversion.* This state can be achieved through stimulated absorption by optical pumping but in a semiconductor laser, it is most commonly achieved via the injection of electrical carriers into the device [2]. When a voltage just lower than the bandgap voltage is applied to a *pn* junction, the potential barrier of the semiconductor is reduced and electrons from the *n*-doped side and holes from the *p*-doped side flow into the depletion region resulting in a population inversion in a narrow area known as the *active region* [3]. Radiative recombination is very likely in this region and the produced radiation can either interact with valence band electrons causing stimulated absorption or conduction band electrons causing stimulated emission. With the further injection of electrical current, the carrier concentration can become large enough that the rate of stimulated emission exceeds that of absorption and optical gain occurs. In a semiconductor, a resonance cavity may be formed simply by cleaving end facets because the material/air interface has a high reflectance due to the high refractive index of the material. Light generated via stimulated emission as described above

gets reflected by the facets back into the cavity and can stimulate further emission of photons leading to amplification [4].

In semiconductor lasers the resonance cavity can generally support a number of longitudinal modes, the spacing of which depends on the length of the cavity. Although lasing will only occur at modes which lie within the gain spectrum of the material as shown in Fig. 5.3, generally the gain spectrum is wide enough and the longitudinal mode spacing narrow enough that the result is a multi-mode laser output. Lasers with multi-mode outputs suffer badly from dispersion and are unsuitable for WDM systems. Methods have been developed, therefore to encourage single mode output and these will be described in section 5.4.

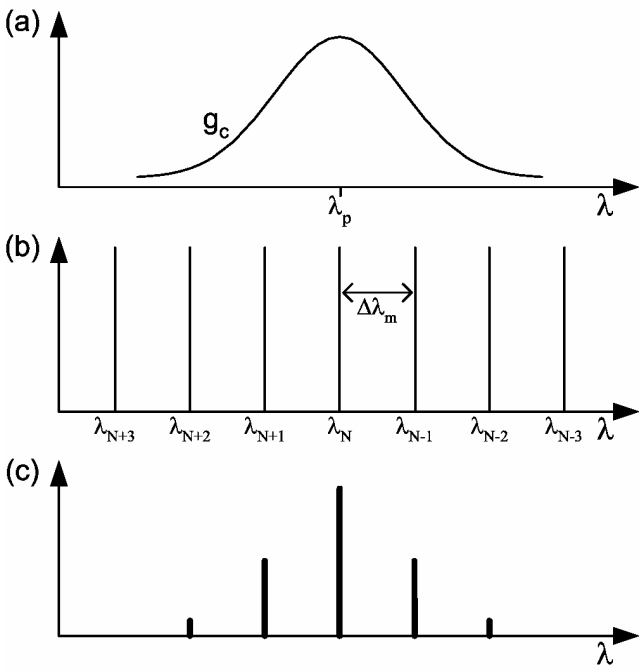

Fig. 5.3: A number of longitudinal modes are present but lasing only occurs for modes which lie within the gain spectrum of the material

5.4 Single Mode Operation

Theoretically, the simplest way to achieve single mode operation is to reduce the cavity length until only a single longitudinal mode is supported. The main problem with this technique in practice is that short cavity lengths result in low output powers. Vertical cavity surface emitting lasers (VCSELs) employ the short cavity technique but to less of an extreme. The cavity is generally long enough to support multiple modes, but short enough that these modes are widely spaced, such that only a single mode will sit under the gain curve

and lase. Another method of gaining single mode operation is to introduce some wavelength dependent feedback element as opposed to the standard mirror in a Fabry-Pérot cavity which reflects all wavelengths equally. Periodic structures, known as Bragg gratings introduced into the cavity, cause wavelength dependent loss, thereby suppressing all undesired modes through deconstructive interference, and providing single mode operation. Two devices based on this technique will be outlined in section 5.7.

5.5 Laser Tuning

The emission wavelength of a tunable laser can be varied through tuning of the gain spectrum, tuning of the mode comb, or through a combination of both [5]. The gain curve of the laser can be tuned by varying the wavelength dependence of the active medium gain, or by using mirrors in which the wavelength selective loss can be tuned. Although wide tuning ranges are available, this method results in strongly discontinuous tuning and issues with multi-mode operation and wavelength ambiguity, as illustrated in Fig. 5.4(a)(ii) where tuning the gain curve results in two modes of equal power. For clarity, in Fig. 5.4 the position of modes which lie outside the gain spectrum are shown dotted in grey.

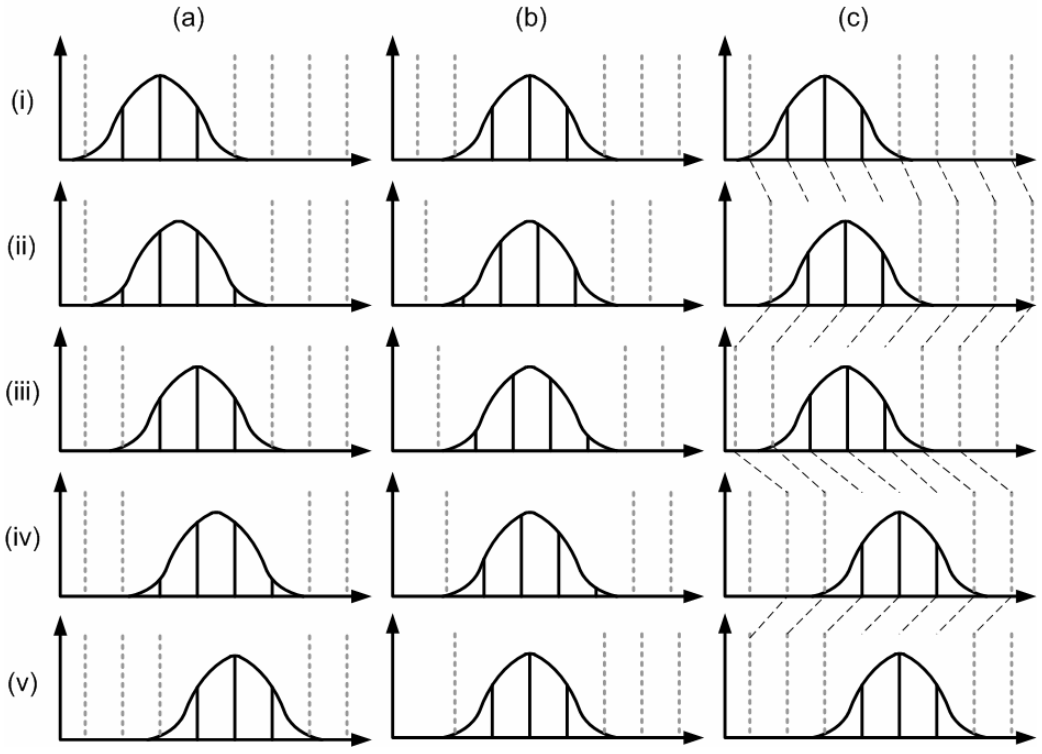

Fig. 5.4: Wavelength Tuning; a) Gain spectrum tuning; b) mode-comb spectrum tuning; c) combined tuning.

The second method of tuning is achieved by varying the spectrum of the mode comb. This is achieved by varying the phase condition in the cavity via adjustments to the length of the cavity, which is the method used in an External Cavity Laser (ECL), or via adjustments to the refractive index in the cavity. This method is shown in Fig. 5.4(b). It results in continuous tuning with a tuning range equal to the mode spacing. Tuning further than one mode spacing results in a mode hop that cancels out the wavelength shift. Clearly this method offers the advantage of continuous tuning but is limited in the range it can tune over due to the shape of the static gain curve. Through simultaneous variation of both the gain spectrum and the mode-comb spectrum, quasi-continuous tuning over a wide range can be achieved as depicted in Fig. 5.4(c). Here, the dashed lines between Fig. 5.4(c) (i) - (v) show that the mode has been tuned across to the point of a mode hop. Between these points, continuous tuning is available giving quasi-continuous tuning across the entire band.

5.6 Laser Diode Tuning Methods

As discussed in the previous section, variation of the gain spectrum, together with variation of the mode comb spectrum allows for quasi-continuous tuning of the laser across a large range of wavelengths. The mode comb is varied by changing the phase condition in the cavity, either via a change in cavity length, or via a change in the refractive index in the cavity. In external cavity lasers (ECLs) the cavity length is varied mechanically in order to achieve this phase condition change. However this results in relatively slow tuning times. In order to achieve very fast tuning times, the refractive index method must be used. With regard to the gain spectrum variation, in general a Bragg grating is used to give wavelength selective loss such that lasing only occurs at the wavelength of minimum loss. This wavelength is set by the pitch of the grating, and the effective refractive index of the grating. Because the pitch of the grating is fixed in the fabrication process, only the refractive index can be easily used to tune the gain spectrum. Therefore in order to tune the output wavelength, it is necessary to vary the refractive index of a phase element and/or an amplitude element of the laser. In semiconductors refractive index tuning can be achieved using field effects, thermal control and carrier injection.

The electric field method, although extremely fast, only causes a small change in the refractive index of a semiconductor, and as such limits the tuning range available. Thermal refractive index changes allow wider tuning than are available with electric field variation,

although excessive heating eventually limits the tuning range. In addition, the speed of thermal tuning is much slower than that of the electric field method. The most suitable method of refractive index variation for tunable lasers destined for WDM applications is carrier injection. It allows much greater changes in refractive index than the electric field method, while offering much faster tuning than thermal tuning.

The following sections will discuss a number of TL designs. Section 5.7 describes three which are fixed single mode lasers in which some degree of tunability is available. Section 5.8 describes some general aspects of widely tunable lasers which employ techniques and technology gleaned from the static lasers. Section 5.9 describes one of these lasers, the SG-DBR in greater detail and details some experimental work carried out on an SG-DBR. Finally in section 5.10, the novel TL known as the tunable SFP laser will be described along with experimental work carried out on it.

5.7 Wavelength Tunable Single Mode Lasers

5.7.1 DFB

The Distributed Feedback (DFB) laser [6] was developed as a single frequency laser, and is perhaps the most common laser used in WDM networks today. With an active region and grating which run the entire length of the device, as shown in Fig. 5.5, DFBs are relatively simple to fabricate. Although facet mirrors can be used to increase the power output, they are not required as frequency selective feedback from the grating provides the conditions necessary for lasing.

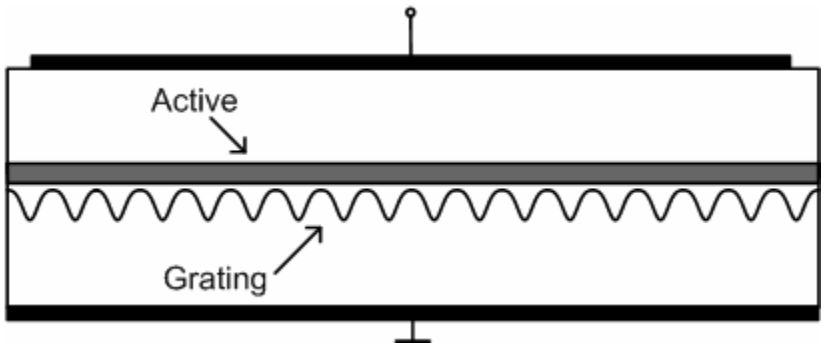

Fig. 5.5: Schematic of a DFB laser

Wavelength tuning in DFB lasers is generally performed via thermal control, therefore slow but very stable, precise and mode-hop free wavelength variation can be achieved. The emission wavelength changes by approximately 0.1nm/°C and hence tuning ranges are

limited to around 5nm with a 50°C change in temperature. To offer wider tuning ranges various component vendors have developed selectable arrays of 8 – 12 DFB lasers that can operate at any wavelength across the C-band. Optical coupling [7,8] or an external Micro-Electro-Mechanical (MEM) mirror [9] is used to output the operating wavelength of the array. The main drawback of using arrays is the power loss associated with the coupler option or the moving part associated with the MEM mirror option. Also the slow tuning times reported, measured in seconds, limit their use for future dynamic functionality.

5.7.2 DBR

Distributed Bragg Reflector (DBR) lasers also make use of a diffraction grating for mode selectivity and tuning, but in contrast to the DFB, the grating section of the DBR is separated from the active region as shown in Fig. 5.6. The leftmost section in Fig. 5.6 is the gain section, and this is separated from the wavelength selective Bragg grating by the central passive phase section. The separation of the gain function and the wavelength or mode selective function in the DBR, reduces the influence of the wavelength tuning on the gain functionality and allows greater tunability, in comparison to DFBs. The facet at the gain section is polished so as to provide reflection, while the other facet is anti-reflection (AR) coated to ensure that reflections are predominantly from the Bragg grating rather than the facet. The output power is determined by I_A, the current into the gain section. The cavity gain peak wavelength is controlled by I_B, the current injected into the Bragg grating and the mode positions can be aligned with the Bragg peak by I_P, the current injected into the phase section. In this way the laser wavelength can be fine-tuned to achieve a higher SMSR. Quasi-continuous tuning ranges of approximately 10nm were achieved in [10] while discontinuous tuning across 17 nm was achieved in [11].

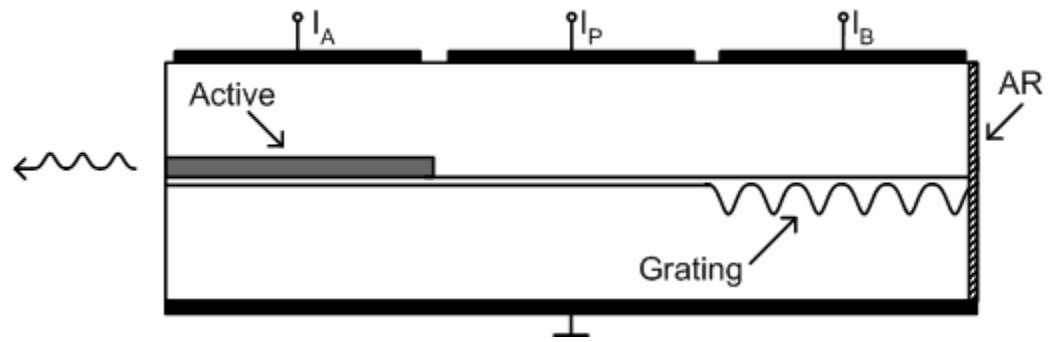

Fig. 5.6: Schematic of a DBR laser

5.8 Widely Tunable Lasers

The DFB and DBR lasers discussed above are limited to a maximum tuning range of ~15nm due to the limitation of the refractive index variation achievable in a waveguide. Tuning action achieved by varying two periodic structures with slightly different pitch is known as Vernier tuning and is illustrated in Fig. 5.7. Here, rather than overlapping modes in a cavity, two combs of reflectance peaks are set up such that only one pair overlaps. Then by slightly tuning one of the combs a large tuning jump is achieved. The Vernier technique is widely used to increase the tuning range of tunable lasers discussed in the subsequent section. For WDM systems it is desirable to have wider tuning ranges covering at least the C-Band. As seen in Fig. 5.7, wider tunability can be achieved by changing a refractive index difference between sections of a laser as opposed to the refractive index itself [5]. Various devices capable of this wide tuning can be grouped according to the headings of the following subsections.

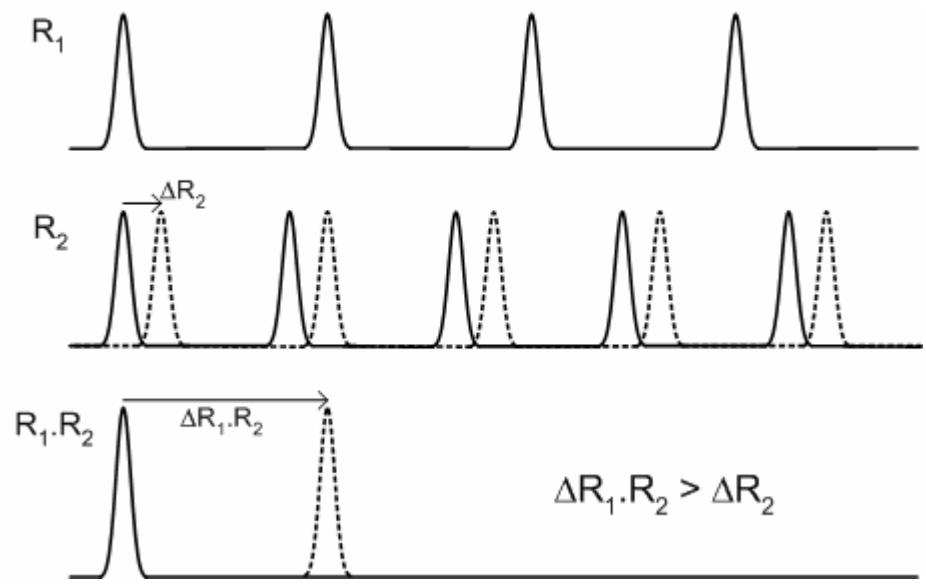

Fig. 5.7: Vernier Tuning

5.8.1 Interferometric structures

Two laser cavities of slightly different length will have mode spectra which are non-identical. If they merge together at a 'Y' junction similar to the output of a Mach-Zehnder interferometer the modes from the two cavities will interfere constructively and destructively and by varying the refractive index of one or both of the cavities wide tunability can be achieved. The lack of a grating in such lasers simplifies fabrication but also reduces the

SMSR of the output. Lasers in this group include the Y-laser [12] and the Vertical Mach-Zehnder (VMZ) laser [13].

5.8.2 Co-directionally coupled structures

In contrast to the previously discussed DFB and DBR lasers where the grating provides coupling between two modes travelling in opposite directions, in this type of design, the coupling is between modes propagating in the same direction. A filtration element is formed by vertically stacking two waveguides of different thickness and material. They will have different propagation constants and so coupling between light travelling in them will be weak. The introduction of a grating in parallel to the waveguides improves the coupling between them where the grating provides phase matching between the modes. Variation of the refractive index provides frequency selective filtration and hence laser tuning. Lasers in this group include the Amplifier-Coupler-Absorber (ACA) laser [14] and the Vertical Coupler Filter (VCF) laser [15].

5.8.3 Grating-based structures

These lasers are similar to the DBR laser in that they employ grating-type reflectors for mode selectivity. Here though, the grating is often modified, such that it provides a periodic comb-like reflection spectrum, as opposed to providing a single reflection window. This is done by periodically 'blanking out' the grating resulting in a sequence of equally spaced bursts of grating. The use of slightly different gratings at either end of the device enables the Vernier tuning effect mentioned previously which greatly extends the tuning range. Lasers in this group include the Sampled Grating DBR (SG-DBR) which is used in this work, the Sampled Grating DFB (SG-DFB), and the Super-Structure Grating DBR (SSG-DBR) [16].

5.8.4 Combination Structures

A number of lasers have been developed which combine elements from more than one of the groups above. For example the SMSR in the basic co-directional coupling lasers is poor due to a wide filtration bandwidth and the Grating Coupled Sampled-Reflector (GCSR) laser [17] adds a sampled reflector at one end to improve the SMSR while keeping the wide tuning range. Another example of this combination is found in the Modulated Grating Y-structure (MGY) laser [18].

5.8.5 Summary

A number of different techniques which can be used to achieve wide tuning ranges in electronically tunable laser diodes have been discussed. The next section describes experimental work which was carried out to characterize two widely tunable lasers. The first is a commercially available SG-DBR laser and the second is based on the SFP structure which does not fit into any of the categories detailed above. This laser will be discussed in detail in section 5.10.

5.9 Experimental Work – SG-DBR

5.9.1 SG-DBR Laser

The SG-DBR laser [19,20,21] is very similar in structure to a DBR laser. It uses Bragg gratings as its mirrors and contains 3 passive sections (front mirror, phase section and back mirror) and one active gain section. Each section can be independently driven to achieve a wide, quasi-continuous tuning range. The sampled gratings are similar to those used in DBR lasers, except that the grating is masked out periodically leaving a repeating pattern of one section of grating followed by an un-etched section similar to the simplified version shown in Fig. 5.8. The resultant reflection profiles is a periodic comb with narrow peaks of reducing amplitude centred on the Bragg wavelength.

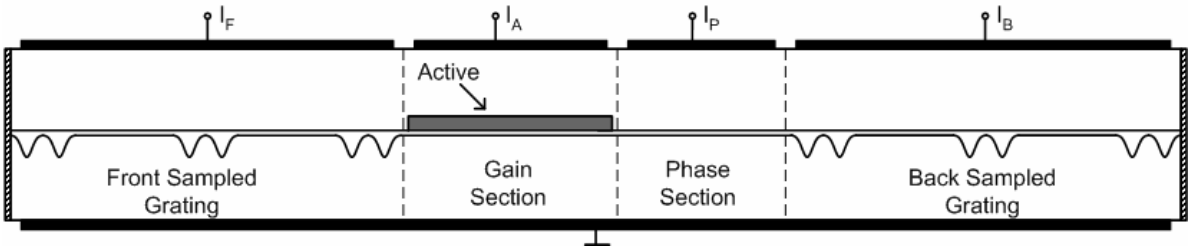

Fig. 5.8: SG-DBR laser structure

Gratings with slightly different periods are used in the front and back mirror in order that only one peak overlaps and the mirror loss seen by the propagating modes is the product of the two mirrors. The wavelength at which two peaks align experiences the lowest mirror loss and hence allows lasing to occur. Tuning is achieved by current injection into one or both of the grating sections; by tuning both mirrors by the same amount, continuous tuning over a small range is available while differentially tuning the sections gives rise to the Vernier effect and wider tuning. As with a regular DBR laser, the phase section is used to ensure that the mode is centred on the peak of the reflection spectrum ensuring good SMSR.

The mid-chip positioning of the active gain section of SG-DBR lasers reduces the output power achievable from them. In addition, because the front mirror may require high drive currents to reach the outer wavelengths, a wavelength dependent loss can occur in this section leading to an output power which varies for different channels. Uniform output power can achieved through tuning of the gain section however gain section variations can also affect the wavelength so more often a semiconductor optical amplifier (SOA) is integrated with the SG-DBR for power control [22]. This SOA also serves as an output blanking mechanism which blocks the laser emission and ensures that spurious modes are not transmitted during a tuning/switching event.

5.9.2 Lookup Table

The complex tuning current arrangements required to obtain quasi-continuous tuning from an SG-DBR laser generally dictates that the laser tuning is controlled by a micro-processor that accesses a lookup table containing the currents required for the three sections in order to tune to a desired wavelength. A block diagram typical of a commercially available SG-DBR laser is shown in Fig. 5.9.

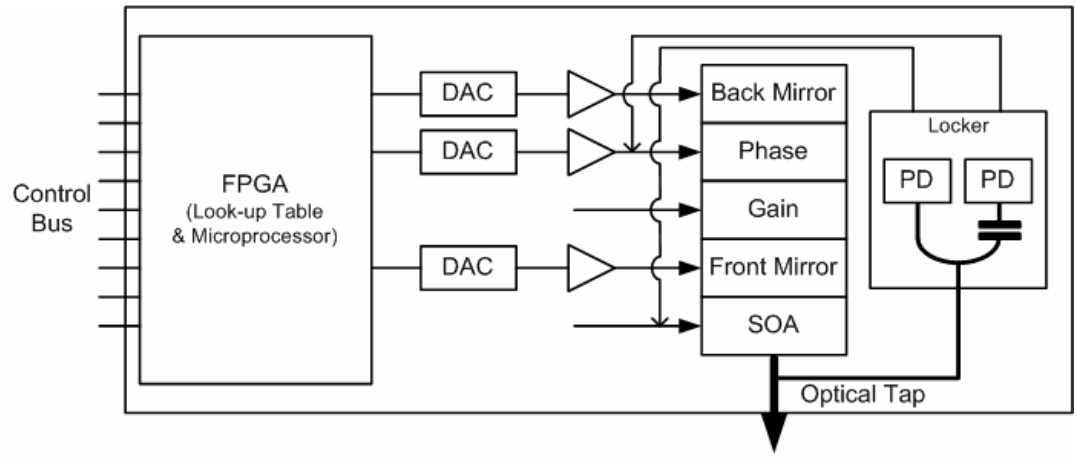

Fig. 5.9: SG-DBR TL module with wavelength and power feedback control block diagram

The lookup table can be generated using simple experiments in which the light output is coupled directly into an optical spectrum analyser (OSA). The gain and phase section currents are then kept constant and the mirror currents are varied in order to obtain information about the peak wavelength, output power and SMSR at each pair of mirror currents. A sample wavelength map is shown in Fig. 5.10. Generally, such maps are generated for a number of phase currents until each wavelength channel on the ITU grid can

be attained. Fine tuning of the output power is performed using the gain section drive current and the four current values are entered into the lookup table against that particular wavelength. Should a particular channel be available using a number of different current combinations the lowest total current is generally used [23]. Generation of lookup tables in this manner is slow and must be performed for each laser. Methods of speeding up this characterisation were reported in [24] in which output power (a faster measurement), and low resolution wavelength measurements are initially performed. Following this, high resolution characterisation is only performed around current levels which look promising for operation.

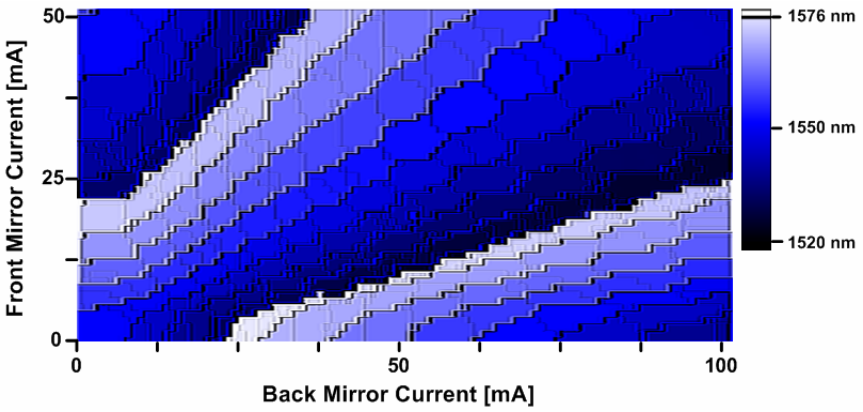

Fig. 5.10:Wavelength map for an SG-DBR laser

5.9.3 Wavelength Locking

The ITU Recommendation G692 [25] advises that the emission frequency of a TL should deviate by no more than $(f_S-2B)/4$, where f_S is the channel spacing and B is the channel bit rate. A tunable laser may sit at a particular channel for widely varying timescales, from nanoseconds in packet switching applications to months or years in sparing applications. Due to environmental factors and ageing, the frequency can drift and so, as shown in Fig. 5.9 feedback based wavelength lockers are often used to ensure that the laser remains within tolerance. A small portion of the laser output power is tapped off and split between two paths, one of which is passed through an etalon filter and detected by a photodiode and the other of which is detected directly. The electrical signal produced by the filtered signal gives information about wavelength drift and can be fed back into the phase section in order to correct for this. On the other hand, the directly detected portion provides an error signal for the output power and this can be fed back into the SOA.

5.9.4 Switching Speed

As mentioned in section 5.6, lasers can be tuned using temperature, electric field variations and carrier injection. The use of the electric field through the electro-optic effect is the fastest, but offers only small changes in refractive index and hence small tuning ranges. Thermal tuning offers wider tuning ranges but is much slower. Carrier injection tuning offers the best compromise for WDM lasers in that wide tuning ranges are available with relatively high speed switching. With carrier injection tuning, the speed of tuning is limited by a number of factors:

1. Carrier Lifetime – Through the injection of current, variation in the carrier density causes the refractive index of the mirror and/or phase sections to change leading to tuning. The tuning speed is inherently limited to the spontaneous carrier lifetime in these passive tuning sections [26]. The required carrier density for the source and destination channels will impact the switching time. Larger differences in carrier densities result in longer switching times.

2. Device Structure – In [27] the authors address issues relating to the structure of the device which can impact the maximum tuning speed available. These issues include thermal management which is improved by mounting the device p-side down to improve the heat-sinking, and reduction of mirror comb spacing which allows tuning to be achieved with lower currents swings.

3. Driving electronics – The speed of the electronics which are used to control the device also limit the total tuning speed available. The 'latency' is the time between the request for a new channel and the time that the laser begins to switch. During this time the look-up and other calculations are performed prior to the currents for the new channel being sent to the device. In addition feedback electronics can add to the settling time. In commercial devices, micro-processors are often used for practical control of the fast tunable lasers. Sub-50ns wavelength switching was reported in [28] for an FPGA based module, with transitions between a large number of random combinations of a 64 channel system on a 50 GHz spaced grid.

5.9.5 Spurious Mode Generation

In WDM applications it is very important that lasers which are tuning do not emit on any wavelength other than the destination wavelength which is being tuned to. Emission at

spurious wavelengths can cause severe interference on other data channels at those wavelengths. However because the drive currents used to tune the laser vary continuously, it is very likely that intermediate currents between the source and destination current will lead to the generation of spurious modes. This is illustrated in Fig. 5.11 in which emission changes over time from a source to a destination wavelength via a number of intermediate wavelengths which may be reached by longitudinal mode hops or by super mode hops.

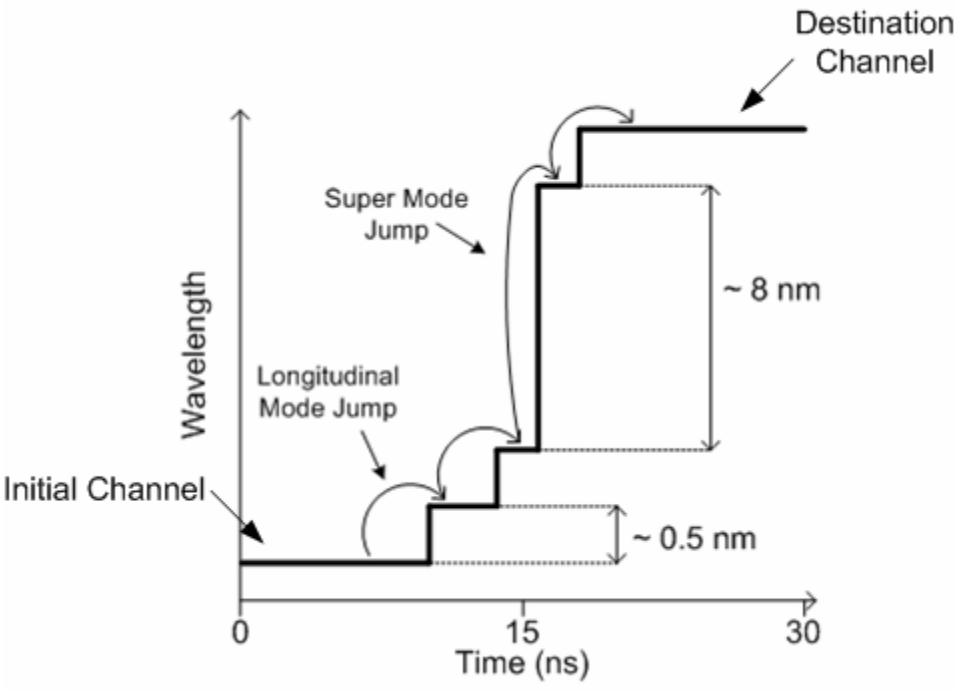

Fig. 5.11:Wavelength variation versus time for channel transition

In [29], spurious mode generation was shown to impact severely on an intermediate wavelength when an un-blanked SG-DBR laser switched across it. Often, due to the low output power of SG-DBRs already mentioned, an SOA is integrated with the SG-DBR in order to boost output power. By reducing the SOA bias condition, from the saturated state used for power boosting, the laser output was reduced to -30 dBm during wavelength switching for an SG-DBR in [30]. Other methods of blanking include reducing the drive current to the gain section (which is not ideal due to the effects that this can have on wavelength), and the use of an external modulator in the 'off' position after the laser.

5.9.6 SG-DBR Experimental Work

A TL module [31] built around a monolithically integrated SG-DBR-SOA chip was used in this work. The continuous wave (CW) module output power was ~8.5 dBm and a good

SMSR (>40dB) was measured for all channels. The tuning range was 33.4 nm and within this range 85 channels spaced by 50 GHz were available as shown in Fig. 5.12. The module could be programmed to switch between any set of these 50GHz channels. For the first 50ns after a switch was initiated the emission on spurious wavelengths was possible and so the SOA was used for blanking for 60ns after the switch is initiated. After this time the laser was guaranteed to be within ±15GHz of its intended frequency. The wavelength locker was then used to reduce the frequency variation and after 200ns the emission frequency was guaranteed to be, and to stay within ±2.5GHz of the target frequency.

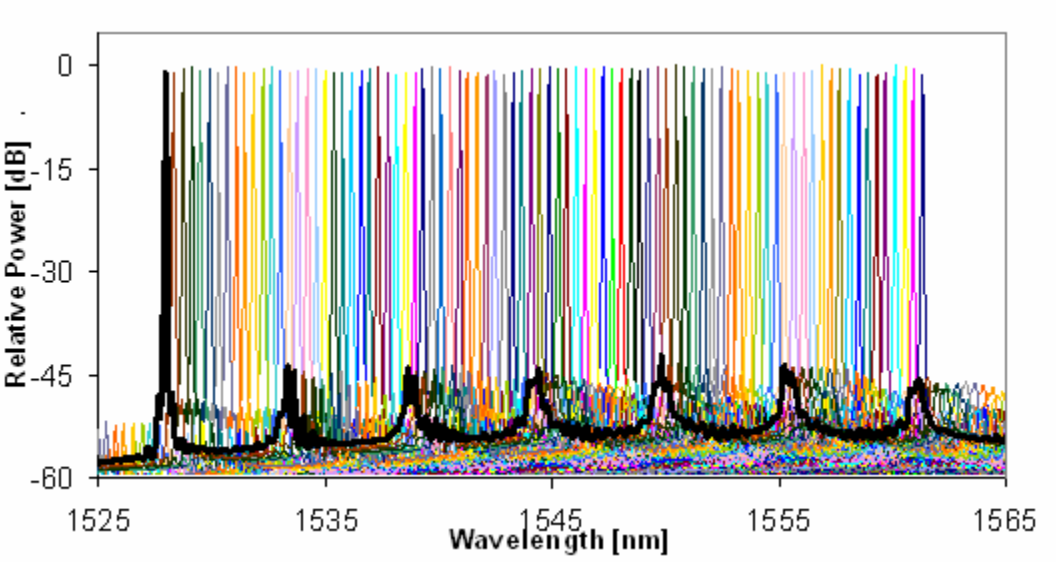

Fig. 5.12:Overlaid channel spectra from the SG-DBR module showing 85 50GHz spaced channels with SMSR > 40dB

5.9.7 Frequency Drift Experiment

As carriers try to pack more data into less bandwidth by reducing the WDM channel spacing or increasing the data rate per channel, the wavelength drift requirements of tunable lasers used in the system become increasingly stringent. In systems with channel spacing of 50GHz or less even a small drift could cause the laser to enter the pass-band of an adjacent channel leading to cross-channel interference. In this section, experimental analysis of the frequency drift of one of the SG-DBR laser modules described above is detailed. The instantaneous frequency drift of a TL module immediately after the blanking period is measured with high resolution using two different techniques. Initial characterisation is performed using an optical filter as a frequency discriminator. The results obtained are then verified using an

optical self-heterodyne technique. While this experiment is concerned with the drift from a single laser, in Chapter 6 this work will be built upon to investigate the effects of the wavelength drift in an optical packet switching system employing these lasers.

5.9.8 Optical Filter Technique

Using the experimental setup shown in Fig. 5.13, a tunable fiber Bragg grating (FBG) filter, with a 3 dB bandwidth of 27.5 GHZ, was operated as a sloped frequency discriminator [32, 33]. This method converts an optical frequency drift to an optical power drift. The filtered power falling on a photodiode was measured as a function of time. A power reference measurement was also taken (indicated by the dashed line in Fig. 5.13) by recording the power falling on the photodiode without the filter. This was then normalized out of the measurement to ensure that only power deviation caused by frequency drift was taken into account.

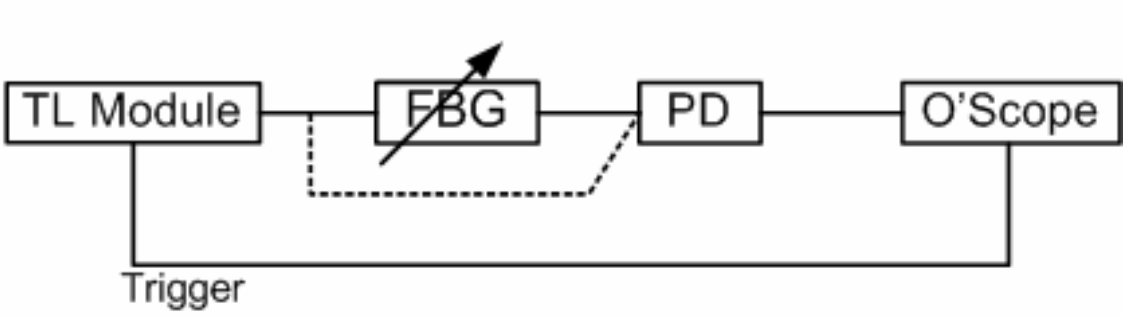

Fig. 5.13:Experimental set-up used to measure the magnitude and duration of the frequency drift after the TL comes out of blanking using an optical filter as a frequency discriminator.

The FBG is tuned to a wavelength such that the TL target channel lies in the middle of the slope of the filter as shown in Fig. 5.14(a). The filter profile was measured using a broadband light source and this provided a translation between power and frequency. Using the logarithmic scale allowed a wider drift to be measured.

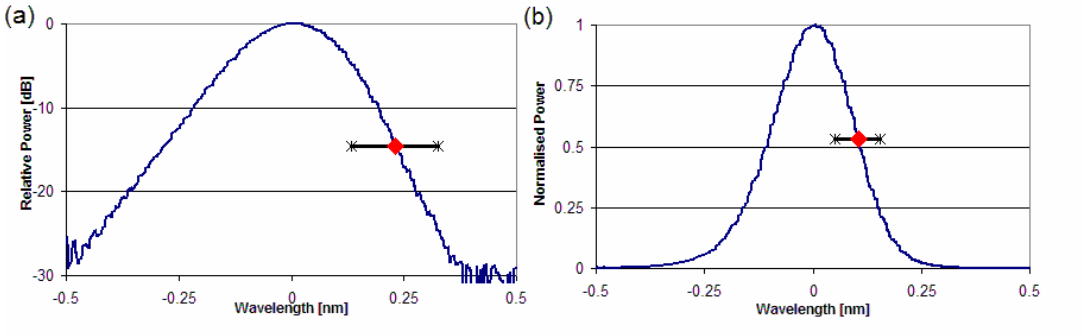

Fig. 5.14:Frequency response of the FBG filter using; a) the logarithmic scale; b) the linear scale and showing the positioning of the TL target wavelength and the maximum drift

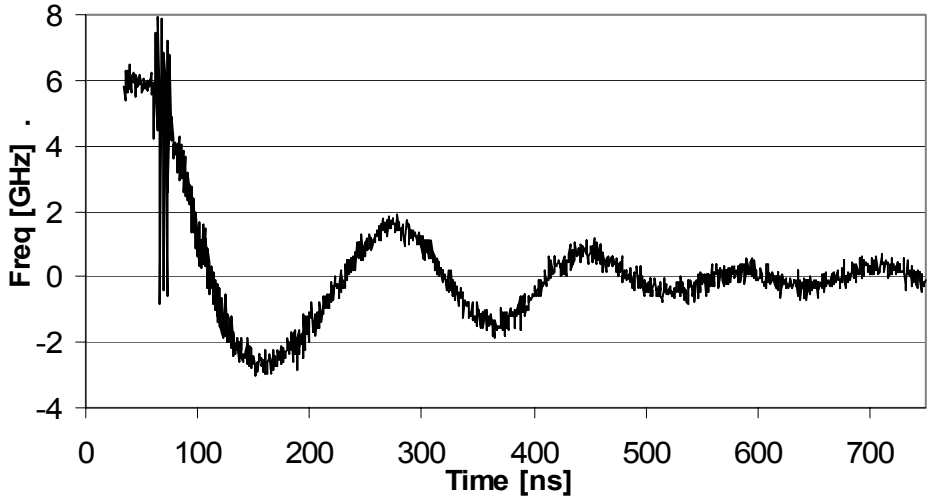

Fig. 5.15:Calculated instantaneous frequency of TL immediately after emerging from blanking

The frequency drift measurement presented is for the transition from Channel 42 (1548.915 nm) to Channel 52 (1544.924 nm). The calculated frequency drift for this transition is presented in Fig. 5.15, which shows the frequency deviation of the module output from the target ITU channel as a function of time. After blanking, the laser emission is approximately 6GHz from the target frequency. The fast fluctuation seen just after the switch is attributable to the wavelength locker switching on. Once the wavelength locker is engaged it takes approximately 100ns to bring the wavelength within the ±2.5GHz range after which it never strays from this range until receiving a new switching request. The total time taken to get within this range is within specifications at just under 200ns.

5.9.9 Optical Self-Heterodyne Technique

The method presented above for instantaneous frequency measurement is somewhat indirect and requires post-measurement data manipulation. To ensure the accuracy of the result, a second technique, based on an optical self-heterodyne measurement was employed. The experimental setup is shown in Fig. 5.16. The light from the TL module was split into a delayed path and a direct path and recombined to fall on a detector. A variable optical attenuator was used on the direct path to ensure that both paths experienced the same losses. By carefully choosing the optical delay the direct path signal appeared like a static source at the target frequency. Hence, when the delayed signal re-combines with the direct signal a beating signal is formed at the difference frequency between them. This beating frequency corresponds to the drift of the laser. Through the use of an electrical low pass filter, the times that this beating signal is within a certain frequency range can be viewed on an oscilloscope and by comparing this with the plot from the frequency discriminator experiment, the accuracy of the former measurement can be determined

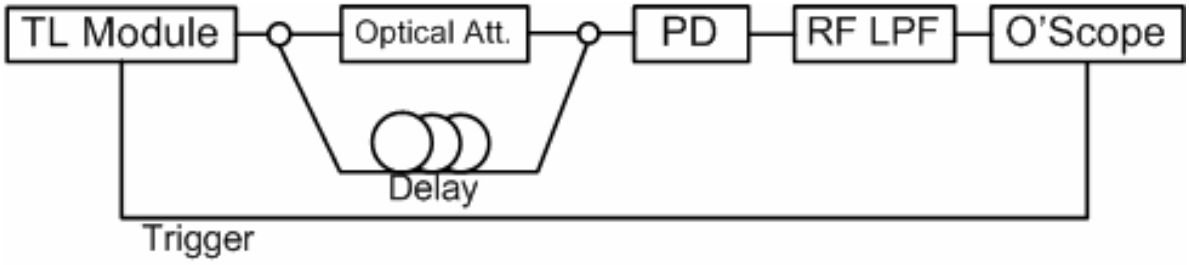

Fig. 5.16:Experimental set-up used characterise the frequency drift after the TL comes out of blanking using an optical self heterodyne measurement.

The lower plot of Fig. 5.17 shows the detected photocurrent after passing through a low pass filter with a 3 dB bandwidth of 117 MHz. Comparison of the figures show good agreement. The points at which the frequency discriminator plot crosses the 0GHz line corresponds well to the points where initial bursts of beating signal are seen on the oscilloscope trace. Any point on this trace where no beating is observed corresponds to time during which the laser is greater than 117MHz from its target frequency. The laser crosses its target wavelength and overshoots four times before finally settling to its target.

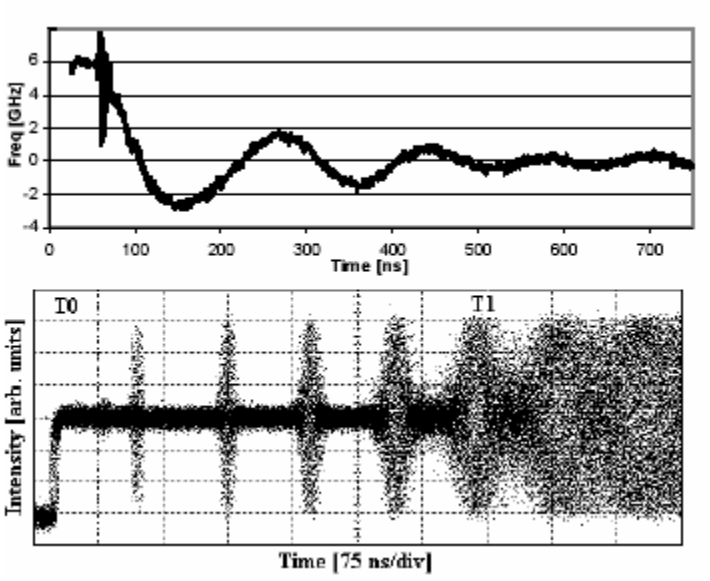

Fig. 5.17:Frequency drift characterisation of TL module for channel transition 42-52 using frequency discriminator (top) with self heterodyne technique for comparison (bottom)

5.9.10 Conclusion

This section discussed the SG-DBR laser in detail and described an initial experiment carried out using one such laser. The frequency drift of the laser was observed to be as much as 7.5GHz which could potentially lead to performance degradation in certain systems. In [34] it is shown that in Ultra Dense WDM (UDWDM) systems such as access networks that may use channel spacing as low as 12.5GHz, critical error floors are observed due to this drift. Furthermore, similar performance impairments which could affect the routing of packets in an optical packet switching system will be demonstrated in Chapter 6.

5.10 Slotted Fabry-Pérot Lasers

5.10.1 Background

Most of the widely tunable lasers available today, including the SG-DBR laser described above, require complex re-growth and processing techniques in fabrication which leads to a low wafer yield and high cost lasers. As such, a widely tunable laser, which can be fabricated using simpler, low cost techniques, is highly desirable. To obtain a single transverse mode from a Fabry-Pérot laser the active layer can be reduced in width to form a so-called 'ridge waveguide' [35]. Reflections caused by perturbations (in this case, short increases in ridge width) added to the ridge waveguides were shown in [36] to provide single longitudinal

mode emission. Later work [37] used a similar technique to obtain single mode operation but rather than varying the waveguide width, slots were etched into the waveguide to a depth just above the active region. This method is simple and cost effective as it does not require any re-growth or complex processing steps. By using slightly larger slots at certain points the device can be isolated into independent sections which can then be driven differentially to achieve a wide tuning range using the Vernier effect [38]. In these lasers the facet reflections are the primary source of feedback while the location and pattern of the slots provides the filtering required for enhanced spectral purity.

Throughout this work, a number of devices with different structures were tested and characterised but the majority of the work reported here refers to two devices which will be referred to as Device 1 and Device 2. During the fabrication the slots were etched into the ridge waveguide to a depth which just penetrates the top of the upper waveguide resulting in an internal reflectance of ~ 1% at each slot. A general schematic of the devices is shown in Fig. 5.18 along with a diagram showing actual dimensions for Device 1 in Fig. 5.19.

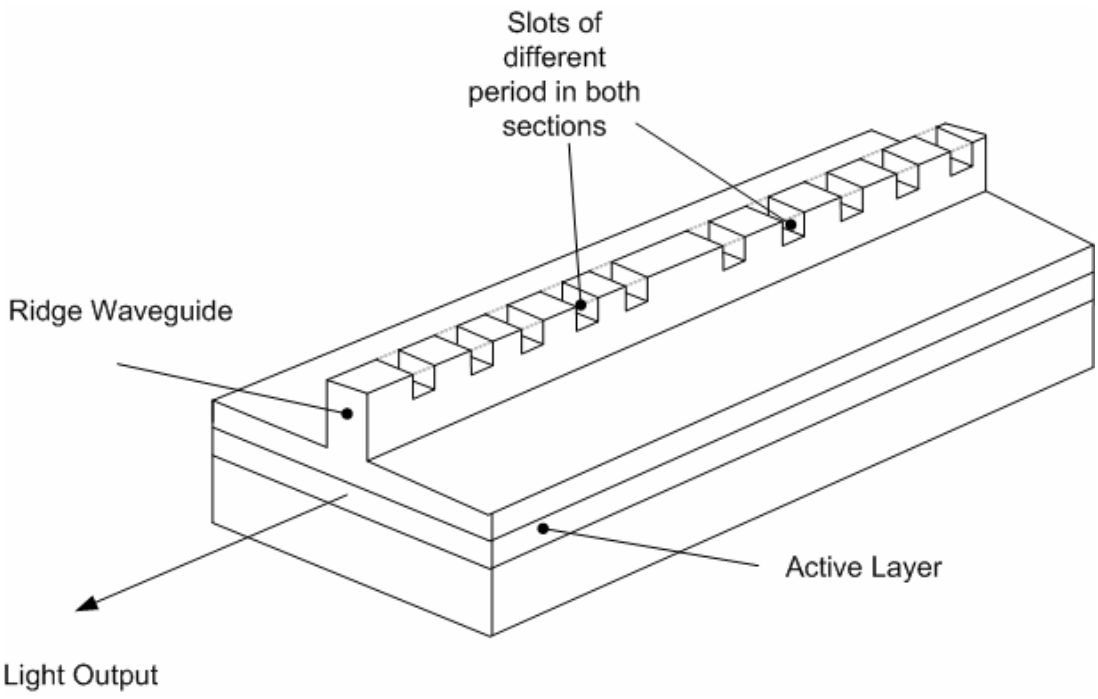

Fig. 5.18:General schematic of the tunable SFP laser

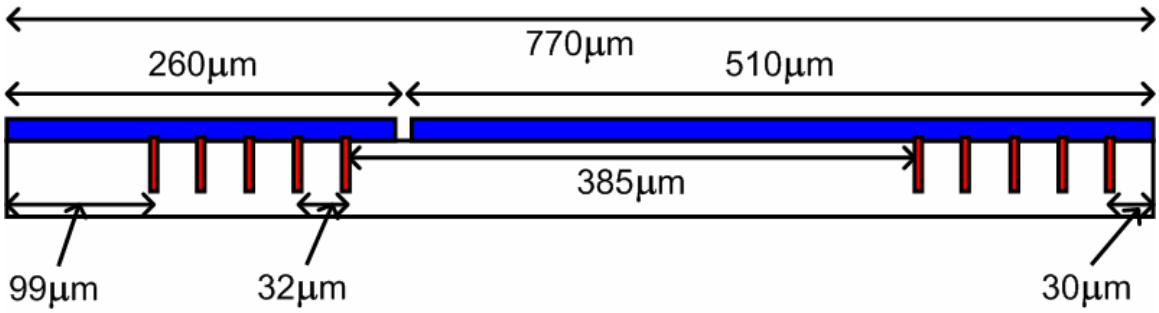

Fig. 5.19:Actual dimensions of tunable SFP 'Device 1'

Device 1 had a total length of 770 µm which is split into two sections by removing the metal and highly doped cap layer near the centre of the ridge allowing each section to be driven differentially. Section 1 had a contact length of 260 µm and contained 5 slots, spaced 32 µm apart, and located 99 µm from the front facet. Section 2 had a contact length of 510 µm and contained 5 slots, also spaced 32 µm apart, and located 30 µm from the back facet. Due to the relatively large reflectivity from the individual slots, a number of sub-cavities are formed. The sub-cavity between both sets of slots sets the dominant FP mode spacing in the laser spectrum. The 32 µm slot separation results in a comb like mirror loss spectrum with a free spectral range of approximately 10 nm which sets the supermode spacing. Finally, the sub-cavities between the facets and the slots set up a modulation of the mirror loss spectrum such that a single mode dominates. As the sections of the laser are differentially driven, the local refractive index is changed resulting in a change in the resonant conditions favouring one of the supermodes.

Further explanation of the physics of tunable SFP lasers can be found in [38] and references therein. Although the paper details work carried out on a laser based around 1310nm, the concepts are all identical. It presents basic characterisations including P-I and V-I curves, and mirror loss and reflectivity spectra. This thesis is more concerned with the devices from a communication and engineering perspective, and so concentrates on aspects including switching times and the modulation and transmission of data using the devices. All experiments were carried out on using the laser in bare chip form, mounted on a ceramic test board and without temperature control. The mounted devices are shown in Fig. 5.20(a). The ceramic test board consisted of a ground plane consisting of two large gold pads connected with a thin gold strip. A screw hole in the back of this ground plane ensured electrical grounding with the aluminium mount used. Ten smaller gold pads around the edge

of the submount were wire bonded to five two-section devices on a single chip. A circuit board with two strip-lines was soldered to the gold pads of the device in use and the circuit board and submount were mounted onto the aluminium block. Sub-Miniature version A (SMA) connectors were connected to the aluminium mount and soldered to the other end of the strip-line to provide drive current. The emitted light was coupled into fiber using a Graded Refractive Index (GRIN) lens mounted on an XYZ translation stage as shown in Fig. 5.20(b).

(a) **(b)**

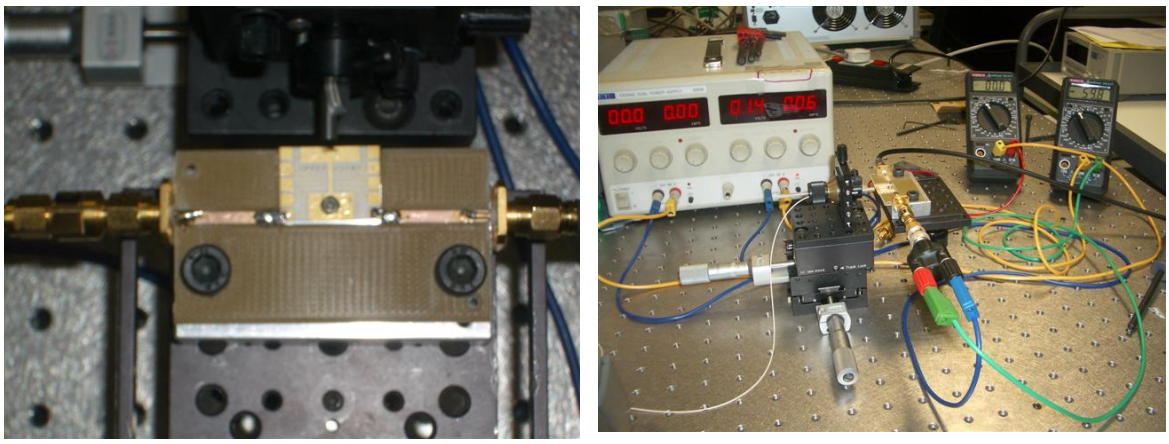

Fig. 5.20:Photographs of mounted laser chips

5.10.2 Wavelength and SMSR Map

Two of the fundamental characterisations which must be performed on a widely tunable laser are the wavelength and SMSR as a function of drive current (or currents). Samples of such plots from a similar device are shown Fig. 5.21 and Fig. 5.22 below. It can be seen from these plots that this laser can tune between 5 different modes by varying the front section alone and driving the back section with a constant current of approximately 50mA. The modes are spaced by approximately 10nm and cover a range of almost 40nm. With these lasers, a trade-off is made between having a large tuning range, quasi-continuous tuning, and a high SMSR. In this case, the quasi-continuous tuning was sacrificed for wide tuning range and a high SMSR of up to 46dB. In the wavelength plot, the large solid patches of colour indicate that a relatively small amount of continuous tuning is occurring and instead, once a boundary is reached, a super-mode hop occurs with very little further tuning. In addition the thin dark borders between the sections in the SMSR plot indicate that very little dual mode

operation is observed especially above 60mA on the back section. Fig. 5.23 shows the five single-mode spectra available from Device 1 overlaid and clearly presents even channel spacing and good single mode operation with SMSR greater than 35dB in all cases.

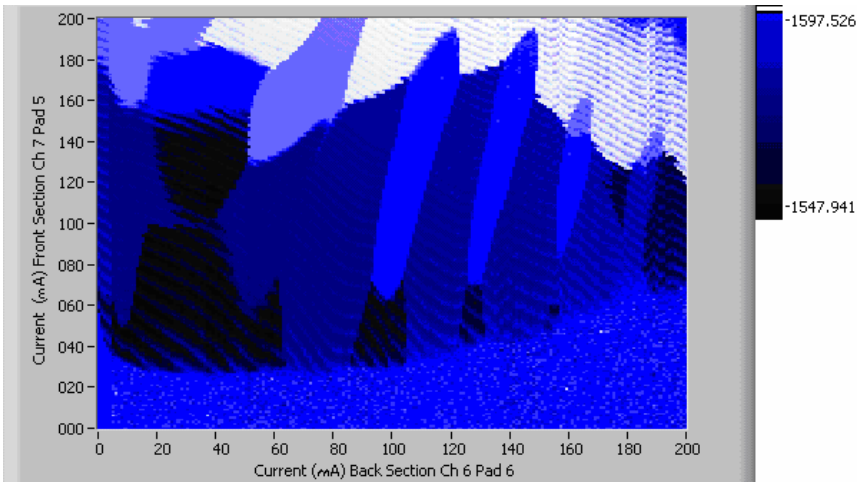

Fig. 5.21:Peak output wavelength as a function of current to the front and back section of an SFP laser.

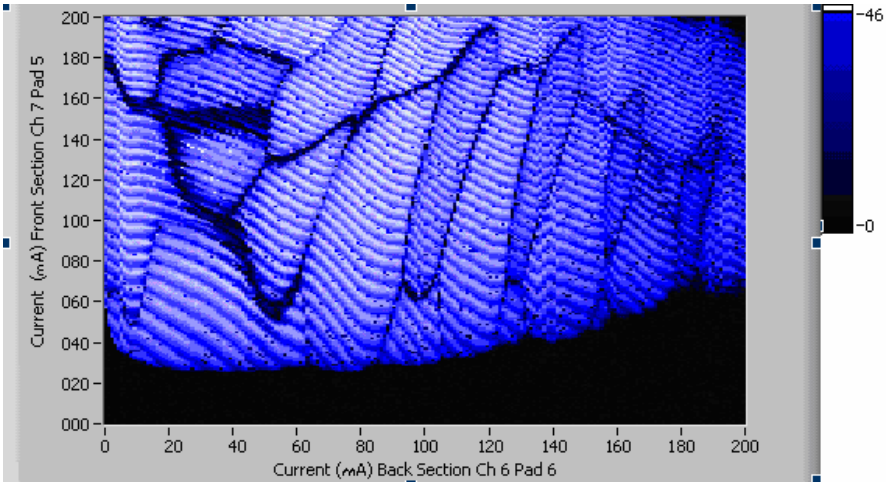

Fig. 5.22:SMSR as a function of current to the front and back section of an SFP laser.

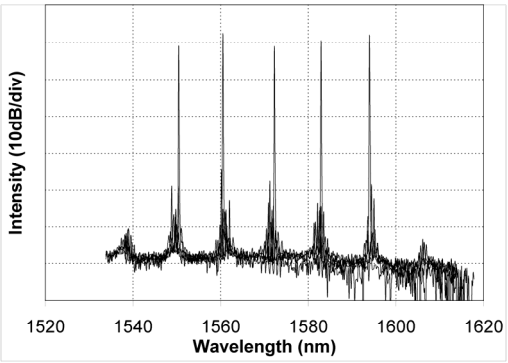

Fig. 5.23:Overlaid single mode spectra of Device 1 showing SMSR >35dB for each channel

5.10.3 Switching Speed

Having tested the channel spacing and the number of channels which could be switched between, the next matter of interest was the speed in which they could be switched. In order to test the switching speed of the device the experimental set up shown in Fig. 5.24 below was initially used. The front section of the Device 1 was driven by a *dc* current of 88mA, and the back section was driven by a square wave signal at a frequency of 50 MHz generated by an Anritsu pulse pattern generator (PPG). The square wave signal switched the current applied to the back section of the laser between 120 mA and 140 mA, which caused the laser to switch from 1560.5 nm (referred to as 'channel 1' henceforth) to 1593.9 nm (referred to as 'channel 2' henceforth) every 20 ns.

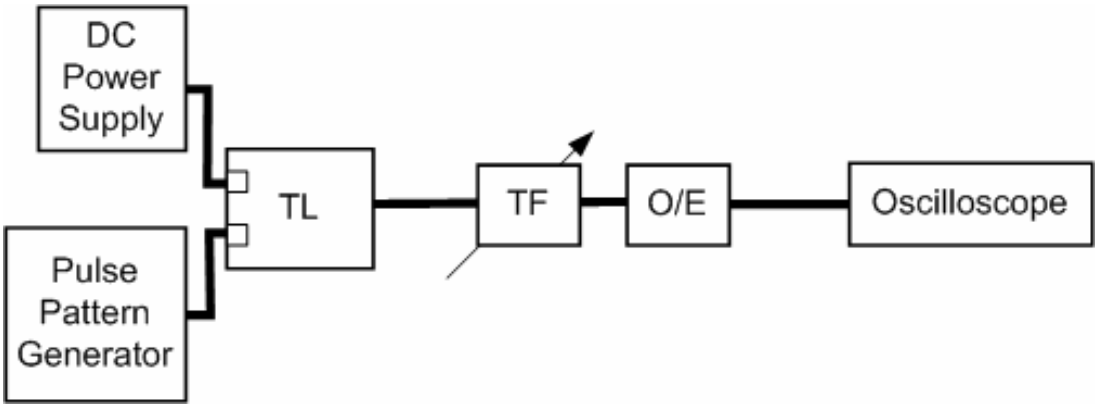

Fig. 5.24:Experimental configuration used to determine switching time of the laser. Comprised of tunable laser (TL), tunable band pass filter (TF), photodetector (O/E)

By aligning an optical band pass filter on channel 1 and passing the output of this filter into a photodetector that channel was selected out and the switch was viewed on an oscilloscope. The high level in the upper waveform in Fig. 5.25 corresponds to the time when channel 1 is on and hence light is passing through the filter. The low level in the upper waveform corresponds to the time that the laser is on channel 2. The lower waveform corresponds to the case when the filter was set to select out channel 2. From this result it is seen that laser switched on a timescale of a few nanoseconds between operating wavelengths.

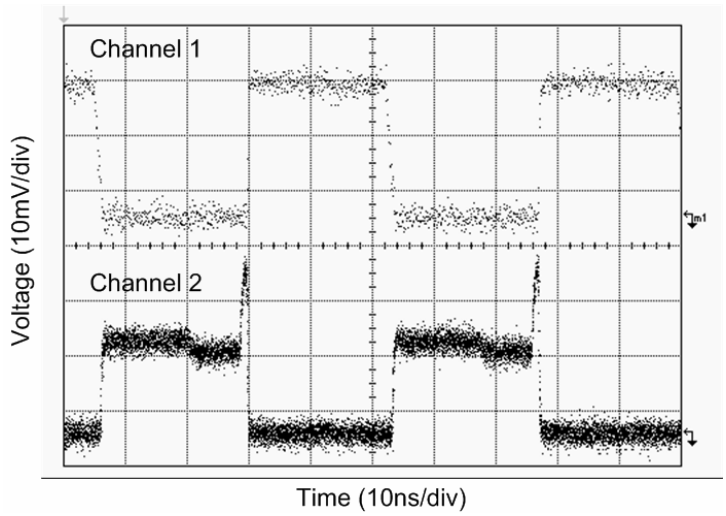

Fig. 5.25:Tunable laser switching between channels one and two with the filter set on channel one (top) and on channel two (bottom).

In order to more accurately measure how long it takes for the laser to switch wavelength, a heterodyne technique similar to that employed in [39] was employed, but in this case the beating signal was determined by setting the output frequency of an external cavity laser (ECL) to be 1 GHz from the channel 1 output frequency of the slotted FP laser. By placing a 1.87 GHz low pass electrical filter after the photodetector, the time taken for the laser to get within 1.87 GHz of the target frequency when it was switching from channel 2 to channel 1 can be determined. The experimental setup is shown in Fig. 5.26 and Fig. 5.27 presents the detected electrical signal as the laser is switching between channel 1 and channel 2 at a repetition rate of 50 MHz. The DC component corresponds to the time that the laser is operating on channel 2, and the modulated portion corresponds to the time the laser is operating on channel 1. It should be noted that the optical output power from the laser is slightly greater on channel 1 than on channel 2, thus the DC level when the laser is operating on channel 2 is below the centre level of the modulated signal. By investigation of the time when the laser switched from channel 2 to channel 1, it can be seen that the laser has completed its switch to within 1.87 GHz of it target wavelength after about 1.3 ns. It should be noted that unlike SG-DBR and GCSR tunable lasers that have passive tuning sections, these two section slotted FP lasers have only active sections. This ensures that the carrier lifetimes that may affect switching speed are limited by stimulated carrier lifetimes, and not spontaneous lifetimes as with SG-DBR and GCSR. It is thus possible to achieve very fast switching times with these devices. In fact, it is likely that the switching times achieved are

limited, not by the device itself but by the rise and fall time of the drive electronics and by the low speed packaging used. A similar switching time can be expected for all channel combinations due to the fact that the same tuning mechanism is responsible for each switch and we have measured the switching time for other combinations to be within 10% of the result presented here.

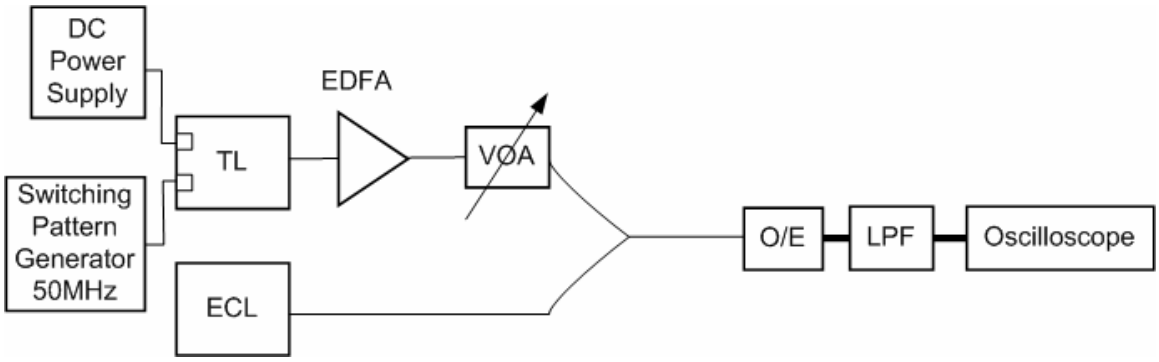

Fig. 5.26:Experimental setup for the heterodyne technique

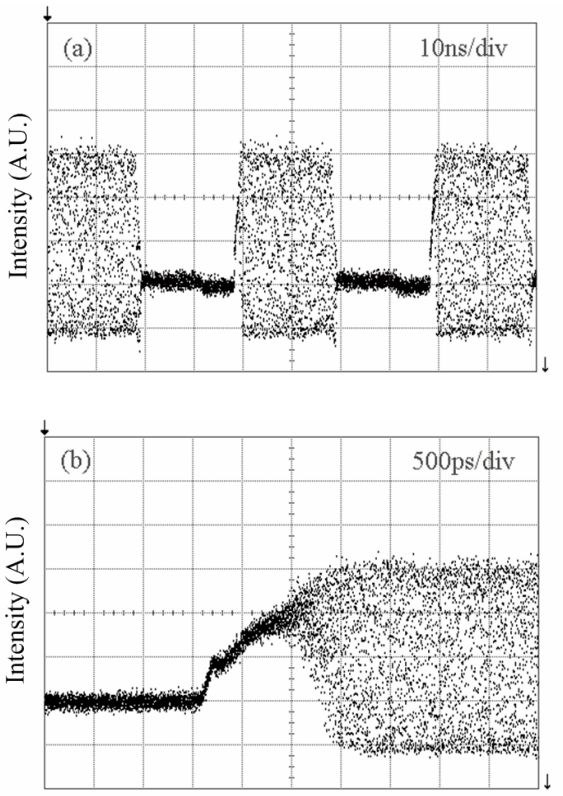

Fig. 5.27:Beating signal generated when output of switching laser is mixed with ECL signal 1 GHz away from 1 channel from slotted laser with (a) 10 ns/div (b) 500 ps/div.

5.10.4 Modulation

For Device 2 the design of the laser was refined in an effort to reduce the spacing between channels. The length of the device was increased to 1040 microns and this length was divided into three sections as opposed to two. The front, middle, and back sections were 180, 690 and 170 microns long respectively and in this work the back and middle sections were tied together electrically allowing simpler control of the device. While all sections were active, only the front and back sections contained slots. Using this design, the average channel spacing was reduced to approximately 2.7nm (340GHz) and the number of channels increased to 8 channels spread over approximately 19nm.

Having shown that tunable lasers based on the SFP structure could be switched very quickly, for use in communication systems it was vital to demonstrate that high speed data could be transmitted error free while the device was switching. In an optical packet switching system, it is important to know how soon after the switching event the laser can be modulated with the data packet, as this will directly affect the network throughput. This was evaluated using the experimental set up shown in Fig. 5.28.

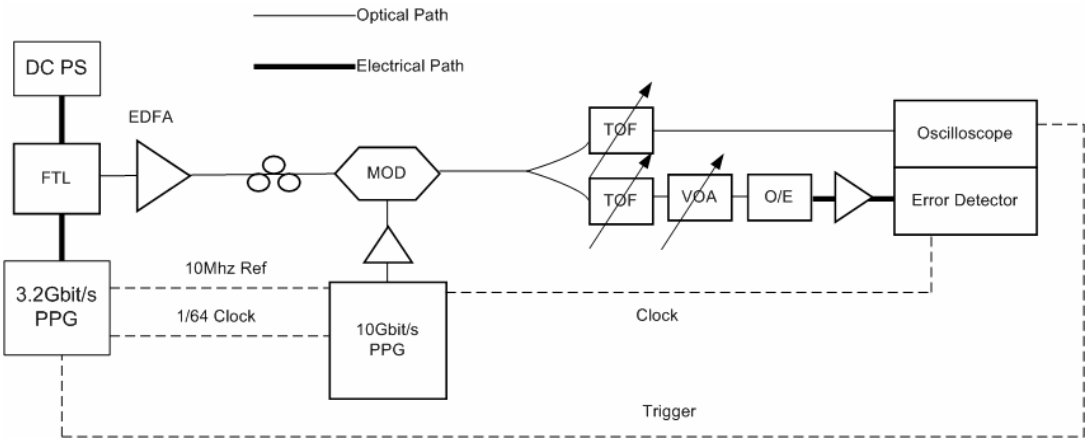

Fig. 5.28:Experimental Setup used to measure the switching speed of a modulated SFP laser

For the switching measurements, the back and middle section were driven with a DC current of 148mA and the front section was directly driven with a Non-Return to Zero (NRZ) pattern generator with rising and falling edge times of 365ps and 130ps respectively, peak to peak amplitude of 185mV and an offset of +387mV. This caused the optical output from the laser to switch between channels at 1537.5nm and 1540nm, which will be referred to as channel 1 and channel 2 respectively. The optical signal was then amplified and externally modulated with a 10Gb/s NRZ Pseudo-Random Bit Sequence (PRBS) data before being

split with a 50:50 coupler. Each portion was then passed through a tunable optical bandpass filter with a bandwidth of 0.2nm centred on the channels. Both filtered channels were viewed on a digital sampling oscilloscope. Fig. 5.29 shows both channels switching on and off. It should be noted that the path lengths for the two channels were not identical due to different filters being used, hence the time difference between the switch on of one channel and the switch off of the other channel are not to scale. In order to view both events on the oscilloscope at the same time different measurement offset times were used for each channel.

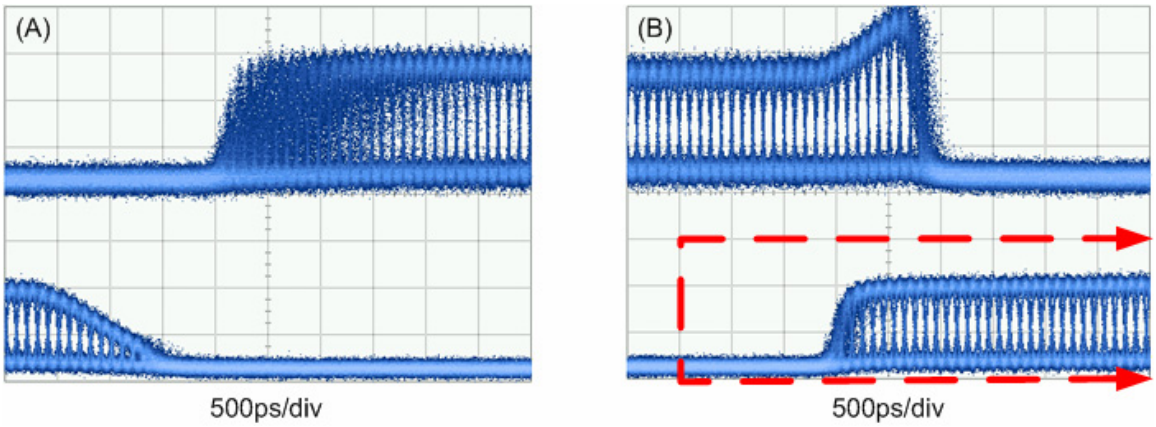

Fig. 5.29:Switching SFP eye diagrams; a) Channel 1 exhibiting a switch on time of less than 500ps and channel 2 showing a switch off time of approximately 1ns; b) Channel 1 exhibiting a switch off time of less than 500ps and channel 2 showing a switch on time of less than 500ps. The dashed red line represents 4.5ns of the 10ns gating window which was stepped across to measure the time resolved BERs. Clearly for 1.5ns of this time 50% of the bits will be in error because the laser is on the other channel.

Fig. 5.29 shows that both channels exhibit a rise time of <500ps and the fall times are <500ps and ~1ns for channel 1 and channel 2 respectively. These times are in agreement with the self-heterodyne measurements described previously. It is also seen that the eyes are open after less than 3ns for the 1540nm channel and less than 1ns for the 1537.5nm channel. It is expected that the closed eye at the beginning of the traces is due to jitter in the switching time accumulating in subsequent acquisitions of the sampling oscilloscope and wavelength drift under the filter passband.

In order to measure how soon after a switch, data could be transmitted error free, time resolved bit error rate (BER) measurements were taken by repeatedly counting and aggregating the number of errors in a 10ns (100 bit lengths) gating window, which could be

moved with a maximum resolution of 10ps. The dashed red line of Fig. 5.29 represents 4.5ns of the 10ns gating window which was stepped across to measure the time resolved BERs. With this sample gating position, 1.5ns of the gating windows lies outside the signal so during this time 50% of the bits will be in error because the laser is on the other channel.

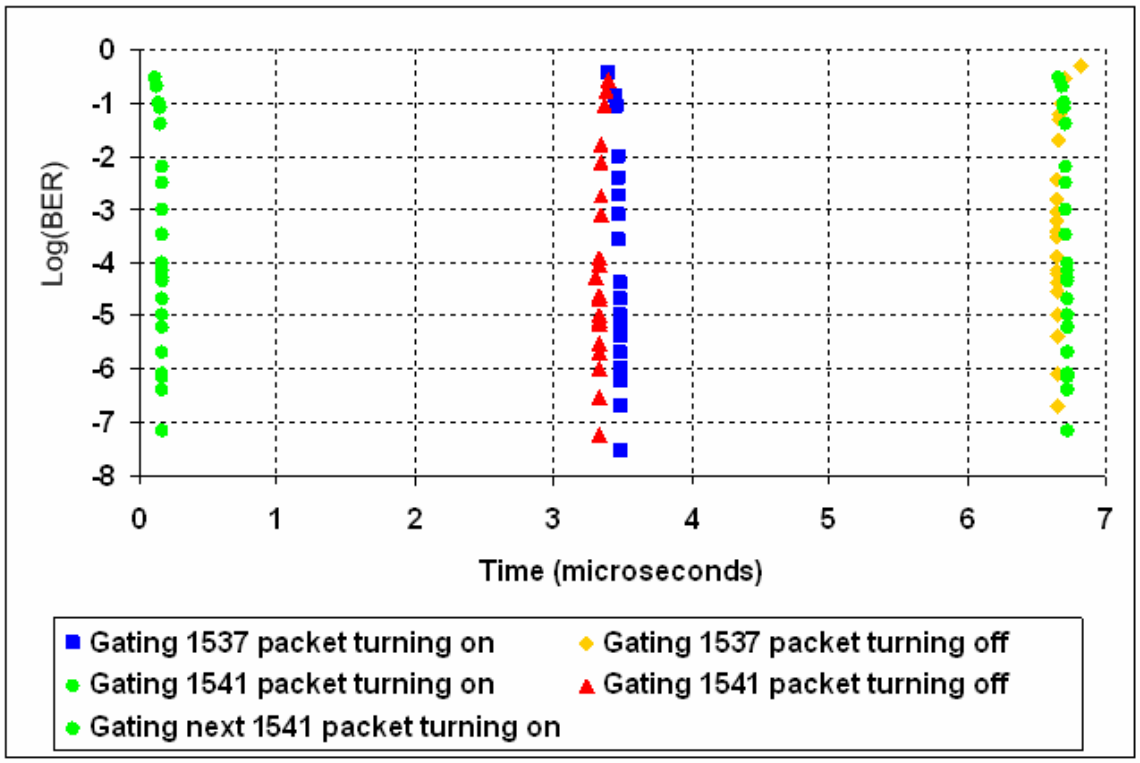

Fig. 5.30:Plot showing the time resolved BERs for the switch on and switch off times of both channels.

The results of the time resolved BER measurements for the switch on time and switch off time of both channels are displayed in Fig. 5.30. Slight differences in the path length for each channel mean that the positioning of the channel 1 measurements with respect to the channel 2 measurements is estimated given that the packet length was approximately 3.2μs. It can be seen that for the majority of that time no error rate is shown because the data packets were error free. Around the switching event however, errors can be seen. It is interesting to note that the error curves seem to cross each other, indicating that both channels are on at some point in time as opposed to one channel switching off before the next channel switches on.

In a scenario where all of the data bits were perfect and the switch on time was instantaneous then a 100ps (1 bit length) shift in the gating window position would place the

gating window over a 1 bit portion of the signal where the channel was not present as shown in Fig. 5.31. This movement would change the error rate from $0x10^{-10}$ (error free) to $5x10^{-3}$ (1 gated bit in error 50% of the time[3]). This implies that any error rate worse than $5x10^{-3}$ represents a point at which at least one bit length of the measurement gate lies at a point where the channel is not present and can therefore be ignored. In a practical system where the data is not always perfect and the switch takes a finite time to complete we can use this point to estimate the point at which the beginning of the packet matches the beginning of the gating window.

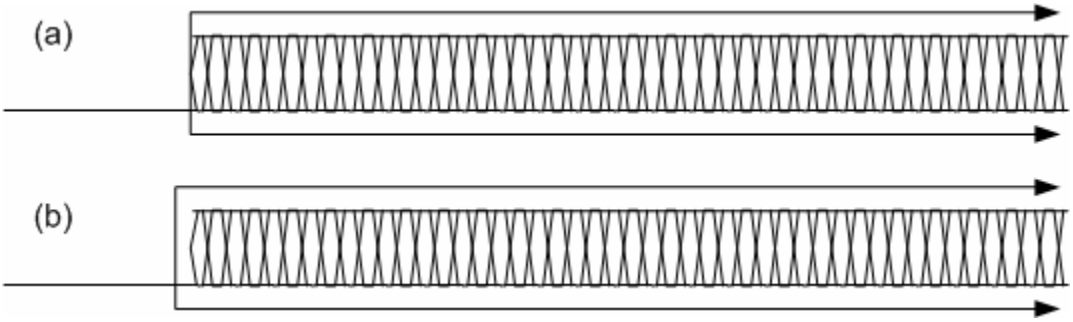

Fig. 5.31:In a system with instantaneous switching and perfect data, movement of the gating window by 1 bit length can cause the error rate to change from a) error free; to b) $5x10^{-3}$ where one bit is in error 50% of the time

Fig. 5.32 shows how the BER varies as the gating window was shifted across each signal as it turns on. The point marked 't_{ref}' shows where the error rate has dropped to error free. The time between $5x10^{-3}$ and 't_{ref}' therefore represents the longest possible time that it takes the laser to switch and transmit without errors. For both channels this occurs within 8ns. This represents the combined latency and settling time and switching time and indicates that these devices switch quickly enough to be suitable for OPS. Indeed, as mentioned commercial devices for this purpose have switching times in the hundreds of nanoseconds when blanking and wavelength locking are employed.

[3] The received bit will always be measured as a '0'. 50% of the time the transmitted bit will have been a '1' and will be measured as an error. The rest of the time a '0' will have been transmitted and no error will be recorded

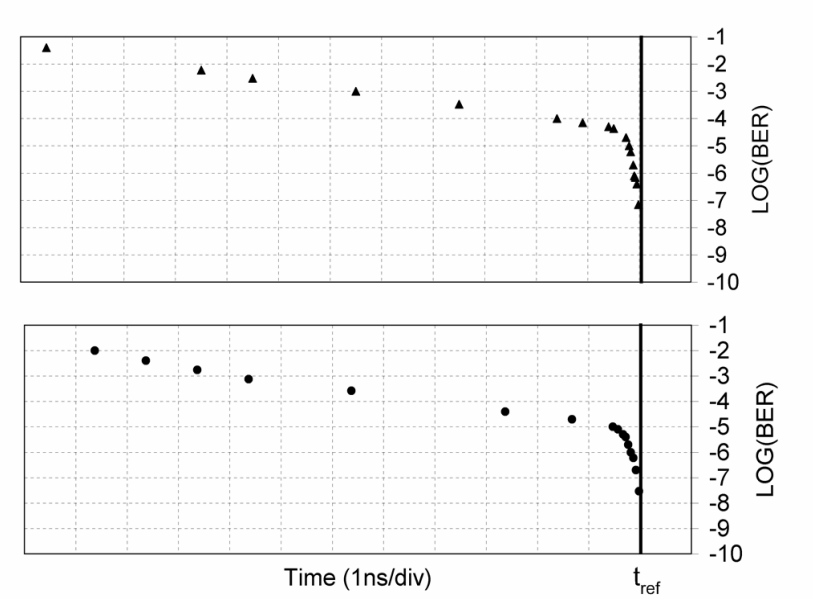

Fig. 5.32:Time resolved BER measurements showing how soon after the switching event, error free transmission is possible on (top) channel 1 and (bottom) channel 2.

5.11 Conclusion

Wavelength tunable lasers are an important component for WDM networks and their importance will rise as networks become more dynamic to the point of being indispensable when fast optical switching is employed. This chapter provided background information about tunable lasers, their applications and requirements as well as some of the basics of operation. A number of TLs were described briefly while two particular designs were described in detail. Experimental work carried out on these lasers was then discussed.

The SG-DBR laser is a commercially available device with control software and evaluation board electronics. As such, much work has been published on the characteristics of these devices. The experimental work carried out using these devices looked at the wavelength drift exhibited after switching and showed this drift to be up to 7.5GHz. In densely packed WDM systems this level of wavelength drift can cause performance degradation. Methods to overcome it would include the use of more sophisticated, but also more expensive wavelength lockers that would operate in a shorter time and keep the wavelength under tighter control [40]. The blanking time could also be increased such that the laser has had more time to settle to its desired wavelength before the output is enabled, however the disadvantage of this technique is the reduction in throughput. The drift examined in this chapter is shown to have a detrimental effect in an optical packet switching system, which

would ultimately cause packets to be routed to incorrect destinations. This issue is examined in the next chapter.

The second laser which was examined was the tunable SFP laser, a simple, inexpensive device which was shown to provide extremely fast wavelength switching with good accuracy over a wide tuning range without the use of temperature control, output blanking or wavelength locking. It is expected that the extremely fast switching times are enabled because the device has no passive sections which would limit the switching time to the spontaneous carrier lifetime. This technology is not yet mature so the experimental work described involved initial characterisation of the device including wavelength and SMSR maps and channel switching times. The devices examined had channel spacing of 1THz and 340GHz and it is expected that the design could be further refined in order to achieve higher channel counts with channel spacing suitable for WDM systems. The fast switching times suggest that devices based on the SFP design may be suitable for use in OPS systems.

Chapter 3 examined aspects of a slow form of optical switching where lightpaths may remain in place for long periods of time. This chapter looked at the tunable laser as a key device to enable the evolution of optical switching. TLs will be employed more and more as WDM networks change from static networks to dynamic optical switching networks. The following chapter examines the SG-DBR laser studied here in a systems role. The system studied represents what is currently viewed as the final step in the evolution of optical switching in WDM networks: optical packet switching.

References

[1] G. Sarlet et al, "Tunable Laser Diodes", in *WDM Technologies: Active Optical Components,* A. K. Dutta, N. K. Dutta, M. Fujiwara, eds. Associated Press, San Diego, USA, 2002.

[2] G. Keiser, Optical Fiber Communication (2nd Edition), McGraw-Hill, 1991.

[3] S.O. Kasap, "Stimulated Emission Devices - LASERS" in *Optoelectronics and Photoncs: Principles and Practices,* Prentice Hall, NJ, USA, 2001.

[4] J. Wilson, J Hawkes "Lasers I" in *Optoelectronics: An Introduction,* Prentice Hall Europe, 1998

[5] J. Buus, M.-C. Amann and D. J. Blumenthal, *Tunable Laser Diodes and Related Optical Sources*, Wiley-Interscience, 2005.

[6] H. Kogelnik, C. V. Shank, "Coupled-wave theory of distributed feedback lasers", *Journal of Applied Physics*, Vol. 43, 1972, pp 2327 – 2335.

[7] T. Mukaihara, Y. Nakagawa, H. Nasu, H. Kambayashi, M. Oike, S. Yoshimi, T. Kurobe, T. Kimoto, K. Muranushi, T. Nomura and A. Kasukawa, "High power, low noise, low power consumption, 25 GHz × 180 ch thermally tunable DFB laser module integrated with stable wavelength monitor," in Proc. Eur. Conf. Optical Commun. (ECOC03), Rimini, Sep. 2003, paper We.4.P.81, pp. 718-719.

[8] M. Bouda, M. Matsuda, K. Morito, S. Hara, T. Watanabe, T. Fujii and Y. Kotaki, "Compact high-power wavelength selectable lasers for WDM applications," in *Proc. Optical Fiber Commun. Conf. (OFC 2000)*, Baltimore, Mar. 2000, vol. 1, pp. 178-180.

[9] B. Pezeshki, E. Vail, J. Kubicky, G. Yoffe, S. Zou, J. Heanue, P. Epp, S. Rishton, D. Ton, B. Faraji, M. Emanuel, X. Hong, M. Sherback, V. Agrawal, C. Chipman, and T. Razazan "20-mW widely tunable laser module using DFB array and MEMS Selection," IEEE Photon. Technol. Lett., vol. 14, pp. 1457-1459, Oct. 2002.

[10] S. Murata, I. Mito and K. Kobayashi, "Tuning ranges for 1.5 μm wavelength tunable DBR lasers," *Electron. Lett.*, vol. 24, pp. 577-579, May 1988.

[11] F. Delorme, G. Alibert, P. Boulet, S. Grosmaire, S. Slempkes, and A. Ougazzaden, "High reliability of high-power and widely tunable 1.55- m distributed Bragg reflector lasers for WDM applications," *IEEE J. Sel. Topics Quant. Electron*., vol. 3, pp 193-202 Apr. 1997.

[12] O. Hildebrand et al, "The Y-laser: A multifunctional device for optical communications systems and switching networks", *IEEE Journal of Lightwave Technology,* Vol. 11, 1993, pp 2066-2075

[13] B. Borchert, S. Illek, T. Wolf, J. Reiger, M. C. Amann, "Vertically Integrated Mach-Zehnder interferometer (VMZ) widely tunable laser diode with improved wavelength access", *Electronics Letters,* Vol. 30, 1994, pp 2047 – 2049.

[14] S. Illek, W. Thulke, M.-C. Amann, "Codirectionally coupled twin-guide laser diode for broadband electronic wavelength tuning" *Electronics Letters,* Vol. 27, 1991, pp 2007-2209

[15] R.C. Alferness et al, "Broadly Tunable InGaAsP/InP laser based on a vertical coupler filter with 57nm tuning range", *Applied Physics Letters,* Vol. 60, 1992, pp. 3209 – 3211.

[16] Y. Tohmori, et al, "Broad-range wavelength tunable superstructure grating (SSG) DBR lasers", *IEEE Journal of Quantum Electronics,* Vol. 29, 1993, pp 1817 – 1823.

[17] P.-J. Rigole, et al, "114nm wavelength tuning range of a vertical grating assisted codirectional coupler laser with a super structure grating distributed Bragg reflector" *IEEE Photonics Technology Letters,* Vol 7, 1995, pp 697 – 699.

[18] J.-O. Wesström, G. Sarlet, S. Hammerfeldt, L. Lundqvist, P. Szabo, P. Rigole, "State of the art performance of widely tunable modulated grating Y-branch lasers", in *Optical Fiber Communications (OFC 2004),* Paper TuE2, Los Angeles, CA, 2004.

[19] V. Jayaraman, D.A. Cohen and L.A. Coldren, "Extended tuning range semiconductor lasers with sampled gratings," in *Lasers and Electro-Optics Society Ann. Meet. (LEOS 1991)*, San Jose, Nov. 1991, Paper No. SDL15.5.

[20] V. Jayaraman, A. Mathur, L.A. Coldren and P.D. Dapkus, "Very wide tuning range in a sampled grating DBR laser," in *Proc. 13th IEEE Int. Semiconductor Laser Conf.,* Takamatsu, Japan , Sep. 1992 , pp. 108-109.

[21] V. Jayaraman, D.A. Cohen and L.A. Coldren, "Demonstration of broadband tunability in a semiconductor laser using sampled gratings," *Applied Physics Letters.* , vol. 60, (19), pp. 2321-2323, May 1992.

[22] B. Mason, J. Barton, G. A. Fish, L. A. Coldren and S. P. DenBaars "Design ofsampled grating DBR lasers with integrated semiconductor optical amplifiers," *IEEE Photon. Technol. Lett.*, vol. 12, pp. 1-3, Jul. 2000.

[23] G. Sarlet, G. Morthier,and R. Baets, "Control of widely tunable SSG-DBR lasers for dense wavelength division multiplexing," *J. Lightw. Technol.,* vol. 18, pp. 1128-1138, Aug. 2000.

[24] J. Dunne, T. Farrell and R. O'Dowd, "Fast generation of optimum operating points for tunable SG-DBR laser over 1535-1565 nm range," in *Proc. Conf. on Lasers and Electro-Optics (CLEO99),* Baltimore, May 1999, pp. 147-148.

[25] ITU-T, Recommendation G.692, "Optical interfaces for multichannel systems with optical amplifiers," Oct. 1998.

[26] Y. Yu, R. O'Dowd, "Influence of mode competition on the fast wavelength switching of an SG-DBR laser," *J. Lightw. Technol.,* vol. 20, pp. 700-704, Apr. 2002.

[27] J.E. Simsarian M.C. Larson H.E. Garrett Hong Xu and T.A. Strand, "Less than 5-ns wavelength switching with an SG-DBR laser," *IEEE Photon. Technol. Lett.,* vol.18, pp. 565-567, Feb. 2006.

[28] J.E. Simsarian and Liming Zhang, "Wavelength locking a fast-switching tunable laser," *IEEE Photon. Technol. Lett.*, vol. 16, pp. 1745-1747, Jul. 2004.

[29] A. Dantcha, L.P. Barry, J. Murphy, J.Dunne, T. Mullane, and D. McDonald, "BER performance in wavelength packet awitched WDM systems during nano-second wavelength switching events," *Elsevier Journal of Optics Commun.,* vol. 242, pp. 171-177, Aug. 2004.

[30] T. Wipiejewski, et al, "Performance and reliability of widely tunable laser diodes" in *Proc. Electron. Compon. and Technol. Conf.*, New Orleans, May 2003, pp. 789 – 795.

[31] Intune AltoNet 1200 FTL Tx Module [Online] http://www.intunenetworks.eu/site/

[32] J.E. Simsarian L. Zhang, "Wavelength locking a fast-switching tunable laser," IEEE Photon. Technol. Lett., vol. 16, pp.1745-1747, Jul. 2004.

[33] V. Polo, A. Ausiro, J. Prat and G. Junyent, "GCSR laser frequency drift compensation using optimized current waveform on one single electrode," in *Proc. 7th Inter. Conf Transparent Optical Networks (ICTON 2005),* Barcelona , Jul. 2005, vol. 2, pp. 17-20.

[34] E. Connolly, F. Smyth, A.K. Mishra, A. Kaszubowska-Anandarajah, L.P. Barry, "Cross-Channel Interference Due to Wavelength Drift of Tunable Lasers in DWDM Networks," *Photonics Technology Letters, IEEE* , vol.19, no.8, pp.616-618, April15, 2007

[35] I.P. Kaminow, R.E. Nahory, M.A. Pollack, L.W. Stulz, J.C. Dewinter, "Single-mode c.w. ridge-waveguide laser emitting at 1.55 μm," *Electronics Letters* , vol.15, no.23, pp.763-765, November 8 1979

[36] J.E. Bowers, L.A. Coldren, B.R. Hemenway, B.I. Miller, R.J. Martin, "1.55 Â¿m multisection ridge lasers," *Electronics Letters* , vol.19, no.14, pp.523-525, July 7 1983

[37] B. Corbett, D. McDonald, "Single longitudinal mode ridge waveguide 1.3 μm Fabry-Pérot laser by modal perturbation," *Electronics Letters* , vol.31, no.25, pp.2181-2182, 7 Dec 1995

[38] R. Phelan, W.-H. Guo, Q. Lu; D. Byrne, B. Roycroft, P. Lambkin, B. Corbett, F. Smyth, L.P. Barry, B. Kelly, J. O'Gorman, J.F. Donegan, "A Novel Two-Section Tunable Discrete Mode Fabry-PÉrot Laser Exhibiting Nanosecond Wavelength Switching," *Quantum Electronics, IEEE Journal of* , vol.44, no.4, pp.331-337, April 2008

[39] H. Joseph, D. Sadot, "A Novel, Self-Heterodyne Method for Combined Temporal and Spectral High Resolution Measurement of Wavelength Transients in Tunable Lasers", IEEE Photonics Technology Letters, vol 16, pp 1921-1923 Aug 2004.

[40] C. C. Renaud, M. Duser, C. F. C. Silva, B. Puttnam, T. Lovell, P. Bayvel, and A. J. Seeds, "Nanosecond channel-switching exact optical frequency synthesizer using an optical injection phase-locked loop (OIPLL)," *IEEE Photon. Technol. Lett.*, vol. 16, pp. 903–905, Mar. 2004.

Chapter 6 – A Novel Optical Label Switching Scheme based on a Fast Tunable SG-DBR Laser

6.1 Introduction

Chapter 4 described experimental work which studied aspects of slow reconfigurable optical networks in which lightpaths are reconfigured on slow timescales for bandwidth provisioning or traffic management for example. This chapter moves a number of years later down the evolutionary path of optical switching and explores an Optical Packet Switching (OPS) system based upon the Sampled Grating Distributed Bragg Reflector (SG-DBR) laser detailed in Chapter 5. OPS was introduced in section 3.11 and the concept of Optical Label Switching (OLS) was briefly described. OLS will be discussed in greater detail in the initial sections of this chapter with the focus on the form used in this work: Sub-Carrier Multiplexed (SCM) OLS. The experimental work will be explained over a number of sections beginning with the concept of the labelling scheme designed. Next the transmitter and receiver will be discussed, followed by the actual packet switching system experiments employing, first a single OPS channel, and later a pair of channels switching on timescales typical of OPS.

6.2 Optical Label Switching

In 'conventional' optical packet switching the packet header and data are transmitted together and at the same data rate in much the same way as packets are transmitted in the electrical domain [1]. In such a scenario, the routing and forwarding of packets may prove to be a bottleneck as fiber link rates approach 1TBit/s. OLS is a more practical approach to packet switching in the optical domain given the technology which is currently available. It is based on the concepts of Multi-Protocol Label Switching (MPLS), an extension of the Internet Protocol (IP), designed to allow the Internet to support multiple service types and simplify traffic management, which has begun to replace legacy protocols such as Asynchronous Transfer Mode (ATM) and Frame Relay.

In OLS, the routing information is separated from the data and placed in a 'label'. The label is much smaller than a data payload, and therefore can be transmitted at a much slower data rate and still arrive in the same time slot as the faster, but larger payload. As payload speeds continue to rise above what can be readily handled by electronic means, a slower label can still be processed. The IP header is only examined once, at the edge of the network and the information that it contains is used to create a label which gets attached to the optical payload. The payload consists of the IP packet *and* IP header in optical format and it remain in the optical domain and gets routed transparently through the network. Although the optical label is created using information from the IP header, it is smaller and simpler than an IP header. It contains routing information such as the source, the destination, and may contain control information such as the priority, the Time-To-Live (TTL) and the length of the packet. IP addresses are mapped into labels and corresponding wavelengths and ports and distributed across the network as routing tables. When an optical packet reaches a node, its label is examined and the switch fabric and wavelength converters are arranged according to the routing table, in order to forward the packet onward towards its destination.

Label *swapping* has received a lot of attention in the literature. It involves erasing the "local significant" label at intermediate nodes throughout the network and attaching a new updated label before forwarding the packet on through the network [2,3]. While label swapping can improve the flexibility and scalability of a network, it significantly increases the cost and complexity of the node and is not a required function in a label switched network. Deterministic labels can be used [4] and provided the label data rate is reasonably high, and hence a large number of addresses are available, scalability should not be overly affected.

The main advantages over of label switched OPS over 'conventional' OPS are as follows:

1) Optical circuits and bursts can be labelled just as easily as packets, therefore OLS offers better interoperability between circuit, burst and packet switching. It seems likely that the future Internet will be based on a combination of protocols and this is well suited to OLS

2) OLS offers protocol and format independent transparency, which is not offered by conventional packet switching because the header and payload are essentially transmitted as a single entity. In order for a conventional OPS header to be readable, the label must be of the same defined format.

3) OLS was developed based on MPLS and this gives excellent backwards compatibility with legacy networks such as MPLS, MPLambdaS, IP and SONET via GMPLS.

4) OLS is interoperable with GMPLS, which provides a simple and effective control plane without tight timing and synchronization

These points, along with the fact that the technology required to read headers at ever-increasing payload data rates would prove prohibitively expensive, means that 'conventional' OPS has been abandoned in favour of OLS based OPS.

Many methods have been studied for the labelling of optical packets but, as mentioned in Chapter 3, three methods have received the most attention: bit-serial, orthogonal, and SCM labelling. Other, less widely studied methods include Wavelength Division Multiplexed (WDM) labelling and Optical Code Division Multiplexed (OCDM) labelling, which is based on work from the late 1980s [5,6] and has seen renewed interest in more recent years. In this section four of these techniques are discussed, with the fifth, SCM labelling, the basis of this chapter, receiving particular attention in a dedicated section following this.

With bit serial labelling, the label and payload are separated in the time domain. This is similar to 'conventional' OPS [1] except that the label is transmitted at a slower data rate than the payload, a technique that was first suggested in [7]. A guard band between the label and payload simplifies the extraction of the label, however tight timing and synchronisation is still required and this represents the major drawback with serial labelling. Nevertheless, in [8] packet rates of 160Gb/s with 10Gb/s labels were reported using Time Division Multiplexing (TDM).

Orthogonal labelling schemes separate the payload and label by modulating them onto different dimensions of the optical carrier and using different modulation formats. For example the payload could be modulated onto the intensity with a Frequency Shift Keyed (FSK) label [9] or vice versa [10]. Other methods use Differential Phase Shift Keyed (DPSK) [11] or Polarization Shift Keyed (PolSK) labels [12]. The advantages of orthogonal labelling lie in the fact that timing is not strict like with serial labelling and spectral efficiency is better than SCM forms, however crosstalk between payload and label can be severe. In addition,

some compromise between the extinction ratio of the payload and label must be made to avoid '0' bits on one causing errors on the other.

In contrast with the other methods in which the label is processed electronically, OCDM labelling has the advantage that label processing is carried out in the optical domain through autocorrelation. This allows extremely fast label processing. In [13] the label is encoded ahead of the payload in the time domain in a similar manner to bit serial labelling and in [14] the payload and label are modulated onto the two orthogonal polarizations of light. In [15] separate areas of the spectrum are used for the labels and the payload but because the label bandwidth is shared among all of the labels this method offers far superior spectral efficiency when compared with the WDM labelling method [16]. WDM labelling is perhaps the least attractive method of all. The label is transmitted on a separate WDM channel [16], and while this allows for it's simple extraction this it does not make good use of the available spectrum and requires two lasers per packet, which is uneconomical.

6.3 SCM Labelling

SCM labelling is similar to WDM labelling in that the label and payload are separated in the wavelength domain. Rather than use a separate optical carrier, however, with SCM labelling the label is placed on an RF subcarrier that is then multiplexed with the payload on the same wavelength. SCM labelling of optical packets was first proposed in 1992 [17]. In this experiment, a 2.5Gb payload was labelled with a 40Mb/s label on a 3GHz subcarrier.

6.3.1 Generation of SCM labelled signals

The SCM labelled optical packet can be generated in 3 ways: Electronically, electro-optically, and optically. The electronic method uses a coupler or diplexer to combine the payload with the SCM signal in the electronic domain. This combined electronic signal is then used to drive a single modulator [18] or to directly modulate a laser [19]. Electro-optic combination uses a single differentially driven modulator [20] with the payload driving one arm and the separately generated label driving the other arm. Both of these methods introduce a power penalty in the baseband data resulting in a trade-off between payload and label performance. The payload and label can also be combined optically as demonstrated in [21]. In this paper a single laser source is split and used to drive 2 modulators, one with the payload and the other with the labels. A Fiber Loop Mirror filter (FLM) is used suppress the carrier in the label signal and to combine the signals in the optical domain allowing the power in both

label and payload to be maximized without affecting the other. The disadvantage of this technique is that it is bulky and requires two modulators.

Generally, the labels are placed at a subcarrier frequency which is equal to or higher than the clock frequency of the payload signal. To improve the spectral efficiency, an in-band SCM technique was presented in [22]. This method uses a combination of orthogonal and SCM labelling. A 40Gb/s DPSK payload was combined with 3GHz subcarrier labels at 25Mb/s. A major advantage of this technique is that the RF components required to generate 3GHz subcarriers are much less costly than those required for 40GHz or beyond. However the system is more complicated due to the coherent detection required and the need for two modulators in the transmitter.

6.3.2 OCSS

One form of SCM labelling is known as optical carrier suppression and separation (OCSS) [23]. Here, a sine wave RF clock and its inverse are used to drive a differential modulator with a CW input. The resulting spectrum consists of two subcarriers spaced by twice the RF clock frequency with the optical carrier suppressed between them. The two modes can then be filtered and modulated independently, one with the payload and the other with the label. Good extinction and low crosstalk make this method attractive but the main problems with method are the complicated transmitter and node design that require three modulators in the transmitter and two in every node.

6.3.3 Reading SCM labels

An SCM label can be read by direct detection of the entire optical channel, and then downconversion using the RF carrier [17]. Downconversion is not ideal because it requires additional high frequency components. In addition RF fading caused by double sidebands experiencing different phase shifts due to fiber dispersion occurs [24]. An alternative method [25], allows direct detection of the labels. Providing that the subcarriers are Amplitude Shift Keyed (ASK), they can be optically band pass filtered and detected directly, because the filter blocks the energy from the other optical carriers and subcarriers with the effect that the photodiode appears to be illuminated by a single intensity modulated signal. This technique removes the need for high frequency components and additionally overcomes the fading problem [26,27]. The fading problem has also been overcome using a more complex

modulation technique to give single sideband (SSB) SCM [28] which also allows for greater spectral efficiency but is more complex to generate.

6.3.4 Swapping

Once the label and payload have been separated it is relatively simple to swap the labels with new ones if required. A modulator in the node, driven with the subcarrier data only will add the new labels to the existing payload prior to retransmission. A sub-optimal extinction ratio is required however to ensure that light is always present to modulate onto.

6.3.5 Advantages of SCM Labelling

The advantages that SCM labelling offer over other forms include:

1. Simple bookkeeping since the same wavelength channel is used for the payload and label. This is in contrast to WDM labelling systems, and systems which use dedicated bandwidth for labelling.
2. In contrast to bit serial labelling in which tight timing and synchronization is required, with SCM the label and payload arrive together in time but can be processed asynchronously. This greatly simplifies the node architectures.
3. Label extraction is very simple, requiring only optical filters, and label swapping is also easily available.

6.3.6 Disadvantages of SCM Labelling

1. The RF fading problem discussed previously is a potential disadvantage of SCM labelling but it can be easily overcome using filtration and direct detection, or SSB modulation.
2. Poor spectral efficiency is achieved when using an out of band subcarrier, however as we show in the next section, the use of the data clock as the RF subcarrier results in good spectral efficiency. In addition, advanced modulation formats can be used to narrow the spectrum further. Finally, in-band SCM labelling has also been demonstrated.
3. Nonlinearities due to imperfect components can cause Inter-Modulation Distortion (IMD) between adjacent labels leading to the creation of spectral components which may lie under and interfere with the payload.

4. Apart from the case of inband labelling, for high payload data rates, high subcarrier frequencies and components are required at every node.

6.4 Optical Labelling Scheme

The OLS scheme used in this work consists of an Amplitude Modulated – Phase Shift Keyed (AM-PSK) payload with an Intensity Modulated (IM) Non-Return to Zero (NRZ) label. Duobinary encoding of the payload data results in a spectrum that is significantly narrower than a standard NRZ spectrum, both in the electrical and optical domains. This point is illustrated in Fig. 6.1.

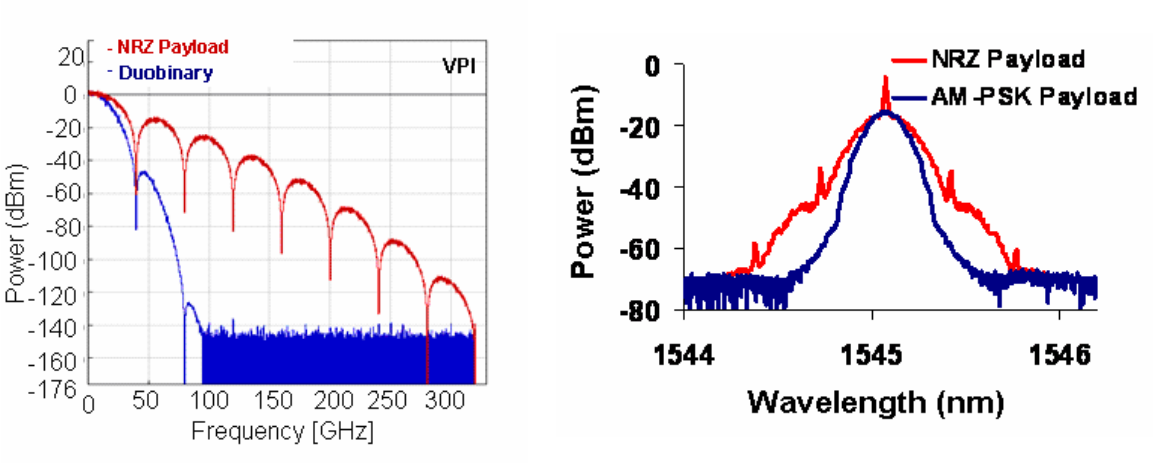

Fig. 6.1: Simulated 40Gb/s duobinary signal vs. 40Gb/s NRZ signal in the electrical domain (left) and experimental measurements in the optical domain (right)

The optical spectrum is 25% narrower than the equivalent NRZ spectrum which allows the label to be modulated onto an RF subcarrier with a frequency equal to the payload data rate. This gives good spectral efficiency in comparison to techniques in which the payload and label are separated by using a subcarrier of a higher frequency. In addition the same clock may be used for the payload data and the subcarrier local oscillator (LO) which represents a cost saving. Low crosstalk between the payload and label allow the use of a high data rate on the label, which improves the scalability of the deterministic labelling system used by allowing a large number of destination addresses. A deterministic labelling system further reduces cost by removing the need for label swapping at every intermediate node.

6.5 Experimental Transmitter Subsystem

The transmitter subsystem used in the work is illustrated in Fig. 6.2. The use of only a single modulator represents a further cost saving in comparison to certain other schemes used for SCM labelling in which two [29], or three [23] Mach-Zehnder Modulators (MZMs) are used in the transmitter. In this work, a 42.6Gb/s NRZ payload data signal is fed from a Pulse Pattern Generator (PPG) through a duobinary electrical amplifier resulting in a 3 level signal in which a '0' or a '1' is mapped to a '0', '1' or '2' depending on the preceding bit. Duobinary encoding can be achieved by extreme low pass filtering using a 3dB bandwidth of 25% of the data rate, or through the use of a digital delay and add and was also used in [30] to achieve high spectral efficiency in a 50GHz spaced system. The labels are generated by mixing a 2.5Gb/s NRZ data signal from a second PPG with the clock signal from the payload PPG yielding double sideband subcarriers at 42.6GHz. The two electrical signals (payload and label) were then passively combined using a custom designed diplexer.

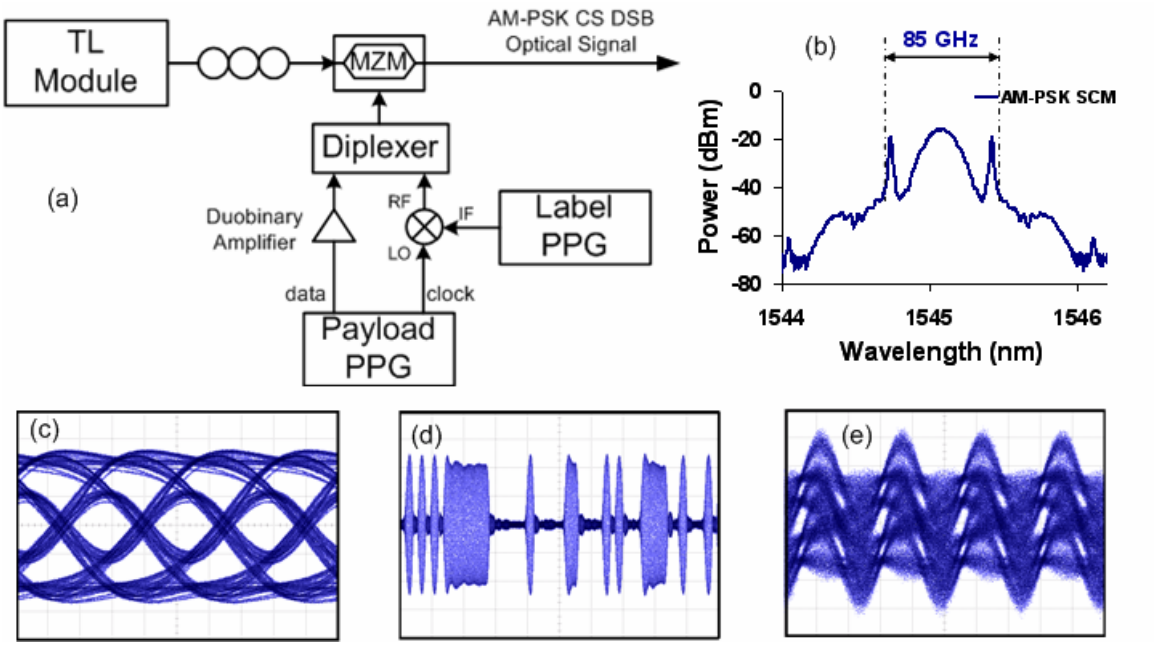

Fig. 6.2: SCM labelling scheme: a) Transmitter subsystem for SCM labelling scheme; b) resulting optical spectrum; Electrical inputs and outputs to diplexer including eye diagram of: c) duobinary payload; d) modulated 40GHz subcarrier; and e) and combined output

The combined electrical signal is used to drive a single MZM that modulates the light output from a SG-DBR TL module and is biased at the null point of its transfer function. The 3-level electrical payload symbols (0, 1 and 2) then get mapped onto both the amplitude and phase of the light (as –E, 0 and +E) resulting in the narrow AM-PSK signal [31, 32]. This

modulation format has the advantage that it can be received using standard NRZ direct detection, however a standard square law detector cannot differentiate between the positive and negative phase components of the optical signal. This means that the detected signal will only recover two symbols (E^2 and 0). The use of differential encoding at the transmitter side allows correct detection and decoding, however its use was not required in this work because PRBS sequences were used, and a differentially encoded PRBS signal is simply a delayed copy of itself. Biasing at the null point of the MZM also benefits the label by suppressing the carrier and hence improving the receiver sensitivity [33]. The drive amplitudes were optimized to minimize crosstalk between payload and label.

6.6 Experimental Receiver Subsystem

The receiver subsystem is shown in Fig. 6.3. The incoming signal is pre-amplified using an Erbium Doped Fiber Amplifier (EDFA) and filtered using a 100GHz Arrayed Waveguide Grating (AWG) with an 80GHz 3dB bandwidth and a flat top filter profile that splits the signal into individual channels and also serves to remove some of the Amplified Spontaneous Emission (ASE) introduced by the pre-amp. A second EDFA boosts the signal once more before it is passed into an Asymmetric Mach-Zehnder Disinterleaver (AMZD) with a Free Spectral Range (FSR) of 85.2GHz. The AMZD acts like a notch filter which when correctly aligned, separates the payload and the Double Side Band (DSB) labels onto separate output ports very effectively as shown in Fig. 6.4. The labels then enter the label receiver which consists of an 6.25GHz Fabry-Pérot optical filter, used to extract a single sideband, allowing direct detection with a receiver optimised for the label bit rate and eliminating any dispersion-induced carrier fading [34] due to fiber transmission. In addition this filter minimized any residual payload crosstalk. After the filter a Variable Optical Attenuator (VOA) is used to control the power onto a low speed photodiode. In the experimental work described here, an error detector is then used to measure system performance. In a deployed system the photodiode would be the interface for the line termination equipment. The payload receiver was similar to the label receiver but it contained a high speed photodiode and did not require the optical filter.

It is important to note that the core nodes can be built using a much simpler receiver setup. As the payload is routed transparently through the network, it need not be detected at every node. As such, the AMZD and Payload receiver sections shown in Fig. 6.3 are not necessary.

Rather, the AMZD could be replaced by an optical tap which would take a portion of the light for label detection and the remainder of the light would enter some form of optical buffer while the label was read and the switches were set. The lack of payload suppression from the AMZD means that a more precise label filter would be required, and this would then extract a single label from the combined payload/label signal as opposed to from the DSB label signal with the payload suppressed.

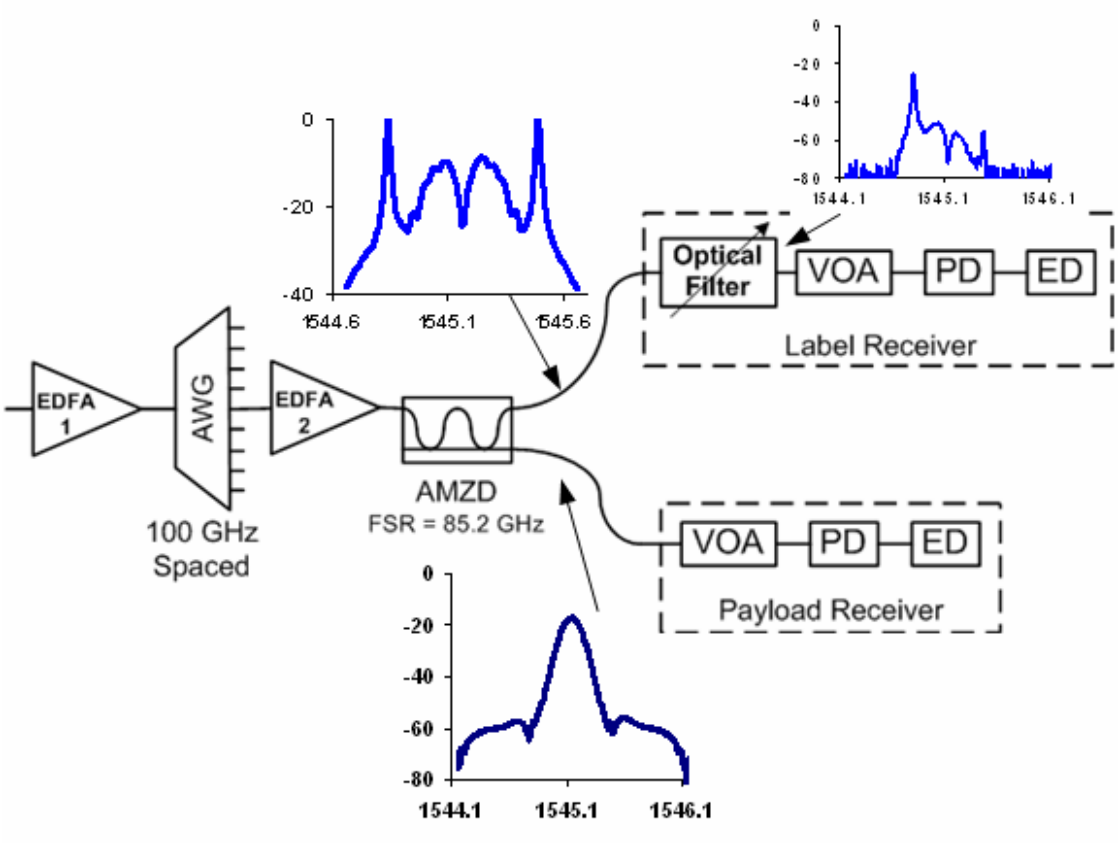

Fig. 6.3: Receiver subsystem showing extracted spectra

6.7 Single channel performance experiment

The first experiment performed was to measure the performance of this particular labelling scheme so only a single channel system was used. The experimental arrangement consisted simply of the transmitter subsystem of Fig. 6.2 connected to the receiver subsystem of Fig. 6.3 via 1km of Standard Single Mode Fiber (SSMF). The optical spectra of the transmitted signal, received payload and the extracted single side-band label are shown in Fig. 6.4.

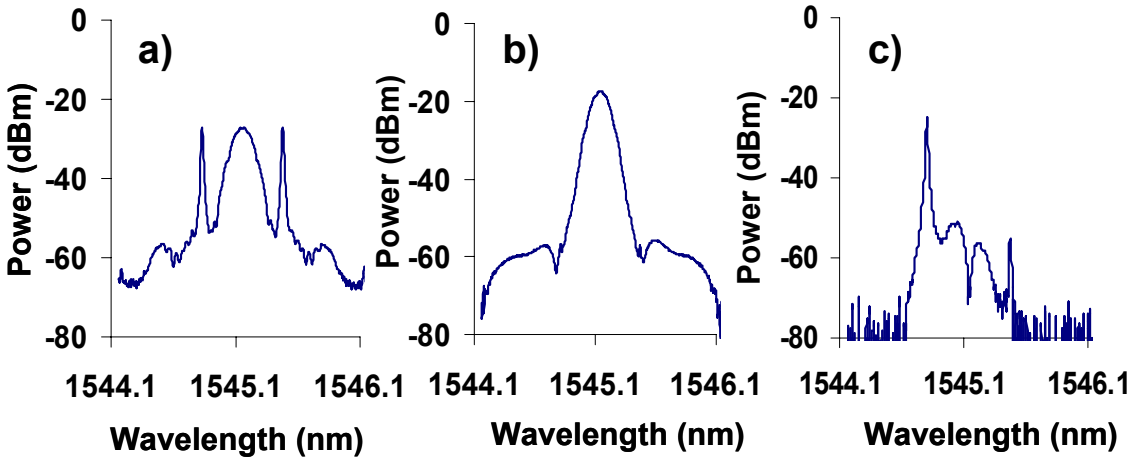

Fig. 6.4: Optical spectra for: a) transmitted subcarrier-multiplexed signal; b) filtered payload; c) filtered single side-band label

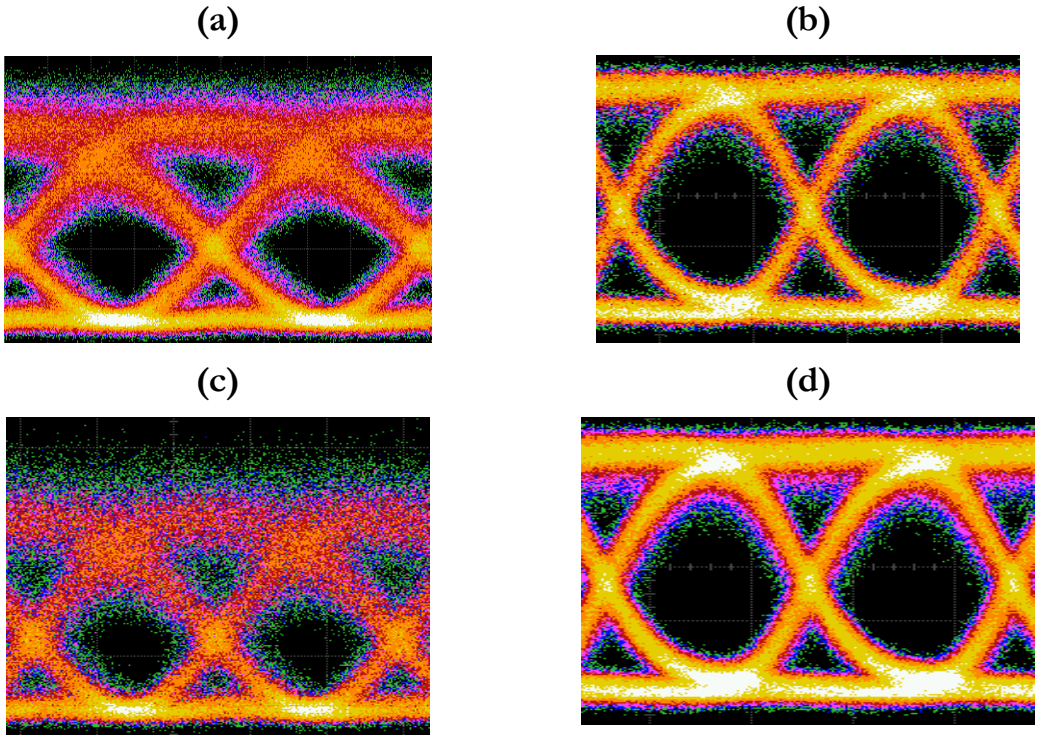

Fig. 6.5: Received Eye diagrams of: a) payload with label off; b) label with payload off; c) payload with label on; and d) label with payload on.

The received eye diagrams corresponding to Fig. 6.4(b) and (c) are shown in Fig. 6.5(c) and (d). The degradation of the payload eye caused by the presence of the label is quite severe while the label is quite resilient to degradation from the presence of the payload. Note that the received payload has lost its 3-level structure. Fig. 6.6(a) compares the Bit Error Rate

(BER) as a function of received power for a 2^7-1 bit PRBS payload when the payload is generated with and without labels of various PRBS lengths. It is shown that the addition of the label introduced a small power penalty of <1 dB, regardless of the label length. The low pattern sensitivity is to be expected, since each payload bit period was much less than bit period of the label. In the following section it is shown that this penalty will be further reduced by aligning the relative phases of the 42.6 GHz subcarrier and 42.6 Gb/s payload signal. As shown in Fig. 6.6(b), the presence of the AM-PSK payload introduced a power penalty of between 3 dB and 4.8 dB on the label for a pattern length of 2^7-1 and 2^{31}-1 respectively. In this case the pattern length is significant. Since each label bit is impacted by up to 16 payload bits, the effective bias point for the subcarrier signal may be modulated by the low frequency content of the payload data.

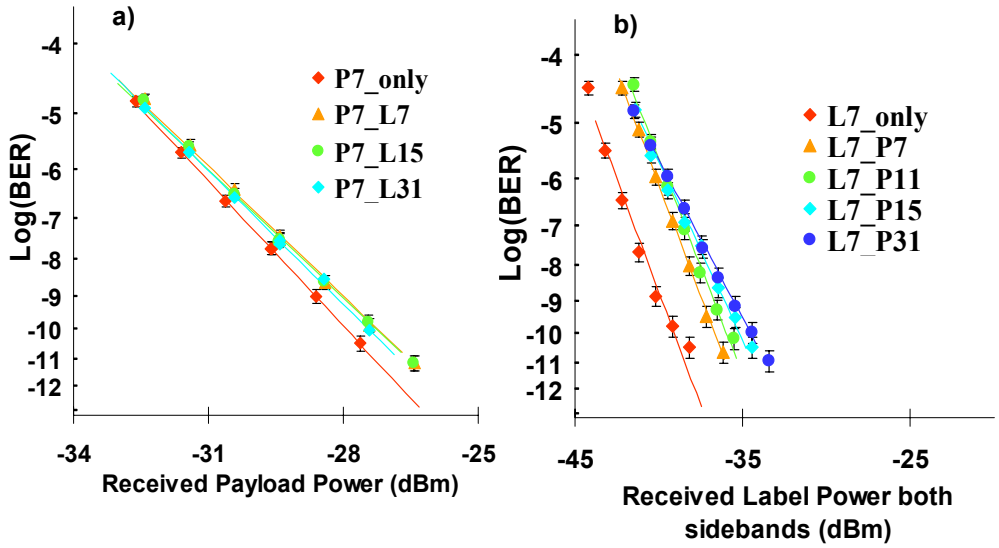

Fig. 6.6: BER versus received power for: a) payload PRBS 2^7-1 with and without various labels; b) labels of PRBS 2^7-1 with and without various payloads, where P^m = payload with PRBS 2^m-1, L^n = label with PRBS 2^n-1

The gain of the duobinary amplifier could be tuned to change the relative power distribution between the payload and labels. Fig. 6.7(a) shows the system performance in terms of the total received power (in payload and labels) required to obtain a BER of $1x10^{-9}$ as a function of the relative gain of the duobinary amplifier. The gain of the duobinary amplifier directly determines the power of the AM-PSK signal, and consequently determines the relative power of the subcarrier label. It can be seen that by controlling the relative power levels in this way it is possible either to achieve BER of $1x10^{-9}$ for the payload and labels at the same

total received power, or to favour the label signal, thus minimising packet loss. Fig. 6.7(b) shows receiver sensitivities of labels versus label PRBS length, with and without a payload of various PRBS lengths. This confirms that the label penalty is determined only by the payload sequence length and not by its own length.

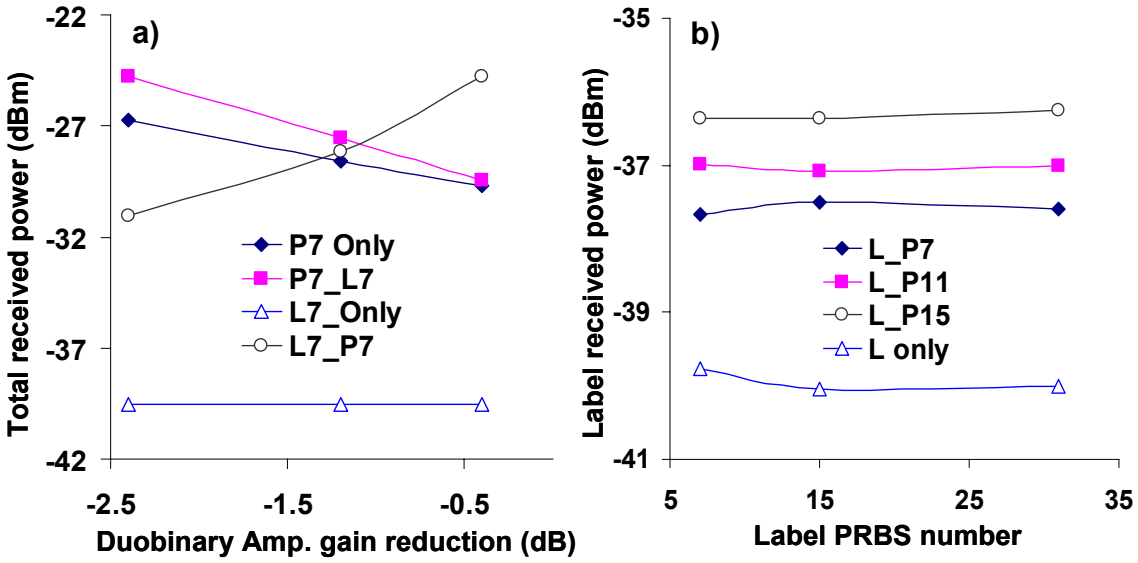

Fig. 6.7: Total received power at BER 10^{-9} vs. reduction in gain of duobinary amplifier with and without labels/payloads; b) Label received power at BER 10^{-9} as a function of PRBS length of label with and without payload. (Pn = payload with PRBS 2^n-1)

6.8 Performance Enhancement

In this section the role of the phase relationship between the payload and subcarrier signals is investigated and optimized to demonstrate a significant improvement in the overall system performance. The performance is further enhanced by appropriate selection of the label filter bandwidth. The experimental set up is as before with the exception of the phase shifter before the diplexer on the label side and the narrower label filter (4GHz rather than 6.25GHz). The arrangement is shown in Fig. 6.8.

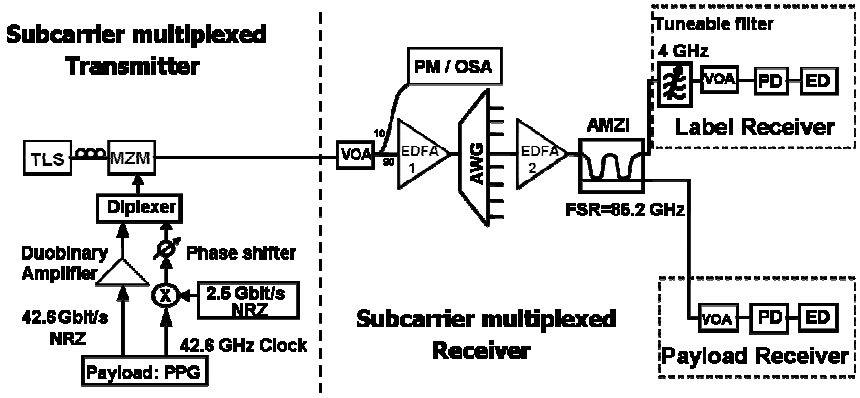

Fig. 6.8: Transmitter and receivers for subcarrier-multiplexed payload and label; TLS: tunable laser source, VOA: variable optical attenuator, PM: power meter, PD: photodiode, ED: error detector

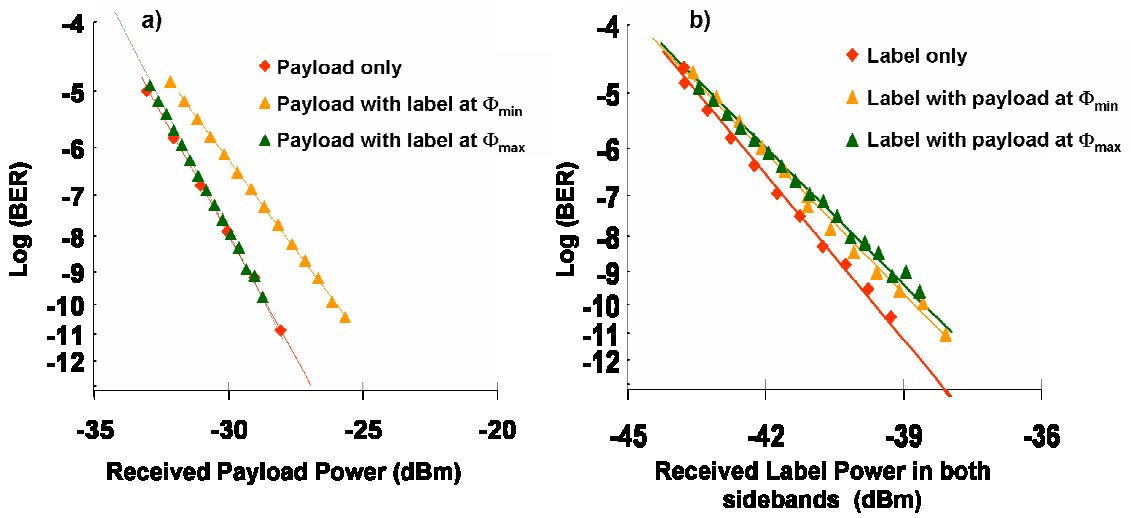

Fig. 6.9: Plot of measured BER versus received power for: a) payload PRBS 2^7-1 with and without label at different subcarrier phases; b) label of PRBS 2^7-1 with and without payload at maximum or minimum subcarrier phases

Fig. 6.9(a) plots detailed BER measurements against a received payload power of a 2^7-1 PRBS payload in presence and absence of a label of 2^7-1 PRBS length. At the optimized phase position Φ_{max}, it can be seen that adding the label introduced a negligible power penalty of <0.1 dB for the BER of $1x10^{-9}$ with the maximum eye opening, whilst this penalty increased to 2.3 dB for the worst phase Φ_{min},. Similarly, as shown in Fig. 6.9(b), the presence of the AM-PSK payload introduced a small power penalty of 0.7 dB on the label sensitivity when the relative phase was adjusted to Φ_{min}. The label receiver sensitivity was degraded by a further 0.3 dB when the relative phase was aligned to the optimum at Φ_{max}, giving a maximum penalty of only 1dB irrespective of the relative phase.

These penalties are examined in more detail in Fig. 6.10(a), which plots the receiver power needed to reach a BER of $1x10^{-9}$ in both label and payload as a function of the phase delay of the 42.6GHz subcarrier. It can be seen that the payload receiver sensitivity follows a sinusoidal trend with the variation of relative phase. The dotted pink line shows the receiver sensitivity of the payload without the label. With the label present and relative phase at its optimum (Φ_{max}), a penalty of <0.1dB was observed. This penalty increased up to 2.3 dB for the worst relative phase (Φ_{min}). The label receiver sensitivity was observed to be largely independent of the relative phase, with a variation of less than 1 dB.

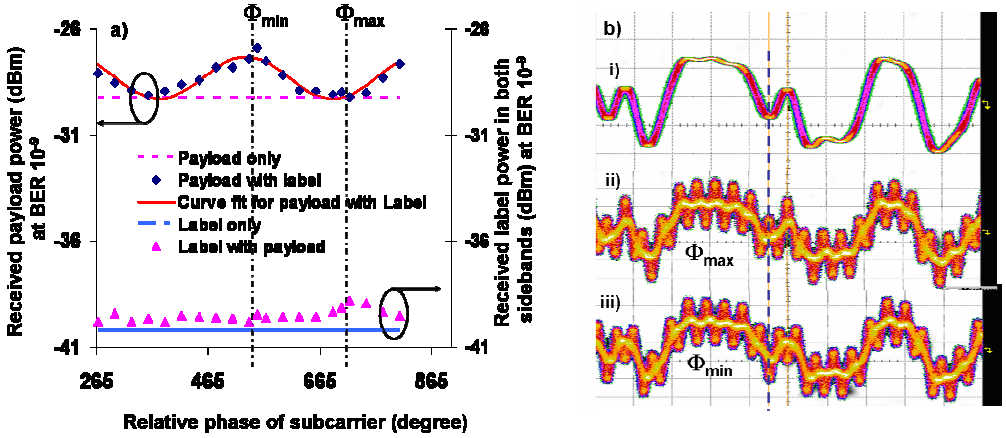

Fig. 6.10:a) Measured receiver sensitivities of the payload and label versus subcarrier phase angle; b) Oscilloscope traces of electrical duobinary drive signal data pattern without subcarrier (i) and with subcarrier at Φmax (ii) and Φmin (iii), respectively.

The origin of the variation in payload receiver sensitivity is illustrated in Fig. 6.10(b), which shows the electrical drive signal data patterns under various conditions. Fig. 6.10(b) (i) shows the 42.6 Gb/s duobinary data pattern applied to the payload in the absence of a subcarrier signal. Fig. 6.10(b)(ii) shows the pattern of the combined signal at the optimum phase, whilst Fig. 6.10(b)(iii) shows the pattern at the worst phase. For a particular payload bit (as indicated by the dotted line), it is apparent that the optimum performance is achieved when the maximum of the subcarrier signal is aligned to the centre of each payload data bit. The reason for this is that the subcarrier bits tend to increase the eye opening of the payload. Conversely, the worst performance is obtained when the minimum of the subcarrier is aligned with the centre of the payload bit. Following the optimisation of this phase, and the label filter width, the overall receiver sensitivity of the subcarrier multiplexed system was

improved by more than 2.0dB for both payload and labels when compared to the initial work.

6.9 WDM packet switching system experiment

Having fully optimized the labelling scheme for a static tunable laser, the next step was to characterize the performance in a multi-channel system with switching tunable lasers. In the previous chapter it was shown that wavelength drift of the tunable lasers on the timescales typical of optical packet switching could cause performance issues. In this section we examine the performance of a one WDM channel as a second channel switches in and out of the adjacent channel. The entire experimental setup is shown in Fig. 6.11. In this work the payload had a data rate of 40Gb/s as opposed to 42.6Gb/s and the label data rate was reduced to 155Mb/s from 2.5Gb/s.

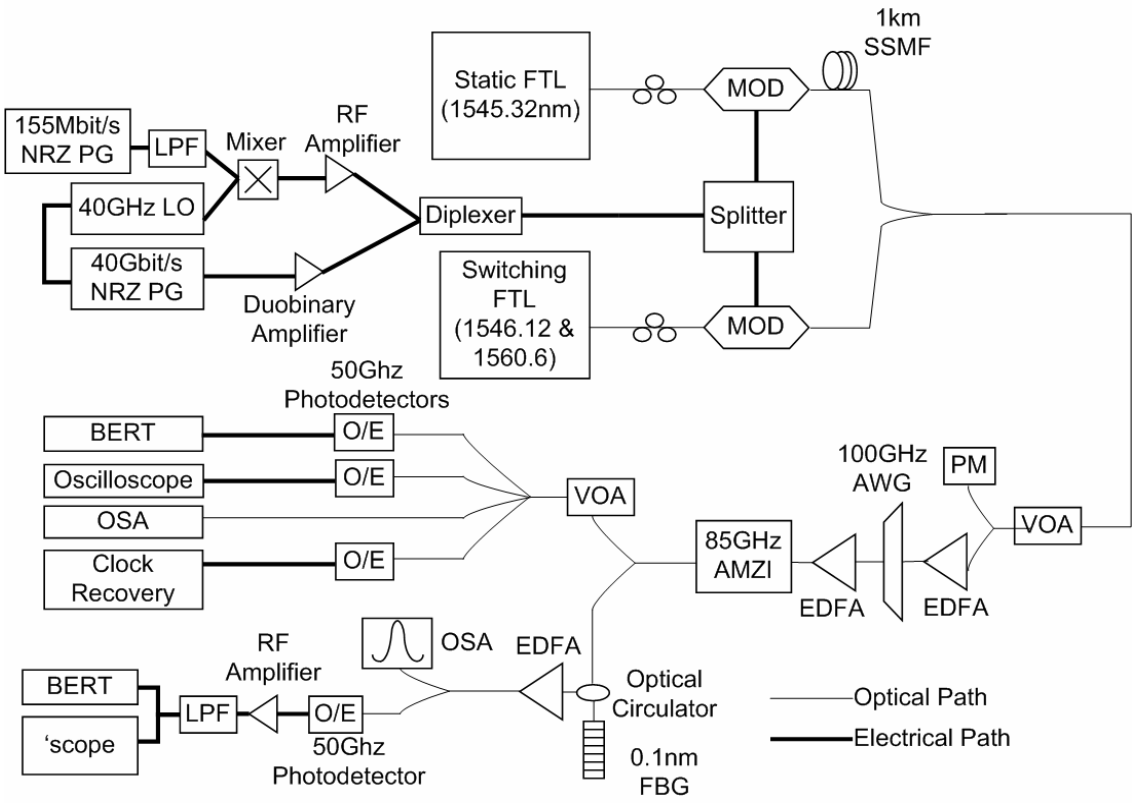

Fig. 6.11:Experimental setup employing two fast tunable lasers (FTLs)

The two laser transmitters used were the same SG-DBR lasers [35] used elsewhere in this work. The signal after the diplexer was electrically split using a 6dB coupler and each path

then drove a 40G MZM. Before coupling the two channels together, one of them was passed through 1km of optical fiber in order to decorrelate the data patterns. This corresponded to 6 word lengths for the label and 15,625 word lengths for the payload.

Fig. 6.12(a) shows the input spectrum to the receiver, with both lasers operating in continuous wave (CW) mode. The receiver was as before except the flat top AWG was replaced with a 100 GHz Gaussian profiled AWG with a 3dB bandwidth of 65GHz. The signals at the output ports of the AMZD are shown in Fig. 6.12(b) and (c). In Fig. 6.12(b) approximately 30dB suppression is shown on the extracted channel's labels at the payload port and in Fig. 6.12(c), a suppression of approximately 10dB of the payload is shown at the labels port.

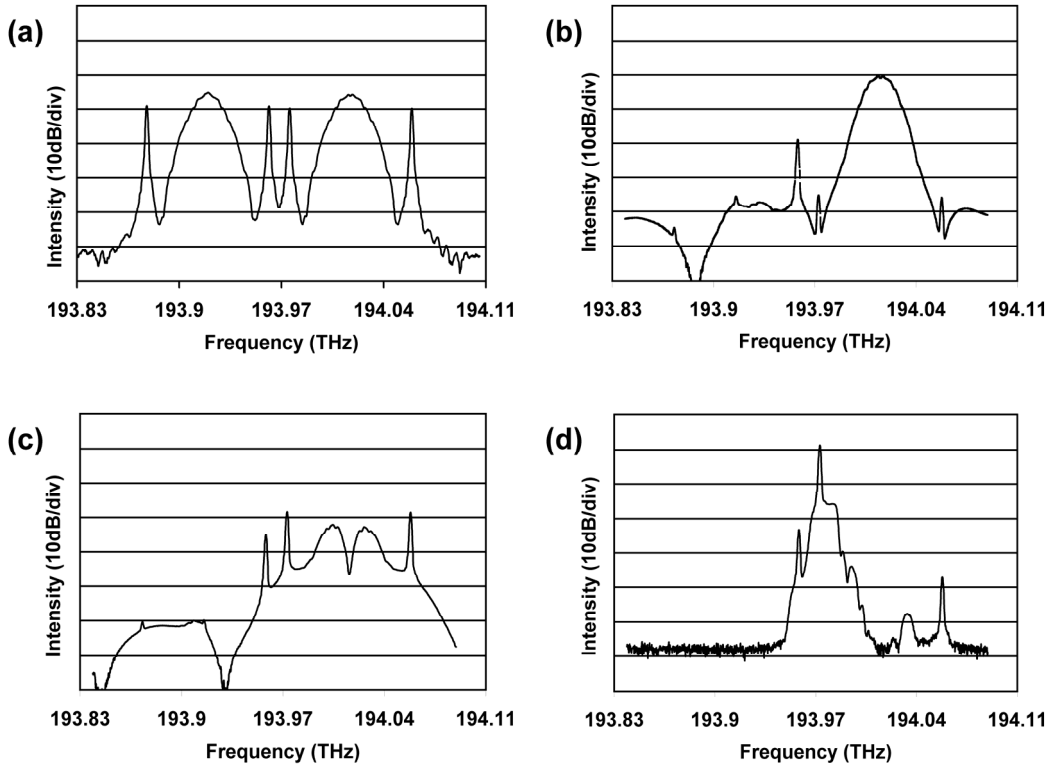

Fig. 6.12:Spectra at different stages of the system: a) Two channels 100GHz apart; b) suppressed labels at one port of AMZD; c) suppressed payload at second port of AMZD; d) extracted Label

In the label receiver, the input arm of a circulator was connected to a tunable Fiber Bragg Grating (FBG) with a 3 dB reflection bandwidth of approximately 12 GHz. This bandwidth is wide enough to ensure correct detection of the label even in the case of wavelength drift

of the tunable laser. The filter was tuned to reflect the lower frequency label of the extracted channel. The reflected label (Fig. 6.12(d)) was directly detected, electrically amplified and low pass filtered. The output of the receiver was split electrically and passed into the Bit Error Rate Tester (BERT) and Oscilloscope.

Due to the slight modifications to the system setup, the single channel system performance was re-characterised. Initial measurements looked at the effects that the label and payload have on each other. The pattern length of both the payload and label was 2^7-1. In Fig. 6.13(a) (○ and △) it is shown that, as before, the presence of the label hardly affects the payload at all. However, the presence of the duobinary payload had a detrimental effect on the label and introduced a power penalty of approximately 13dB. This can be seen in Fig. 6.13(b) (○ and △). Of this label penalty, 11.4 dB was attributable to the power distribution between the payload (93%) and label (7%). The remaining 1.6 dB penalty was attributed to the aggregate modulation of the bias position of the 40 GHz sub carrier by the payload data (averaged over 258 bits). This increased penalty over the single channel system comes about from the insertion of the 6dB power splitter, the use of different electrical amplifiers and the wider bandwidth of the label filter. Owing to the low label signal amplitude, this pattern dependant penalty increased by 5dB when the payload pattern length was increased to 2^{15}-1. To overcome this limitation it may be feasible to use Manchester encoding on the payload as this ensures that there are never more than five zeros in a row [36]. However, through use of optimized components the penalty can be significantly reduced as seen in the previous section.

Next the performance (BER vs. received power) of the payload and label respectively, in three different circumstances was measured. The first case is a single labelled channel. The second case is with two channels 100GHz apart but without any switching of the fast tunable laser. Received eye diagrams corresponding to this static dual-channel case are shown in Fig. 6.14. The final case is when the channel being measured is static and the other is switching from the adjacent channel to a distant channel every 260ns. The laser output is blanked for the first 60ns of this time. As before the 60ns ensures that after coming out of blanking the laser is always within ±12.5 GHz of its target frequency for all channel combinations. The wavelength locking circuit is then activated which holds the output within ±2.5GHz of the target channel after a maximum delay of 200ns after blanking.

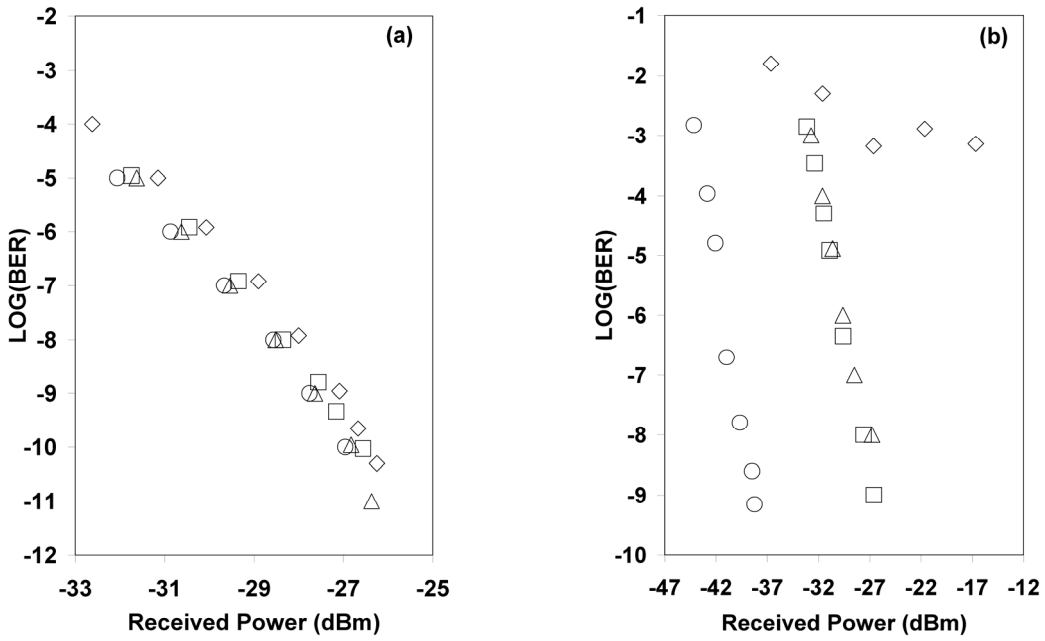

Fig. 6.13:(a) Bit error rate of the 194 THz channel *payload* versus received power in one channel for 4 cases: single channel without label (○); single labelled channel (△); two static labelled channels (□); two switching labelled channels (◇). (b) Bit error rate of the 194 THz channel *label* versus received power in one channel for 4 cases: single label without payload (○); single channel label with payload (△); two static channels (□); two switching channels (◇).

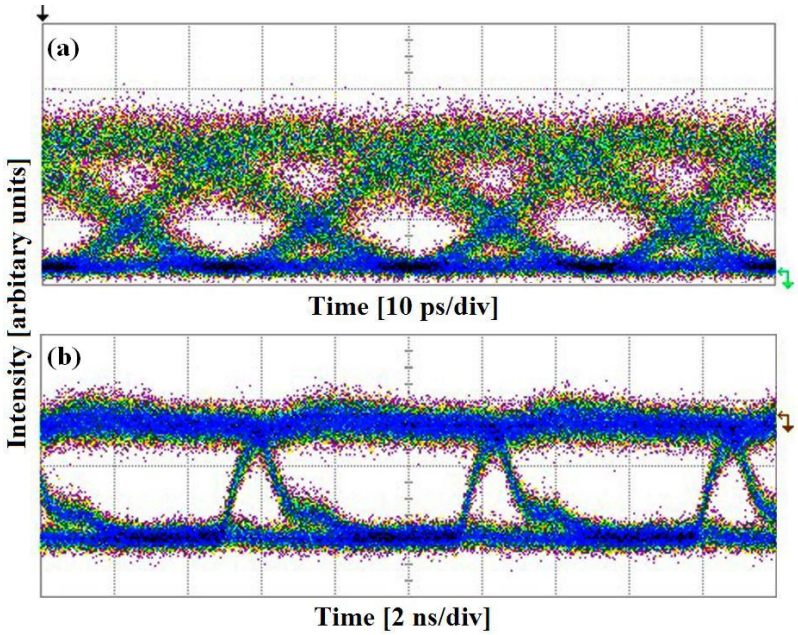

Fig. 6.14:Received eye diagrams of the payload (a) and label (b) for 2 static channel case

It can be seen that for the payload (Fig. 6.13(a); △,□,◇), by simply having two channels adjacent to each other, a power penalty of approximately 0.5 dB is introduced due to crosstalk from the label of the adjacent channel. This could be reduced or even eliminated by optimizing the profile of the AWG which is used to select the channels. Further degradation due to the switching of the adjacent channel is negligible. This is the expected behaviour because of the wide spacing between the payloads in comparison to any drift of the tunable laser that may occur. For the label (Fig. 6.13(b);△,□,◇), again the presence of an adjacent channel introduces very little penalty. However, when one of the lasers is switching, an error floor around $5x10^{-4}$ is introduced due to the label of the switching laser entering the filter pass band of the measured label. This is caused by the wavelength drift of the tunable laser around its target wavelength. The main cause of this drift after blanking is attributed to the wavelength locking circuit. When this is disabled, although tuning takes longer, the wavelength drift is greatly reduced.

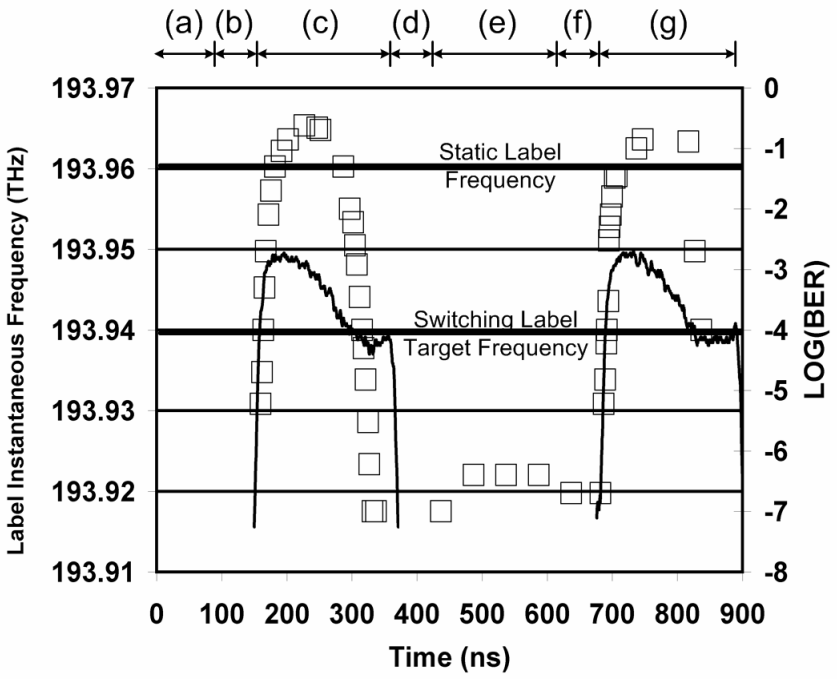

Fig. 6.15:Time Resolved Bit error rate measurements for the extracted label (□) and instantaneous frequency of the switching laser's label. The received power was approximately -28.5 dBm (a) laser at freq 192.1 THz, (b) laser blanked for 60ns, (c) laser settling into freq 193.94 THz for 200ns, (d) laser blanked for 60ns, (e) laser at freq 192.1 THz for 200ns, (f) laser blanked for 60ns, (g) laser settling into freq 193.94 THz for 200ns

This effect is further illustrated in Fig. 6.15, which shows time resolved bit error rate measurements with a received power of -28.5 dBm along with the instantaneous frequency of the label of the switching laser. The instantaneous frequency was extracted from complimentary outputs of the 85GHz AMZD biased at quadrature for the target frequency by using the measured frequency response of the AMZD to resolve the laser output frequency. The gating interval used for the time resolved BER measurements was 8ns and this gating window could be stepped across the signal with a maximum resolution of 500ps.. The time in the plot is divided into 7 sections labelled (a) to (g).

1) During time (a) the switching laser is at the distant channel hence no errors are observed in the measured label and no instantaneous frequency is present.

2) During time (b) the switching laser has switched to the channel adjacent to the measured channel but it is blanked for 60ns so again, no errors are observed.

3) During time (c) the laser comes out of blanking, hence there are now two adjacent labels, one at the frequency marked "static label frequency" and the other settling into the frequency marked "switching label target frequency". It can be seen that during this time, the instantaneous frequency of the switching label comes within 10GHz of the measured label and accordingly, a burst of errors are seen during this time with the error rate at its worst when the two labels are closest together and then reducing as the switching laser settles into it's target frequency.

4) During time (d) the laser is laser has switched to the distant channel again and is blanked for another 60ns and no errors are seen.

5) During times (e) the laser comes out of blanking on the distant channel and the errors seen on the label during this time are caused by its own payload.

6) During times (f) and (g) the cycle is repeated once again.

It can clearly be seen that the switching events in the tunable laser correspond to the time intervals when there are significant errors on the received label data. While the laser is blanked and also while it sits at the distant channel, the error rate of the measured channel

drops considerably. However as the laser tunes towards and begins settling on the 193.94 THz channel the error rate increases dramatically.

6.10 Conclusions

This chapter described the development of transmitter and receiver subsystems for a label switched OPS system. The transmitter was based on a fast tunable SG-DBR laser module and work was carried out that explored the system effects of the wavelength drift of lasers, which had been characterised in the previous chapter.

A number of OLS schemes and methods were described in the early part of the chapter with the focus then turning to the particular labelling method used in this work, SCM labelling. Some of the literature on this topic was then reviewed before the experimental work was described. Three experiments were detailed: The first was the basic design and characterisation of label switching scheme which aside from the common benefits of SCM labels, also offers good spectral efficiency with low payload/label crosstalk. The second set of experiments involved further refinement and improvement of the transmission characteristics of the labelling method by optimization of the amplitude and phase of the label and payload relative to each other. The third experiment expanded the work from a single static channel to a two channel dynamic system. To date, much of the literature on OLS has looked primarily at static single channel systems. Work has focused on the labelling techniques and schemes but the use of these schemes in a system employing multiple switching channels has been somewhat neglected. Error free transmission for both payload and label in a static dual-channel system with 0.4b/s/Hz spectral efficiency was achieved. However, it was shown that in WDM systems when the lasers employed in the transmitters were switching, the labels were severely impaired and a bit error floor was observed. By time resolving the error measurements it was shown that this error floor corresponded to and was due to the wavelength switching effects of the tunable lasers. Clearly, this interference must be overcome to avoid routing errors and possible methods include increasing the blanking time and/or channel spacing. However both of these solutions reduce network throughput. More attractive solutions include optimised channel and label filter profiles, the use of single side band subcarrier generation to eliminate interference between labels of adjacent channels, and optimisation of the transient laser dynamics including operation of wavelength locking technique during the existing blanking period.

References

[1] X. Dai, L.N. Binh, Y.H. Ja, "Novel realtime time-division-multiplex optical packet switching, using nonlinear effect," *Optoelectronics [see also IEE Proceedings-Optoelectronics], IEE Proceedings J* , vol.137, no.3, pp.141-146, Jun 1990

[2] D.J Blumenthal, A. Carena, L. Rau, V. Curri, S. Humphries, "All-optical label swapping with wavelength conversion for WDM-IP networks with subcarrier multiplexed addressing," *Photonics Technology Letters, IEEE* , vol.11, no.11, pp.1497-1499, Nov 1999

[3] J. Capmany, D. Pastor, S. Sales, B. Ortega, 'Subcarrier Multiplexed Optical Labels Swapping Based on Subcarrier Multiplexing: A Network Paradigm for the Implementation of Optical Internet'. ICTON 2003

[4] S. J. B Yoo, 'Optical Label Switching, MPLS, MPLambdaS and GMPLS'. *Optical Networks Magazine*, May/June 2003, p 17-31

[5] P. Pruncal, M. Santoro, T. R Fan, "Spread-spectrum fibre optic local area network using optical processing" *J Lighw. Technol.,* Vol LT-4, no. 5, pp 547-554, May 1986.

[6] P. Pruncal, D. J. Blumenthal, P. A. Perrier, "Photonic switch with optically self-routed bit switching", *IEEE Commun. Mag.* Vol 25, no 5., pp 50-55, May 1987

[7] W. L. Ha, R. M. Fortenberry, R. S. Tucker, "Demonstration of photonic fast packet switching at 700Mb/s data rate" *Electron Lett*, vol 27. no 10. pp 789 – 790., May 1991

[8] W. Wang, L. G. Rau, D. J Blumenthal, "160Gb/s variable length packet/10Gb/s label all-optical label switching with wavelength conversion and unicast/multicast operation", *J. Lightw. Technol.*, vol 23, no 1. pp 211 – 218, Jan 2005

[9] N Chi, et al, "Experimental Demonstration of cascaded transmission and all-optical label swapping of orthogonal IM/FSK labelled signal", *Electron Lett.* Vol 39, no. 8, pp 676-678, Apr 2003

[10] N. Deng, Y. Yang, C.K Chan, W. Hung, L.K Chen, "Intensity Modulated Labelling and all optical label swapping on angle-modulated packets", *IEEE Photon. Technol. Lett.,* vol 16. no 4, pp 1218 – 1220, Apr. 2004.

[11] N. Chi et al. Optical label swapping and packet transmission based on ASK/DPSK orthogonal modulation format in IP-over- WDM Networks, presented at the *Optical Fiber Communications Conf. (OFC 2003)*, Atlanta, GA, Paper FS2.

[12] C. Chow and H. K. Tsang, Optical packet label using polarization shift keying (PolSK) label and amplitude shift keying (ASK) payload, presented at *Optical Fiber Communications Conf. (OFC 2005)*, Anaheim, CA, Paper OME73.

[13] W.-H. Yang; C.-S. Wu, "Optical CDMA Label Encoding for Optical Packet Switching in All-Optical Networks," *Networks, 2006. ICON '06. 14th IEEE International Conference on* , vol.2, no., pp.1-5, Sept. 2006

[14] D.-Z. Hsu, "A novel photonic label switching based on optical code division multiplexing," *Telecommunications, 2003. ICT 2003. 10th International Conference on* , vol.1, no., pp. 634-640 vol.1, 23 Feb.-1 March 2003

[15] A. Teixeira, P. Andre, P. Monteiro, M. Lima, R. Nogucira, and J. da Rocha, "All-optical routing based on OCDMA headers," in Proc. 16th Annual Meeting IEEE LEOS, 2003, vol. 2, pp. 1046–1047.

[16] S.-C. Lee, R. Varrazza, I.B. Djordjevic, S. Yu, "Optical label detection and packet switching using a 4/spl times/4 optical crosspoint switch matrix," *Optical Fiber Communication Conference, 2004. OFC 2004* , vol.1, no., pp.-, 23-27 Feb. 2004

[17] A. Budman, E. Eichen, J. Schlafer, R. Olshansky, F. McAleavy, "Multigigabit Optical Packet Switch for self-routing networks with subcarrier addressing", in *Proc. Optical Fiber Commun. Conf. (OFC 1992),* San Jose, CA, USA, Feb. 1992, paper TUO4.

[18] M. Jeon, Z. Pan, J. Cao, S.J.B. Yoo, "All-optical sub-carrier label swapping with 2R regeneration," *Optical Fiber Communications Conference, 2003. OFC 2003* , vol., no., pp. 277-279 vol.1, 23-28 March 2003

[19] E. Park, A.E. Willner, "Network demonstration of self-routing wavelength packets using an all-optical wavelength shifter and QPSK subcarrier routing control," *Optical Fiber Communications, 1996. OFC '96* , vol., no., pp. 114-115, 25 Feb.-1 March 1996

[20] R. Gaudino; D.J. Blumenthal, "A novel transmitter architecture for combined baseband data and subcarrier-multiplexed control links using differential Mach-Zehnder external modulators," *Photonics Technology Letters, IEEE* , vol.9, no.10, pp.1397-1399, Oct. 1997

[21] T. Dimmick, R. Doshi, R. Rajaduray, D. Blumenthal, '"Optically Multiplexed Transmitter for hybrid baseband and subcarrier multiplexed signals". *European Conference on Optical Communications (ECOC '00)*, 2000

[22] T. Flarup, C. Peucheret, J. J. V. Olmos, Y. Geng, J. Zhang, I. T. Monroy, P. Jeppesen, 'Labeling of 40Gb/s DPSK Payload using In-Band Subcarrier Multiplexing'. *Proc. Optical Fiber Communications Conference (OFC) 2005*, Vol. 3 p 3

[23] G.-K. Chang; J. Yu; A. Chowdhury, Y.-K. Yeo, "Optical carrier suppression and separation label-switching techniques," *Lightwave Technology, Journal of* , vol.23, no.10, pp. 3372-3387, Oct. 2005

[24] G.H. Smith, D. Novak, "Broad-band millimeter-wave (38 GHz) fiber-wireless transmission system using electrical and optical SSB modulation to overcome dispersion effects," *Photonics Technology Letters, IEEE* , vol.10, no.1, pp.141-143, Jan 1998

[25] P.A. Greenhalgh, R.D. Abel, P.A. Davies, "Optical prefiltering in subcarrier systems," *Electronics Letters* , vol.28, no.19, pp.1850-1852, 10 Sept. 1992

[26] M. Popov, A. Martinez, J. Capmany, D. Pastor, P.-Y. Fonjallaz, B. Ortega, "Fiber-Bragg-grating-based device for payload and label separation in highly packed subcarrier-multiplexed optical label swapping," *Photonics Technology Letters, IEEE* , vol.17, no.11, pp. 2445-2447, Nov. 2005

[27] H.-J. Lee; S.J.B. Yoo, V.K. Tsui, S.K.H Fong, "A simple all-optical label detection and swapping technique incorporating a fiber Bragg grating filter," *Photonics Technology Letters, IEEE* , vol.13, no.6, pp.635-637, Jun 2001

[28] Y.M. Lin, W.I. Way, G.K. Chang, "A novel optical label swapping technique using erasable optical single-sideband subcarrier label," *Photonics Technology Letters, IEEE* , vol.12, no.8, pp.1088-1090, Aug 2000

[29] N. Chi, J. Zhang and P. Jeppesen, "All-optical subcarrier labeling based on the carrier suppression of the payload," *IEEE Photonics Technol. Lett.,* vol.15, pp. 781-783, May 2003.

[30] M. Deulk, J. Gripp, J. Simsarian, A. Bhardwaj, P. Bernasconi, M. Zirngibl, and O. Laznicka, "Fast packet routing in a 2.5 Tb/s optical switch fabric with 40 Gb/s duobinary signals at 0.8 b/s/Hz spectral efficiency" in *Proc. Optical Fiber Commun. Conf. (OFC 2003)* , Georgia, Mar. 2003, vol. 3, postdeadline paper PD8-1-3.

[31] P. J. Winzer and R.-J. Essiambre, "Advanced modulation formats for high-capacity optical transport networks," *J. Lightw. Technol.,* vol. 24, pp. 4711-4728, Dec. 2006

[32] G. Charlet, "Progress in optical modulation formats for high-bit rate WDM transmissions," *IEEE J. Sel. Topics Quant. Electron*., vol. 12, pp. 469-483, Jul./Aug. 2006.

[33] R. Hui, B. Zhu, R. Huang, C. T. Allen, K. R. Demarest, D. Richards, "Subcarrier multiplexing for high-speed optical transmission," *J. Lightw. Technol.,*vol. 20, pp. 417-427, Mar. 2002.

[34] GH. Smith, D. Novak, D., Z. Ahmed, 'Overcoming chromatic dispersion effects in fibre-wireless systems incorporating external modulators', *IEEE Trans. Microw. Theory Tech.*, 1997, 45, pp. 1410–1415

[35] J. Buus, M.-C. Amann, D. J. Blumenthal, "Widely Tunable Monolithic Laser Diodes" in *Tunable Laser Diodes and Related Optical Sources*, Wiley, New Jersey, 2005.

[36] J. Zhang, N. Chi, P. V. Holm-Nielsen, C. Peucheret, P. Jeppesen, "Performance of Manchester-Coded Payload in an Optical FSK labelling scheme". *IEEE Photonics Technology Letters*, vol 15, pp 1174-1176, Aug 2003.

Chapter 7 – Discussion and Conclusion

Optical networks are constantly evolving; from single channel point to point Synchronous Optical Network/Synchronous Digital Hierarchy (SONET/SDH) links, they have grown to multi-channel Wavelength Division Multiplexed (WDM) networks carrying terabits of data every second. Now, as the first true optical switching components are being deployed, the next step in the evolution is from optical transport networks to optical switching networks. In their earliest forms these networks will be somewhat analogous to early telephone switching networks, in which a user will request some bandwidth, and a network manager will meet the request by reconfiguring the network. Gradually, the majority of manual intervention will be removed from the network as systems are put in place to enable automatic self-reconfiguration in response to changing network conditions. The network will recognise network faults or traffic congestion and automatically re-route high priority data around them. The beginnings of this automated optical circuit switched network are already being seen with the deployment of the Generalized Multi-Protocol Label Switching (GMPLS) control plane as described in Chapter 2 of this thesis.

Optical Circuit Switching (OCS) is desirable for telecommunication carriers because it provides significant cost saving without requiring a total overhaul of the network. Network flexibility without the need to deploy personnel to each node site, and the removal of Optical-Electrical-Optical (OEO) conversions in the node together represent a huge cost saving. In addition these cost savings come without requiring a total overhaul of the network. Current transport networks can be relatively easily upgraded to optical switching networks with the replacement of electronic switching components in the node with their optical counterparts.

In order to move to the next stage of in the evolutionary chain of optical networks however, the capital investment may be much higher, and as such carriers will need to see a significant cost saving or revenue gain before they will be willing to make that investment. While the nodes in an OCS network simply *switch* data transparently without regard for its contents optical burst and packet switching networks will *route* data transparently, meaning that nodes will need to examine the data (or at least the label) passing through. In addition tunability is

required in the nodes raising the possibility that every laser transmitter in the network would require replacement. The upgrade from OCS to Optical Burst Switching (OBS) or Optical Packet Switching (OPS) ,therefore is not straightforward and certainly, if their current network can provide the services they want to offer, then carriers will not invest simply because the technology is available. Nevertheless, as component costs drop and the technology matures it seems likely that OBS and OPS will be deployed in the network due to the massive flexibility and efficiency that it offers. Indeed, OBS networks are already being offered commercially for the access and metro spaces. The wide range of services that can be offered by optical networks mean that it is quite possible that the network of the future will consists of a combination of OCS, OBS and OPS all controlled by Optical Label Switching (OLS).

At each stage of the evolution a whole host of new issues arise. Problems solved to enable the previous stage of evolution often arise again in more complicated forms. The experience and knowledge gained from the first time around is then built upon to come up with novel solutions. An example of this would be dispersion management; now well understood for point to point optical transport networks. However as optical switching emerges, and greater connectivity between nodes is seen, dispersion management becomes a whole new problem due to the diversity of paths that signals can travel to their destination. This thesis dealt experimentally with a small fraction of the vast range of issues affecting future optical switching networks.

The first two chapters provided background information regarding optical networks, WDM and optical switching. While not intended to be a complete reference, the chapters and the references therein were aimed to give the reader the knowledge required to understand the motivation behind the experimental work and to provide a starting point for further reading on topics of interest. Two of the most important sections of Chapter 2 dealt with the primary switching techniques of interest in this work: OCS and OPS, however both sections were dealt with quite differently. Because OCS, is for the most part a mature technology, at least in terms of hardware and understanding, this section was concerned with higher level topics such as the control plane and the applications enabled by OCS. In contrast, OPS is still a long way from maturity and as such, its section discussed the possible implementations of OPS, and the technological obstacles.

Chapters 3 – 5 were the experimental chapters and the three were similarly structured. Detailed background information and a review of the literature on the topic was given initially, followed by a description of the experiment, the results and some concluding remarks. In all cases the actual numerical results obtained are specific to the system used in the experiment. However, more important than these are the conclusions which are drawn from these results and which apply to all similar systems.

Chapter 3 reported on experiments carried out to investigate the effect of channel reconfiguration on network performance. A circulating loop based WDM testbed was used for this work which involved measuring the transmission performance of channels as the channel configuration changed and the network was then re-optimized for the new configuration. The technique of Applied Constant Gain (ACG) was used to enable the study of constant-gain based systems in a constant-power based circulating loop.

A number of issues were investigated including the performance of channels at different launch powers, and with different dispersion maps. The main lesson learned from the work however, is that wavelength dependent gain of the amplifiers results in a network arrangement that is optimized for a certain channel configuration, but sub-optimal for others. Reconfiguring the network therefore, can cause channel power divergence, which may causing severe transmission penalties. In the worst case studied, the transmission reach for the channel in question was reduced by nearly 1000km simply by changing the wavelength of the other 4 channels in the configuration from a uniformly spread channel configuration to a banded configuration. Clearly such penalties will have a considerable impact on network throughput as transmission cannot begin until the network is re-optimized for the new configuration, a process which can take anywhere from seconds to minutes.

The set of experiments performed was intended to stimulate further study of these effects in order that control mechanisms can be developed to avoid the penalties. An investigation of different approaches to reconfiguration is required and one of the first tests would be to return the system to a known state prior to reconfiguration. For example, in this work the per channel attenuators were not adjusted prior to reconfiguration but if they were returned to a known state (for example the fully loaded arrangement) it is possible that the effects of gain error would be reduced. Another prospect for further work would be the development

of techniques which predict the response of the EDFA to a new channel configuration based on the current configuration and known EDFA models. The system could then be arranged using the predicted response during re-configuration and then fine tuned over time. Furthermore, the gain error could be automatically accounted for with the use of dynamic GEFs within the EDFA. A control circuit which monitored the wavelength dependent gain, rather than the total gain would be required and this could feed back into the dynamic GEF to keep the EDFA gain flat at all times. Finally, work should be carried out which investigates the time resolved system performance as channels configurations are switched. In such an experiment, transient EDFA gain effects will affect performance as well as steady state effects.

Chapter 4 and 5 moved away from the relatively slow switching speeds typical of OCS and toward the much faster form of optical switching: OPS. With wavelength switching taking place so quickly in an OPS network, it is likely that the work from Chapter 3 would be rendered redundant because the EDFAs would never reach a steady state; rather they would experience constant gain transients.

In Chapter 4 fast tunable lasers were the subjects of the experiments. A novel tunable laser design based on the slotted Fabry-Pérot (SFP) laser was shown to exhibit extremely fast wavelength switching despite a very simple and inexpensive fabrication process. In most commercially available fast tunable lasers the switching speed is limited by the spontaneous carrier lifetime in the passive sections however all of the sections in these devices are active and therefore switching times can be expected to be much faster. The devices are crudely packaged and it is expected that the switching times measured are in fact limited by the drive circuitry and crude packaging rather than by the devices themselves. These devices were fully characterised and modulated with 10Gb/s data and it was shown that error free data transmission was possible within a few nanoseconds. This indicates that devices based on the SFP structure may be suitable for use in OPS systems.

Further advances in the design of the tunable SFPs have resulted in increased channel counts and reduced channel spacing. Recently the SFP devices have been packaged in a high speed butterfly package. Further work in this area would include the integration of such a device into a system module employing control electronics and a lookup table which ensured accurate and reliable wavelength switching between any of the available wavelengths. This

would allow the use of the devices in full systems-based experiments which are difficult currently due to the crude packaging and control employed.

A commercially available SG-DBR laser was the subject of experiments detailed in chapters 4 and 5. Although the devices met their design specifications, initial work focussed on the wavelength drift of these devices and the effect that it may have in an SCM labelled OPS system. A wavelength drift of up to 7.5GHz was reported. In densely packed WDM systems this level of wavelength drift can cause performance degradation. The drift can be improved by increasing the blanking time or using more sophisticated wavelength lockers but the disadvantages are reduced throughput and increase expense, respectively. Having characterised the drift the TL was used in a novel SCM labelling scheme which offered excellent spectral efficiency. The problem that the wavelength drift of the lasers can cause was then investigated in a two channel system using the labelling technique. Severe performance problems were observed which in a real system would cause incorrect routing of packets.

Further work in this area would include the expansion of the WDM system from 2 lasers up to 4 or 8 and to perform measurements while all of these lasers were switching between channels concurrently, including the channel being measured. While significant errors were seen with the measured laser in static mode it is expected that the performance would be even worse when switching, due mainly to the static filters employed and the drift of the lasers. In addition the labelling scheme could be developed to investigate single sideband (SSB) operation or in band labelling. The technique could be modified to include label swapping and in this case, a transmitter – node – receiver experiment could be designed.

The ongoing evolution of optical switching brings up new challenges and obstacles with every new idea formed. The experiments reported in this thesis yielded important conclusions, relevant to any researcher working in the areas studied and should stimulate further investigation of the issues covered.

Appendix A – List of Publications

Refereed Journals

1) F. Smyth, E. Connolly, A.K. Mishra, A.D. Ellis, D. Cotter, A. Kaszubowska, L.P. Barry, "Effects of Crosstalk in WDM Optical Label Switching Networks Due to Wavelength Switching of a Tunable Laser," *IEEE Photonics Technology Letters,* vol.18, no.20, pp.2177-2179, Oct. 2006

2) F. Smyth, E. Connolly, B. Roycroft, B. Corbett, P. Lambkin, L.P. Barry, "Fast Wavelength Switching Lasers Using Two-Section Slotted Fabry-Pérot Structures," *IEEE Photonics Technology Letters,* vol.18, no.20, pp.2105-2107, Oct. 2006

3) A.K. Mishra, A.D. Ellis, D. Cotter, F. Smyth, E. Connolly, L.P. Barry, "Spectrally compact optical subcarrier multiplexing with 42.6 Gb/s AM-PSK payload and 2.5 Gb/s NRZ labels," *Electronics Letters*, vol.42, no.22, pp.1303-1304, Oct. 26 2006

4) E. Connolly, F. Smyth, A.K. Mishra, A. Kaszubowska-Anandarajah, L.P. Barry, "Cross-Channel Interference Due to Wavelength Drift of Tunable Lasers in DWDM Networks," *IEEE Photonics Technology Letters,* vol.19, no.8, pp.616-618, April15, 2007

5) R. Phelan, W-H Guo, Q. Lu, D. Byrne, B. Roycroft, P. Lambkin, B. Corbett, F. Smyth, L.P. Barry, B. Kelly, J. O'Gorman, J.F. Donegan, "A Novel Two-Section Tunable Discrete Mode Fabry-Pérot Laser Exhibiting Nanosecond Wavelength Switching," *IEEE Journal of Quantum Electronics,* vol.44, no.4, pp.331-337, April 2008

6) F. Smyth, D.C. Kilper, L.P. Barry, S. Chandrasekhar, "Applied Constant Gain Amplification in Circulating Loop Experiments", Submitted to *IEEE Journal of Lightwave Technology*

Reviewed Conferences

1) F. Smyth, L.P. Barry "Performance Issues in SCM label switched networks due to tunable laser switching events", *International Conference on Applications of Photonic Technology (Photonics North 2006)*, pp 170, Quebec, 5-8 June 2006

2) G. Mulvihill, M. Ruffini, F. Smyth, L.P. Barry, L. Doyle, D. O'Mahony, "Optical IP Switching a Solution to Dynamic Lightpath Establishment in Disaggregated Network Architectures," *International Conference on Transparent Optical Networks, 2006*, vol.3, pp.78-81, June 2006

3) F. Smyth, B. Roycroft, B. Corbett, P. Lambkin, L.P. Barry, "Fast Wavelength Switching Lasers Using Two-section Slotted FP Structures", *European Conference on Optical Communications (ECOC 2006)*, Paper We3.P.42 Cannes, France, 24 – 28 September 2006

4) A.K. Mishra, A.D. Ellis, D. Cotter, F. Smyth, E. Connolly, L.P. Barry, 'Spectrally Compact Optical Subcarrier Multiplexing for Label-Switched Networks with 42.6 Gb/s Duobinary Payload and 2.5Gb/s NRZ Labels', *European Conference on Optical Communications (ECOC '06)*, Paper We2.4.4, Cannes, France, 24-28 September, 2006

5) F. Smyth, A.K. Mishra, E. Connolly, A.D. Ellis, D. Cotter, A. Kaszubowska, L.P. Barry, "SCM optical label switching scheme in a WDM packet transmitter employing a switching SG-DBR laser," *International Conference on Photonics in Switching, 2006. PS '06.*, pp.1-3, 16-18 Oct. 2006

6) R. Phelan, D. Byrne, W.-H. Guo, Q.Y. Lu, B. Roycroft, F. Smyth, L.P. Barry, J.F. Donegan, "A Novel Two-Section Tunable Slotted Fabry-Pérot Laser Exhibiting ns Wavelength Switching," *Optical Fiber Communication and the National Fiber Optic Engineers Conference, 2007. OFC/NFOEC 2007.* pp.1-3, 25-29 March 2007

7) B. Roycroft, S.K. Mondal, P. Lambkin, P. Engelstaedter, B. Corbett, F.H. Peters, F. Smyth, L.P. Barry, R. Phelan, J.F. Donegan, A.D. Ellis, "Fast Switching Tunable Laser Sources for Wavelength Division Multiplexing in Passive Optical Access Networks," *IEEE 19th International Conference on Indium Phosphide & Related Materials, 2007. IPRM '07.*, pp.606-609, 14-18 May 2007

8) F. Smyth, J. O'Dowd, D.C. Kilper, J.E. Simsarian, L.P. Barry, B. Roycroft, B. Corbett, "10Gbit/s Modulation of a Fast Switching Slotted Fabry-Pérot Tunable laser," *European Conference on Lasers and Electro-Optics, 2007 and the International Quantum Electronics Conference. CLEOE-IQEC 2007*, 17-22 June 2007

9) D. C. Kilper, S. Chandrasekhar, F. Smyth, L. P. Barry, "Dynamic Circulating-Loop Methods for Transmission Experiments in Optically Transparent Networks" *10th International Conference on Transparent Optical Networks (ICTON)*, Invited Paper, June 22-26, 2008 - Athens, Greece

10) D. C. Kilper, F. Smyth, L. Barry, S. Chandrasekhar "Power Divergence Due to Wavelength Re-routing in Long Haul Circulating Loop Experiments", accepted for presentation, *European Conference on Optical Communication (ECOC 08)*, Brussels, Belgium, Sept 21st – 25th 2008